Ocean-Land-Atmosphere Research
A SCIENCE PARTNER JOURNAL

REVIEW ARTICLE

A Review of Arctic–Subarctic Ocean Linkages: Past Changes, Mechanisms, and Future Projections

Qiang Wang[1*], Qi Shu[2,3], Shizhu Wang[2,3], Agnieszka Beszczynska-Moeller[4], Sergey Danilov[1,5], Laura de Steur[6], Thomas W. N. Haine[7], Michael Karcher[1,8], Craig M. Lee[9], Paul G. Myers[10], Igor V. Polyakov[11,12], Christine Provost[13], Øystein Skagseth[14], Gunnar Spreen[15], and Rebecca Woodgate[9]

[1]Alfred Wegener Institute Helmholtz Centre for Polar and Marine Research (AWI), Bremerhaven, Germany. [2]First Institute of Oceanography, and Key Laboratory of Marine Science and Numerical Modeling, Ministry of Natural Resources, Qingdao, People's Republic of China. [3]Shandong Key Laboratory of Marine Science and Numerical Modeling, Qingdao, People's Republic of China. [4]Institute of Oceanology, Polish Academy of Sciences, Sopot, Poland. [5]Department of Mathematics and Logistics, Jacobs University, Bremen, Germany. [6]Norwegian Polar Institute, Fram Centre, Tromsø, Norway. [7]Earth & Planetary Sciences, The Johns Hopkins University, Baltimore, MD, USA. [8]Ocean Atmosphere Systems GmbH, Hamburg, Germany. [9]Applied Physics Laboratory, University of Washington, Seattle, WA, USA. [10]Department of Earth and Atmospheric Sciences, University of Alberta, Edmonton, AB, Canada. [11]International Arctic Research Center and College of Natural Science and Mathematics, University of Alaska Fairbanks, Fairbanks, AK, USA. [12]Finnish Meteorological Institute, Helsinki, Finland. [13]Laboratoire LOCEAN-IPSL, Sorbonne Université (UPMC,University Paris 6), CNRS, IRD, MNHN, Paris, France. [14]Institute of Marine Research and Bjerknes Centre of Climate Research, Bergen, Norway. [15]Institute of Environmental Physics, University of Bremen, Bremen, Germany.

*Address correspondence to: qiang.wang@awi.de

Citation: Wang Q, Shu Q, Wang S, Beszczynska-Moeller A, Danilov S, de Steur L, Haine TWN, Karcher M, Lee CM, Myers PG, et al. A Review of Arctic–Subarctic Ocean Linkages: Past Changes, Mechanisms, and Future Projections. *Ocean-Land-Atmos. Res.* 2023;2:Article 0013. https://doi.org/10.34133/olar.0013

Submitted 3 November 2022
Accepted 31 May 2023
Published 26 June 2023

Arctic Ocean gateway fluxes play a crucial role in linking the Arctic with the global ocean and affecting climate and marine ecosystems. We reviewed past studies on Arctic–Subarctic ocean linkages and examined their changes and driving mechanisms. Our review highlights that radical changes occurred in the inflows and outflows of the Arctic Ocean during the 2010s. Specifically, the Pacific inflow temperature in the Bering Strait and Atlantic inflow temperature in the Fram Strait hit record highs, while the Pacific inflow salinity in the Bering Strait and Arctic outflow salinity in the Davis and Fram straits hit record lows. Both the ocean heat convergence from lower latitudes to the Arctic and the hydrological cycle connecting the Arctic with Subarctic seas were stronger in 2000–2020 than in 1980–2000. CMIP6 models project a continuing increase in poleward ocean heat convergence in the 21st century, mainly due to warming of inflow waters. They also predict an increase in freshwater input to the Arctic Ocean, with the largest increase in freshwater export expected to occur in the Fram Strait due to both increased ocean volume export and decreased salinity. Fram Strait sea ice volume export hit a record low in the 2010s and is projected to continue to decrease along with Arctic sea ice decline. We quantitatively attribute the variability of the volume, heat, and freshwater transports in the Arctic gateways to forcing within and outside the Arctic based on dedicated numerical simulations and emphasize the importance of both origins in driving the variability.

1. Introduction

The Arctic Ocean is located at the northern end of the global ocean and surrounded by the continents of Asia, Europe, and North America (Fig. 1A). Different from the polar seas in the Southern Hemisphere, which are widely exposed to the global ocean, the Arctic Ocean is connected with the Subarctic seas only through a few straits. Water and sea ice fluxes through

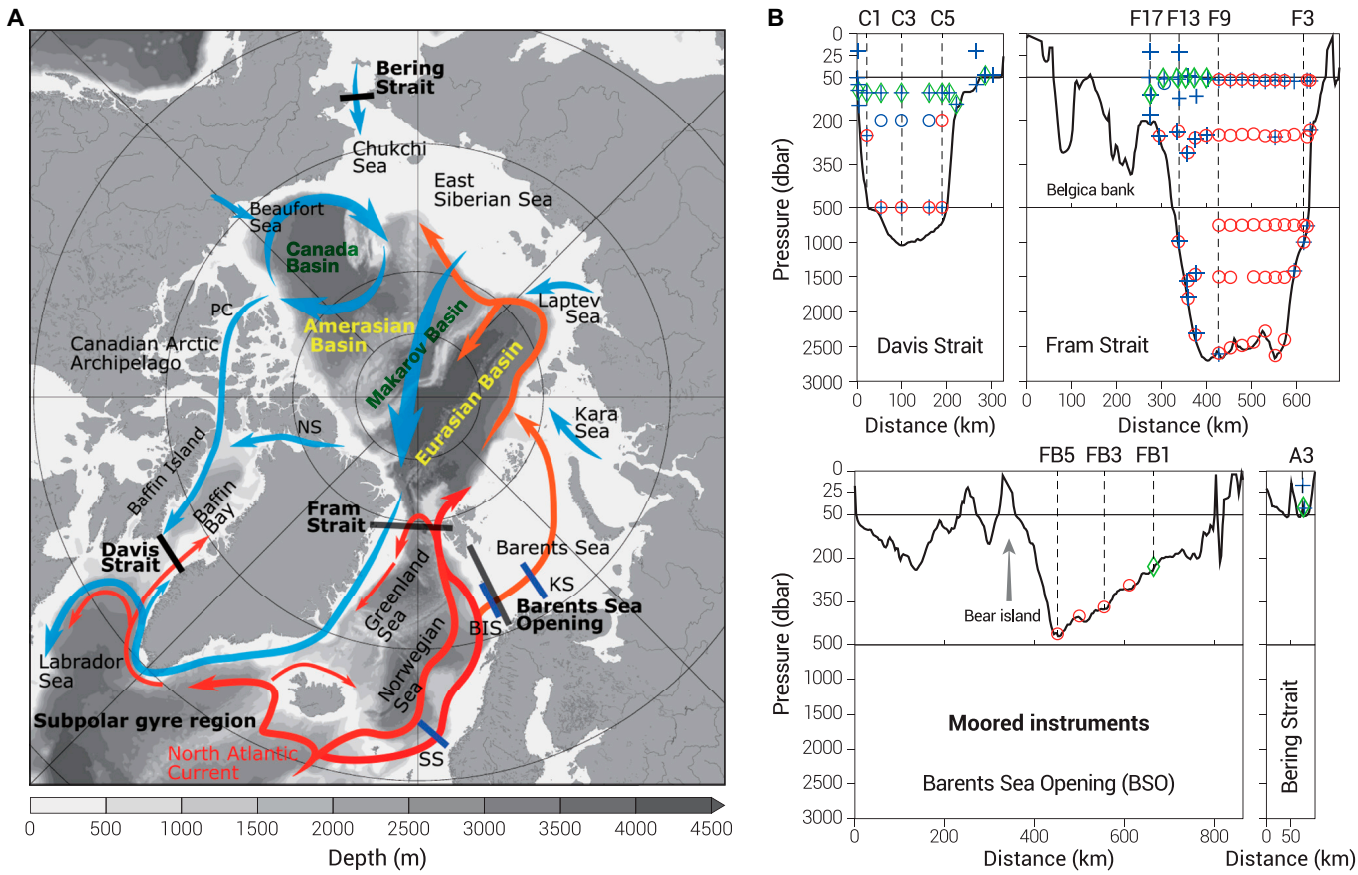

Fig. 1. (A) Schematic of pan-Arctic Ocean circulations. Blue arrows denote the circulations of low-salinity water, and red arrows denote the circulations of Atlantic Water. The background gray color denotes bottom bathymetry. The 4 Arctic gateways reviewed in this paper (Bering, Fram and Davis straits, and the Barents Sea Opening) are indicated with black lines. SS, Svinoy Section; BIS, Bear Island Section; KS, Kola Section; NS, Nares Strait; PC, Parry Channel. (B) Location of mooring instruments in the 4 Arctic gateways [indicated by black lines in (A)]. Red circles depict single-point current meters that measure velocity and temperature. Blue circles depict current meters with both temperature and salinity sensors. Blue crosses depict SeaBird MicroCAT devices that measure temperature and salinity. Green diamonds depict acoustic Doppler current profilers (ADCPs), which measure velocity. (B) is modified from [115] (©American Meteorological Society; used with permission) with new instruments added.

these straits carry water mass, heat, salt, and nutrients, linking the Arctic with the rest of the globe.

The narrow (85 km) and shallow (50 m) Bering Strait is the only oceanic gateway between the Pacific and Arctic oceans. The Pacific inflow is approximately 1 Sv [1]. It has relatively low salinity (~32.5) compared to the Arctic mean salinity (~34.8) and is therefore considered an important freshwater source of the Arctic Ocean [2–4]. It is a conduit for heat in warm seasons, causing sea ice melting in the western Arctic [5]. In winter, it contributes to the renewal of the cold halocline in the Canada Basin, a layer that insulates surface mixed layer and sea ice from the underlying warm Atlantic Water layer [6]. After transiting the Arctic, the Pacific Water can impact the upper ocean stratification in the subpolar North Atlantic and thus the Atlantic meridional overturning circulation (AMOC) and climate [7–11]. Through its impact on the AMOC, the Pacific Water could further influence the melting of ice sheets in North America and Europe, associated with sea-level fluctuations of approximately 20 to 30 m (thus the reopening and closing of the Bering Strait) throughout the last glacial period [12]. In addition to its climate impacts, the Pacific Water is rich in nutrients, feeding Arctic ecosystems [13–15].

In addition to the low-salinity Pacific inflow, the Arctic Ocean receives a large amount of freshwater (zero-salinity water) from river runoff and precipitation [16,17]. Poleward moisture transport in the atmosphere as part of the global hydrological cycle supplies these freshwater sources [18]. The Arctic freshwater source is largely counterbalanced by exports to the North Atlantic through the Davis and Fram straits in the form of both liquid freshwater (low-salinity seawater) and sea ice [2,16,19–25].

The Davis Strait is relatively wide (approximately 300 km) and deep (sill depth of 640 m). However, the straits in the Canadian Arctic Archipelago (CAA) are narrow and shallow. The 2 largest CAA straits, Parry Channel and Nares Strait, are approximately 52 and 28 km wide, respectively, at their narrowest locations, constraining ocean and sea ice transports. The shallow sill depths (approximately 120 and 220 m) in these straits only permit fresh Arctic surface water to flow through the CAA region [26–31], supplying the Baffin Island Current along the western boundary of Baffin Bay.

The Fram Strait is the deepest Arctic Ocean gateway (sill depth 2,600 m, more than 500 km wide including the wide Greenland continental shelf). On its western side, both freshwater at the surface and saline water at depth are exported from the Arctic Ocean via the East Greenland Current. The ocean exports through both the Davis and Fram straits are important freshwater sinks of the Arctic Ocean, while Arctic sea ice is mainly (~90%) exported through the Fram Strait [19,20,32].

Freshwater exported from the Arctic Ocean has long been believed to influence the upper-ocean salinity, stratification, and dense water formation in the subpolar North Atlantic, thus impacting the AMOC [33–37]. Indeed, low-salinity pulses, called Great Salinity Anomalies, were observed in the 1970s, 1980s, and 1990s in the northern North Atlantic, which were attributed to positive anomalies of freshwater export from the Arctic Ocean [38,39]. It has been suggested that future increases in Arctic freshwater export could reduce the strength of the AMOC [40–42]. Model simulations showed that not only the total amount of freshwater exported from the Arctic Ocean to the North Atlantic but also the changes in the distribution of the export between the Fram Strait and Davis Strait may impact the overall dense water formation in the subpolar North Atlantic [43,44]. Arctic waters also contain chemical constituents that are different from those in Atlantic waters, so they can influence the ecosystems in the northern North Atlantic [45,46].

In terms of inflows from the North Atlantic, the Arctic Ocean receives warm and saline Atlantic Water through the southern Barents Sea Opening and eastern Fram Strait [47–53]. In total, approximately 8.0 Sv Atlantic Water enters the Nordic Seas at their southern boundary [54]. The Norwegian Atlantic Current in the eastern Norwegian Sea carries Atlantic Water in 2 main branches toward the Arctic Ocean [55–57]. The eastern branch (Norwegian Atlantic Slope Current) is the main supplier of the Atlantic Water to the Arctic Ocean through both the Barents Sea Opening and Fram Strait, and the western branch (Norwegian Atlantic Front Current) may also contribute to the Atlantic Water inflow via these gateways [58,59]. Nutrients and planktonic organisms are transported in the Atlantic Water into the Arctic Ocean through these 2 gateways [60–62].

The Barents Sea Opening (sill depth of approximately 450 m) connects the northern Norwegian Sea with the Barents Sea, a broad continental shelf sea. The ongoing increase in poleward ocean heat transport through the Barents Sea Opening has driven the declining trend in winter sea ice cover in the Barents Sea [63–66], caused Barents Sea warming and northward displacement of the polar front [67,68], increased the temperature of the Barents Sea Water that feeds the Arctic deep basin [69,70], and contributed to Arctic amplification (surface air warms faster in the Arctic than the global mean in a warming climate) in wintertime [71,72]. Compared to other Arctic regions, the Barents Sea is characterized by the most extensive winter sea ice decline [73] and largest ocean and atmosphere warming [74,75], with potential impacts on mid-latitude weather [76,77]. Due to warming inflows through the Barents Sea Opening, the Barents Sea has been shifting to a state more closely resembling that of the Atlantic (with warmer waters and weaker halocline stratification), a phenomenon called Atlantification [78,79], which has a notable influence on marine ecosystems [80,81]. The linkage between the Barents Sea and North Atlantic through poleward Atlantic Water heat transport implies the potential decadal predictability of the winter sea ice extent [82,83] and fish stocks [84] in the Barents Sea, although air-sea heat fluxes along the Atlantic Water pathways make such predictions challenging [85].

The West Spitsbergen Current (WSC) carries Atlantic Water through the Fram Strait. A large fraction (approximately 50%) of the Atlantic derived water recirculates in the Fram Strait [86–89] and flows southward as the outer branch of the East Greenland Current [90]. The remaining poleward fraction of the WSC feeds the warm Atlantic Water layer of the Arctic Ocean [47,50,91,92]. Notable increases in both the WSC ocean temperature and ocean volume transport were observed over the past 2 decades [52,93]. These changes resulted in a warming trend in the Arctic Atlantic Water layer [78,94,95] and enhanced winter sea ice decline and ocean surface heat loss north of Svalbard and along the Eurasian continental slope [96–103]. The increasing impact of poleward Atlantic Water heat transport on the Arctic Ocean and sea ice has already been manifested in the progression of Atlantification in the Eurasian Basin and Barents Sea [78,81,104].

Warm water originating from the Irminger Sea circulates around the southern tip of Greenland and propagates northward in the West Greenland Current into Baffin Bay [24,105,106]. An increase in the northward ocean heat transport into Baffin Bay has implications for enhanced melting of marine-terminating glaciers over western Greenland [107–111].

The crucial roles of Arctic–Subarctic ocean transports for climate, weather, and ecosystems warrant sustained observations and improved understanding of their ongoing and future changes. In this paper, we review the past changes in ocean volume, heat, and freshwater transports in Arctic gateways, synthesize the mechanisms driving their variability, and summarize our current knowledge about their possible future changes. Our paper is an update of previous reviews [2,16–18,32,81,112,113] with new observations and new understanding included in the review.

Our review focuses on the Bering Strait, Davis Strait, Fram Strait, and Barents Sea Opening; therefore, in this paper, we define the Arctic Ocean as the ocean area enclosed by these 4 gateways. Note that our definition differs from that of the International Hydrographic Organization, which includes the Nordic Seas in the Arctic Ocean [114].

In section 2, we explain the observational and modeling data used in this study and the way the ocean transports are calculated. In section 3, we review water mass properties and ocean and sea ice transports in the main Arctic Ocean gateways in the past. We examine trends over the past 5 decades, compare the first 2 decades of the 21st century with the last 2 decades of the 20th century, and address recent abnormal changes in the 2010s. For these tasks, we synthesize historical (hindcast) model simulation results and available observations. In section 4, we review current knowledge about mechanisms driving ocean and sea ice transports with corroboration of dedicated numerical simulations. In section 5, we discuss projected changes in Arctic Ocean heat and freshwater budgets using recent climate model simulations. Summaries are given at the end of each section for sections 3, 4, 5. A final discussion is presented in section 6.

2. Materials and Methods

2.1. Observations

To monitor the ocean volume, heat, and freshwater transports in the Arctic gateways, moorings have been deployed and maintained in the main gateways since the 1990s. The instruments and technologies developed to deal with challenges related to acquiring oceanography data near the ocean surface in the ice-hazard zone and measuring current direction at high latitudes were reviewed before [112]. The locations of mooring instruments in the Arctic gateways are depicted in Fig. 1B, which is adopted from [115] and modified to include new instruments that were not used in [115]. The spatial resolution

of the mooring instruments is still relatively low, and some shelf regions are not yet covered by moorings.

Our review focuses on the Bering, Fram, and Davis straits and the Barents Sea Opening, which are indicated by black lines in Fig. 1A. The time series of temperature and salinity in the inflows and outflows in the main Arctic gateways from mooring observations, such as the Pacific Water inflow in the Bering Strait [1,116], Atlantic Water inflow in the Fram Strait [52,117] and Davis Strait [24], and freshwater outflow in the Fram Strait [23,118] and Davis Strait [24], are shown in this paper. For the temperature and salinity in the Atlantic Water in the Norwegian and Barents seas, we utilize the long-term data from onboard measurements in the Svinoy, Bear Island, and Kola sections (locations indicated by dark blue lines in Fig. 1A) [119]. For the discussion of ocean transports in the Arctic gateways, available estimates based on mooring observations are depicted together with model results. In addition, time series of sea ice volume transport in the Fram Strait from satellite observations [25] are presented.

2.2. Model results

Due to limited ocean observations, especially long-term velocity observations covering the full width and depth ranges of the Arctic Ocean gateways, model simulations are often used to complement observations for understanding ocean transport variability and driving mechanisms. We employ the model data from the Ocean Model Intercomparison Project (OMIP [120]), which consist of data from a suite of ocean–sea ice models, each driven by 2 different atmospheric reanalysis fields [121]. The simulations driven by the CORE2 atmospheric forcing [122] belong to OMIP1 with a simulation period of 1948–2009, and those driven by the JRA55-do atmospheric forcing [123] belong to OMIP2 with a simulation period of 1958–2018. The Arctic Ocean simulations in OMIP were evaluated in [124], and we make use of their analyzed multi-model-mean ocean transports. OMIP models can relatively well represent observed variability in Arctic Ocean hydrography and gateway transports, but the simulated mean ocean state displays considerable bias [124], similar to the findings in the previous CORE-II project [125]. As a common practice, using multi-model-mean results can reduce the imprint of extreme biases that might be present in individual models, although common model biases cannot be alleviated with this approach. With 2 sets of simulations, we can check their (in)consistency in representing the Arctic–Subarctic ocean transports.

To present projected future changes in ocean transports through the Arctic gateways, we show the results of volume, freshwater, and heat transports in the Shared Socioeconomic Pathway 585 (SSP585) scenario from the Coupled Model Intercomparison Project phase 6 (CMIP6) models analyzed in recent studies [74,126]. With an additional radiative forcing of 8.5 W/m^2 by 2100, the SSP585 scenario represents the highest CO_2 emission scenario in CMIP6 [127]. To date, this is the most commonly investigated CMIP6 scenario in studies on future changes in Arctic Ocean hydrography and gateway transports [74,126,128,129]. Projected changes in the Arctic freshwater budget in other scenarios investigated in previous studies will also be discussed in comparison with those in the SSP585 scenario.

We examine the mechanisms driving the variability of the Arctic–Subarctic ocean transports by employing new sensitivity simulations using the global multi-resolution ocean–sea ice model FESOM (Finite Element Sea Ice-Ocean Model) [130,131]. We use a version with a regionally high horizontal resolution of 4.5 km in the Arctic and a medium resolution of 24 km in the subpolar region. A set of 3 forced simulations is used to determine the local or remote origin of the variability in ocean transports. One simulation is a historical simulation driven by the JRA55-do atmospheric reanalysis dataset [123]. In the other 2 simulations, the atmospheric reanalysis fields are replaced by a repeating one-year forcing [122] either outside or inside the Arctic. Thus, in the region where the atmospheric forcing is replaced, there is no interannual variability or trend in the applied atmospheric forcing (seasonality is present because the forcing is 6 hourly). The boundaries of the Arctic domain for replacing the forcing are at the Bering Strait (66°N), Davis Strait (66°N), Fram Strait (77°N), and Barents Sea Opening (17°E).

The aforementioned method of applying different atmospheric forcings in different regions has already been successfully used to understand the variability of Arctic–Subarctic ocean transports, such as Atlantic Water heat transport through the Barents Sea Opening [132], Bering Strait throughflow [133], and Davis Strait freshwater export [134]. Different model resolutions and simulation periods were used in the studies mentioned above. In the new simulations presented in this review paper, we use high model resolution (regionally 4.5 km in the Arctic) and a long model integration period of 1958–2019.

To synthesize the mechanisms driving the Atlantic Water inflow and Arctic freshwater export, the model results from a set of FESOM simulations that were described in a previous Arctic study [135] are used here. This set of simulations consists of a control simulation (the same as the historical simulation described above) and 6 wind perturbation experiments. Wind perturbations representing the negative and positive phases of the leading Arctic atmosphere circulation mode (the Arctic Oscillation [136]), the second Arctic atmosphere circulation mode (the Arctic Dipole Anomaly [137]), and the Beaufort High variability [138] are separately added to the wind forcing over the Arctic Ocean in different experiments. The differences in the results between the wind perturbation experiments and the control simulation can elucidate the impact of wind perturbations. We illustrate the impacts of large-scale Arctic winds on Atlantic Water inflow through the Fram Strait and on Arctic freshwater exports through the Fram and Davis straits.

2.3. Definitions of transports

The ocean volume (VT), heat (HT), and freshwater (FWT) transports (that is, horizontal fluxes) through a gateway transect are defined as follows:

$$VT = \iint u_n \, \mathrm{d}z \, \mathrm{d}\ell, \tag{1}$$

$$HT = \iint \rho_o c_p u_n \left(\theta - \theta_{\mathrm{ref}}\right) \mathrm{d}z \, \mathrm{d}\ell, \tag{2}$$

$$FWT = \iint u_n \left(S_{\mathrm{ref}} - S\right) / S_{\mathrm{ref}} \, \mathrm{d}z \, \mathrm{d}\ell, \tag{3}$$

where u_n is the ocean velocity perpendicular to the transect, θ is the potential temperature, θ_{ref} is the reference temperature, S is salinity, S_{ref} is the reference salinity, ρ_o is ocean density, and

c_p is the specific heat capacity of sea water. The integration is over height z from ocean bottom to surface and over distance ℓ along the transect.

As in most Arctic Ocean studies, freshwater transports from models and observations are calculated relative to the reference salinity $S_{\text{ref}} = 34.8$ psu, an estimate of the mean Arctic Ocean salinity [2]. If this is an accurate measure of mean Arctic Ocean salinity, then the freshwater transports can be taken as an indicative measure of how much the gateway exchange freshens/salinizes the Arctic Ocean.

The choice of reference temperature in the calculation of heat transports is less straightforward. In the literature, ocean heat transports are often calculated relative to $\theta_{\text{ref}} = 0^{\circ}\text{C}$, which can then be taken as an indicative measure of how much the gateway exchange increases/decreases the heat content relative to 0°C in a studied domain (in our case, the Arctic Ocean). We follow this practice here to be able to synthesize available data in the literature. Note that with this choice, an outflow with negative volume transport and temperature colder than 0°C has a positive heat transport, which is considered a heat source for the Arctic Ocean. Similarly, an inflow with positive volume transport and a salinity higher than 34.8 has a negative freshwater transport, which is considered a sink for the Arctic Ocean freshwater content.

However, there has been a strong motivation to employ an alternative reference temperature to calculate the heat transport associated with the Bering Strait inflow. Pacific waters leave the Arctic Ocean at around freezing point temperature [139]; therefore, heat transport through the Bering Strait calculated relative to freezing point is a measure of how much heat is lost from the Pacific waters during their transit of the Arctic Ocean [5]. In the literature, estimates of Bering Strait heat transport based on moorings were provided with reference to −1.9°C. As mentioned above, we will discuss heat transports calculated relative to 0°C in this paper, but we will also provide estimates relative to −1.9°C for the observed Bering Strait inflow. In the literature, Bering Strait heat transport based on mooring observations has only been estimated relative to −1.9°C [1]. We recomputed the heat transport relative to 0°C (denoted as HT_0) from the original estimates relative to −1.9°C (denoted as HT_{freezing}):

$$HT_0 = HT_{\text{freezing}} + \rho_o c_p \theta_{\text{freezing}} \cdot VT, \tag{4}$$

where $\theta_{\text{freezing}} = -1.9^{\circ}\text{C}$ and VT is ocean volume transport. The calculated Bering Strait heat transport relative to 0°C is approximately 8 TW lower than that relative to −1.9°C. However, the increase in heat transport from the 1990s to 2000–2018 is approximately 2 TW based on both heat transport definitions (see section 3.1). Throughout the paper, if the reference temperature is not explicitly mentioned in conjunction with heat transports, the heat transports are relative to 0°C.

Freshwater transport in sea ice ($SFWT$) at a given transect is calculated as follows:

$$SFWT = \int u_i h_i \left(\rho_i / \rho_o\right)\left(S_{\text{ref}} - S_i\right) / S_{\text{ref}} \, \mathrm{d}\ell \approx 0.79 \int u_i h_i \, \mathrm{d}\ell, \tag{5}$$

where u_i is the sea ice drift velocity perpendicular to the transect, h_i is the sea ice thickness averaged over each grid cell, $S_i = 4$ is the sea ice salinity, $\rho_i = 910$ kg m^{-3} and $\rho_o = 1{,}024$ kg m^{-3} are the sea ice and ocean density, respectively, and the last integral $\int u_i h_i \, \mathrm{d}\ell$ represents sea ice volume transport. The constants used here are consistent with those used in previous studies [25]

In this paper, we calculate heat and freshwater transports in sections with non-zero mass transport. Previous studies have highlighted the need for caution when interpreting ocean heat and freshwater transports [140–142]. As heat transports depend on the chosen reference temperature, they are ambiguous to interpret physically without additional information about ocean temperature and volume transports. For example, consider a single gateway section with a non-zero mass transport, such as the Bering Strait. The heat transport values vary with the reference temperature, so without further contextual qualification, the following heat transport quantities are ambiguous (meaning they depend on the reference temperature used): record (high or low) values, changes over time, importance relative to another gateway, and attribution of changes to volume transport change or temperature change [141,142]. To make the heat transports physically interpretable, examples of further qualifications are as follows: (i) Assumptions or information about the heat and volume transports across other gateways. Such assumptions allow the construction of a control volume with zero net volume transport, for instance. The dependence on the reference temperature disappears for a control volume with zero net volume transport. (ii) Assumptions about the subsequent fate of the water flowing through the gateway, such as how it mixes with other water masses or interacts with sea ice. It is also legitimate to compare heat transport across an open gateway between observations and ocean model results (using the same reference temperature). Assessing model realism this way requires caution, however, because such agreement between model results and observations can be coincidental and specious. A stronger test of model realism requires agreement between model results and observations for any reference value, not just one. Satisfying this test means that both the volume transport and the relationship between velocity and temperature are realistic; the same is true for freshwater transport. A robust comparison requires inclusion of volume transport, salinities, and temperatures. The above factors should be considered when assessing the heat and freshwater transports across gateways with non-zero volume transport. We repeat here that our choices of reference salinity and temperature in this paper are not arbitrary, as described above in this section.

3. Historical changes

3.1. Pacific Water inflow

Mooring observations of temperature, salinity, and currents for the Pacific inflow in the Bering Strait have been carried out since the 1990s [1,54]. Over the observation period, the Pacific inflow displayed a warming trend of approximately 0.5 ± 0.2°C per decade, with the annual warm (≥0°C) water duration increasing from 5.5 months in the 1990s to more than 7 months in recent years, mainly due to earlier warming; it also experienced a dramatic wintertime freshening (salinity decrease of 0.3 per decade), implying changes to the ventilation of the Arctic's cold halocline [1]. The warming and freshening trends in the observation period were enhanced due to increased warming and freshening since the mid-2010s (Fig. 2A and E).

The FESOM simulation reproduced the observed variability in the Pacific inflow temperature and salinity well, except for the strongest freshening event in 2016 (Fig. 2A and E;

model-observation correlation coefficients are shown on the plots). It was speculated that the freshening could be partially attributed to glacial melt over mainland Alaska [1,143]. The absence of this freshening event in the model might be because changes in glacial melt were not adequately accounted for in the runoff data set used to drive the model. However, the overall good skill of the model may allow us to better understand hydrography changes in long periods without observations. The model shows that the Pacific inflow experienced a significant warming trend of $0.13 \pm 0.03^{\circ}$C per decade over the past 5 decades (Fig. 2A) and no significant trend in salinity (Fig. 2E). The model suggests that there were warming events in the 1970s and 1990s, which were characterized by interannual to multi-year variability superimposed on a persistent warming trend. The model also shows that at the end of the 2010s the temperature and salinity changed and approached prior values. However, with the currently available observations (until 2018), we still cannot tell whether this reversion is reflected in the real world.

Mooring data show that the Pacific Water volume transport displayed a significant upward trend of 0.10 ± 0.06 Sv per decade in the observation period of 1990–2019 [1]. Averaged from 2000 to 2018, the observed volume transport was 1 ± 0.1 Sv, 0.2 Sv higher than the climatological value of 0.8 ± 0.2 Sv [3]. The Bering Strait freshwater transport continues to account for about one-third of the Arctic total freshwater input and displays an interannual variability of about 1,000 km^3, greater than the variability of any other Arctic freshwater source [144]. Averaged from 2000 to 2018, the freshwater transport based on mooring observations was $3{,}000 \pm 280$ km^3/year, higher than the early mooring observations of $2{,}500 \pm 300$ km^3/year [1]. For heat transport, the mean value for 2000–2018 was 14 ± 4 TW (relative to -1.9°C; 6 TW relative to 0°C), which is higher than the estimate of 12 ± 4 TW (relative to -1.9°C; 4 TW relative to 0°C) for the earlier period [1].

It is challenging to use the OMIP simulations to synthesize the Bering Strait ocean transports, because they did not reproduce the observed upward trends, although the interannual variability was well represented (Fig. 3A). The correlation coefficient between the observed and OMIP2-simulated annual mean volume transports for 2000–2018 is 0.85 ($P < 0.01$; after detrending). Not only does the simulated volume transport fail to reflect the observed increase during 2000–2018, but it is also even lower in the 2010s compared to the simulated long-term mean. The simulations also did not reproduce the observed upward trends in heat and freshwater transports in the observation period (since the 1990s; Fig. 3E and I) because volume transport makes a considerable contribution to these changes [1]. It is not clear whether the model bias is mainly due to deficiencies in atmospheric forcing, runoff data, or model configurations. It is interesting that in the common period of OMIP1 and OMIP2 (1958–2009), the 2 sets of OMIP simulations are nearly identical in their simulated Bering Strait volume, heat, and freshwater transports, although the models were forced with different atmospheric reanalysis products (Fig. 3A, E, and I). Similarly, a long coarse-resolution simulation driven by a 20th century atmosphere reanalysis product showed that the modeled Bering Strait volume transport remained close to 0.8 Sv through the 20th century [145]. However, without observations, we cannot judge the reliability of model simulations for the 20th century, especially considering that they cannot simulate the observed trend in the early 21st century. It is also noteworthy that the simulated interannual variability is weaker than the observed (Fig. 3A, E, and I), possibly due to the low resolutions of the ocean models and the applied atmospheric forcing as well.

3.2. Atlantic Water inflow

The Atlantic Water enters the Nordic Seas mainly across the Iceland–Scotland–Ridge [54,146–148] and passes through the Norwegian Sea before reaching the Barents Sea and Fram Strait [51,54]. Poleward propagation of warming and cooling episodes along the Atlantic Water pathway through the Norwegian Sea was observed [149] and reproduced in model simulations [92,150]. The Atlantic Ocean influences the Arctic Ocean through ocean transports, and the impact could even be seen in the multidecadal variability of the Arctic Ocean temperature [151,152]. We first review the past changes in the Atlantic Water in the Norwegian Sea region, which underpins later discussions of the Atlantic Water inflow in the Barents Sea Opening and Fram Strait.

3.2.1. Norwegian Sea inflow

The Atlantic Water at the Svinoy Section, which is close to the southern end of the Norwegian Atlantic Current (see Fig. 1A for location), experienced a warming trend after the 1970s according to the observations [51,149] (Fig. 2B, upper panel). The warming trend lasted until the mid-2000s [153], followed by a cooling trend (Fig. 2B, upper panel). Until 2020, the temperature at the Svinoy Section dropped to a level close to that in the mid-1990s, so there was no significant temperature trend if only considering the relatively short period of 1995–2020 with mooring observations [154]. However, considering the last 5 decades, there was a mean warming trend of about $0.20 \pm 0.03^{\circ}$C/decade in the upper ocean at the Svinoy Section in the observations, and the FESOM results displayed a similar trend (Fig. 2B). Despite the low temperature of the Atlantic inflow in the 2010s, the total ocean heat content in the Norwegian Sea has increased because of the reduction in ocean surface heat loss [155].

The annual mean salinity in the Atlantic inflow at the Svinoy Section is highly correlated with the annual mean temperature ($r = 0.71$, $P < 0.01$ without a time lag), with warming (cooling) episodes coinciding with salinification (freshening) episodes (Fig. 2B and F, upper panels). Following a salinification trend between the 1970s and the mid-2000s, the salinity of the Atlantic inflow dropped in the 2010s. The Norwegian Sea displayed a freshening anomaly in the 2010s, mainly due to the freshening of the Atlantic inflow; therefore, it experienced a decoupling of temperature and salinity, with simultaneous warming (due to reduced heat loss to the atmosphere) and freshening [155]. Considering the last 5 decades, the observed salinity trend was not significant at the Svinoy Section (Fig. 2F).

Systematic monitoring of volume transport has been established between Greenland and Scotland since the mid-1990s. Over this period, the Atlantic Water volume transport into the Norwegian Sea did not display a significant trend [54]. The recent estimates of mean poleward Atlantic Water volume transport between Greenland and Scotland are 8.0 ± 0.7 Sv [54] and 7.7 ± 0.8 Sv [156], which are not very different from the previous estimate of 7.6 Sv for the Svinoy Section [157]. Based on mooring observations and an inverse model, the Atlantic Water heat transport across the Iceland–Faroe–Scotland Ridge averaged over 1993–2016 was estimated to be 281 ± 24 TW [158]. A similar value of 273 ± 27 TW

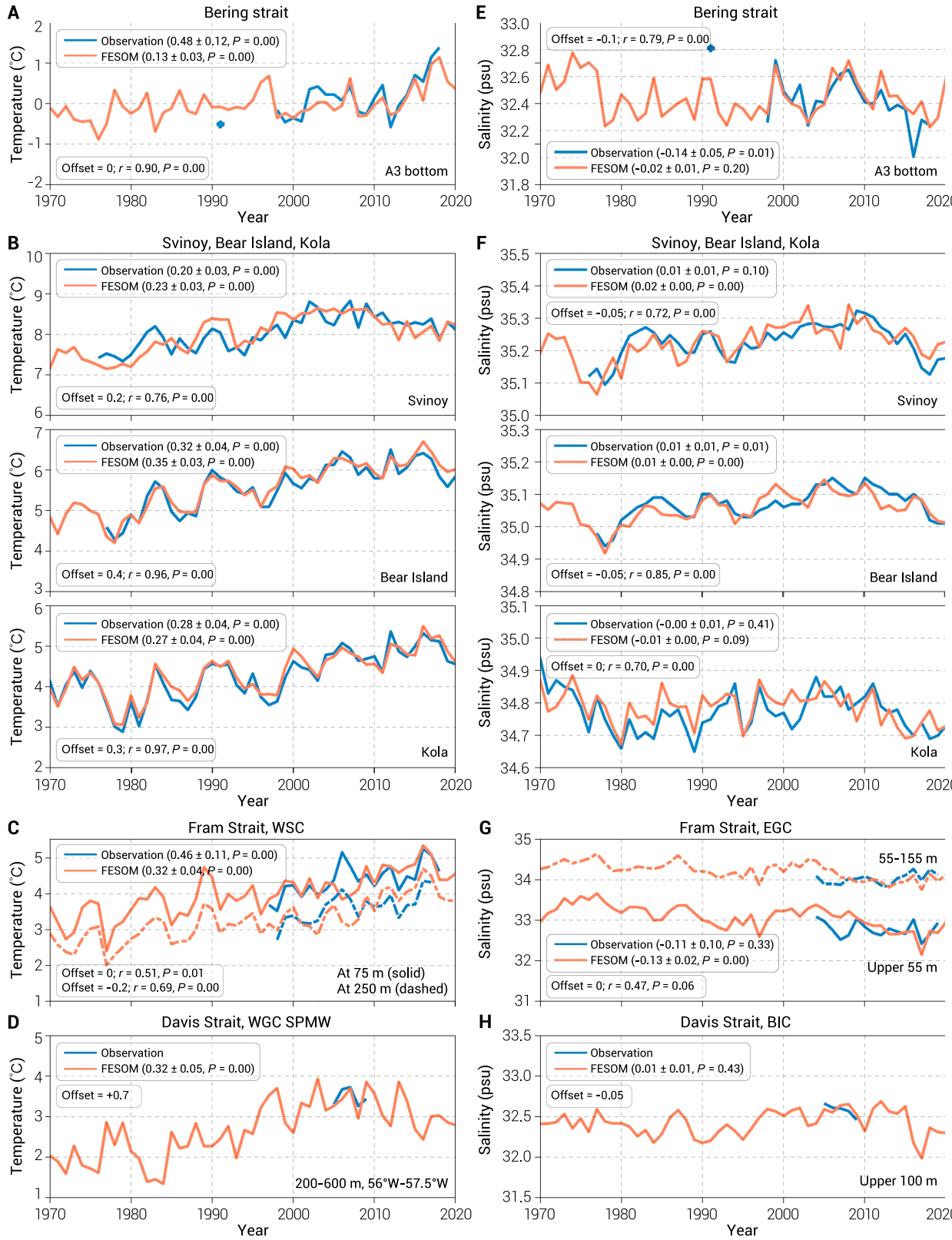

Fig. 2. Annual mean (left) potential temperature and (right) salinity. (A and E) Temperature and salinity at the bottom of the Bering Strait. (B and F) Temperature and salinity at 50 to 200 m in the Svinoy, Bear Island, and Kola sections (from top to bottom). (C) Temperature at 75 m (solid) and 250 m (dashed) depths in the core of the West Spitsbergen Current in the Fram Strait. (G) Salinity in the upper 55 m (solid) and 55 to 155 m (dashed) depths in the East Greenland Current in the Fram Strait. (D) Temperature of the Subpolar Mode Water in the West Greenland Current in the Davis Strait. (H) Salinity in the upper 100 m in the Baffin Island Current in the Davis Strait. Observations are in blue, and FESOM simulated results are in red (see section 2 for data references and descriptions). The offsets added to the model results for plotting are indicated in the panels. The correlation coefficients between the observations and model results are indicated with *r*. In legends, the linear trends over the periods of the model (1970 to 2020) and the observations (variable, see the length of blue lines) are cited.

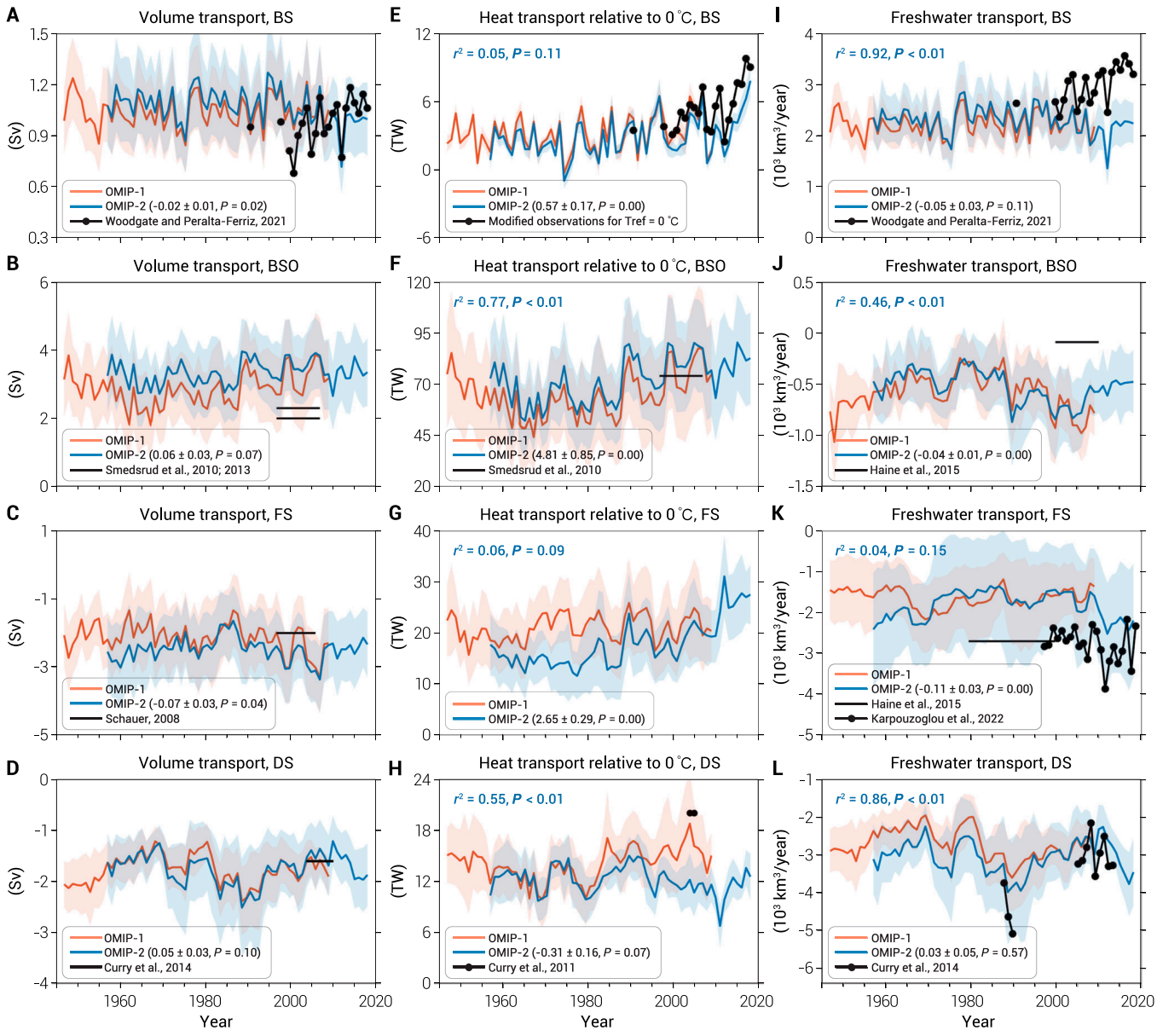

Fig. 3. Simulated annual mean ocean volume transport (A to D), heat transport (E to H, relative to 0°C), and freshwater transport (I to L, relative to 34.8) in OMIP1 (red) and OMIP2 (blue) models. From top to bottom: Bering Strait (BS), Barents Sea Opening (BSO), Fram Strait (FS), and Davis Strait (DS). The multi-model-mean results are given together with model spreads as background shading. The linear trends of the OMIP2 results from 1970–2018 are shown in the legends. r^2 values in the middle and right columns indicate the coefficient of determination between ocean volume transport and the corresponding heat/freshwater transport in OMIP2. Available observations are also shown. Note that the observed Bering Strait heat transport was modified from the original data by changing the reference temperature to 0°C, and the original Bering Strait heat transports relative to −1.9°C are approximately 8 TW higher than the numbers presented here. Positive values indicate inflows to the Arctic Ocean. The model data used in this figure are described by Shu et al. [124].

was obtained using shipboard velocity and temperature measurements along the ridge between 2009 and 2016 [159].

It was estimated that the ocean heat transport across the Iceland–Faroe–Scotland Ridge increased by 21 TW after 2001 [158]. However, when considering the period of 1995–2020, the ocean heat transport does not exhibit a significant trend due to the cooling of the Atlantic inflow after the mid-2000s [154]. Based on a model simulation, Smedsrud et al. [113] suggested that the poleward Atlantic Water volume transport and heat transport across the Iceland–Faroe–Scotland Ridge increased by 1 Sv and 50 TW, respectively, over the 20th century. Therefore, the insignificance of the trends in Atlantic volume and heat inflows into the Norwegian Sea in the short observation period might be due to masking by decadal and multidecadal variability. The presence of strong multidecadal variability was evident in the century-long temperature observations at the Svinoy Section: The Atlantic Water at the Svinoy Section experienced a few warm decades before a strong cooling in the 1970s [145,149].

3.2.2. Barents Sea Opening

The observed temperature and salinity in the Atlantic Water inflow at the Barents Sea Opening (the Bear Island Section) are significantly correlated with those at the Svinoy Section (Fig. 2B and F) [51,160,161]. For the observed annual mean

temperature, the correlation between the Barents Sea Opening and Svinoy Section is r= 0.74, 0.73, and 0.68 ($P < 0.01$) for 0-, 1-, and 2-year lags, respectively, but the correlation strongly decreases for the detrended time series, with r= 0.49, 0.44, and 0.31 ($P < 0.05$) for 0-, 1-, and 2-year lags, respectively. The correlation for the observed annual mean salinity between the 2 transects is r= 0.81, 0.88, and 0.79 ($P < 0.01$) for 0-, 1-, and 2-year lags, and the correlation coefficients do not change much if the time series are detrended. The fact that the temperature correlation between the 2 transects becomes much lower when the time series are detrended reflects the strong impacts of surface heat loss along the Atlantic Water pathway on ocean temperature and water mass transformation, which were demonstrated in different studies (e.g., [155,161,162]). The salinity correlation coefficients indicate an advection timescale of approximately 1 year between the 2 transects. Our updated analysis is somewhat in contrast to earlier studies that reported a lag of 1 to 2 years in temperature anomalies from the Svinoy Section to the Barents Sea Opening [51,160].

A cooling anomaly started in the late 2000s at the Svinoy Section, while cooling was visible only in the second half of the 2010s at the Barents Sea Opening and was not obvious at the Kola Section in the 2010s (Fig. 2B). This further demonstrates the effect of atmospheric modulation on the Atlantic Water temperature along its pathway. The salinity at the Barents Sea Opening dropped by about 0.15 in the 2010s, similar to the change at the Svinoy Section, but with a lag of approximately 1 year (Fig. 2F). The signal of salinity decline further propagated to the Kola Section, although the overall salinity correlation between the Barents Sea Opening and Kola Section is not very high ($r = 0.59$, $P < 0.01$), possibly due to the entrainment of freshwater in the southern Barents Sea. Considering the past 5 decades, the warming trend in the Atlantic Water inflow at the Barents Sea Opening was 0.32 ± 0.04°C per decade based on the observations, and the model simulation obtained a similar trend. The trend of the Atlantic Water salinity at the Barents Sea Opening over the past 5 decades was small (approximately 0.01 ± 0.01 per decade), similar to that found in the Svinoy Section.

Mooring observations of ocean currents in the Atlantic Water inflow at the Barents Sea Opening have been maintained since 1997 [162]. The Atlantic Water volume transport, about 2 Sv, did not display a significant trend in the mooring observation period [69]. Combining the Atlantic Water inflow, the Norwegian Coastal Current along the southern continental slope, and the recirculation flow in the northern Barents Sea Opening, the net ocean volume transport through the Barents Sea Opening was estimated to be 2.3 Sv [53]. The OMIP2 simulations show that the net ocean volume transport was slightly lower in the 2010s than in the 2000s, and the mean over 2000–2018 was slightly higher (by 0.1 Sv) than that over 1980–2000 (Fig. 3B). Considering the past 5 decades, there was a small but statistically significant upward trend of 0.06 ± 0.03 Sv per decade in the OMIP2 simulations, which can be mostly attributed to an increase at the end of the 1980s.

The OMIP2 simulations show that the net heat transport through the Barents Sea Opening displayed a pronounced drop in 2010 (Fig. 3F), mainly due to the reduction in ocean volume transport (Fig. 3B). After this event, the heat transport was restored to the level in the 2000s. On average, the heat transports in the 2010s and 2000s were similar, so the earlier synthesized net heat transport of 70 ± 5 TW [53] can be used to represent the mean state over the past 2 decades. The mean heat transport (relative to 0°C) in 2000–2018 was about 13% higher than that in 1980–2000 in OMIP2. Over the past 5 decades, the heat transport has displayed a significant upward trend of 4.81 ± 0.85 TW per decade in OMIP2.

The Atlantic Water salinity is higher than the Arctic mean salinity, so the Atlantic Water inflow through the Barents Sea Opening is equivalent to a freshwater sink of the Arctic Ocean [16], outweighing the freshwater source of the Norwegian Coastal Current, which carries freshwater originating from the North and Baltic seas into the Barents Sea [163]. The synthesized freshwater transport through the Barents Sea Opening is −90 km^3/year [16,32]. The OMIP simulations considerably overestimate this transport strength (Fig. 3J), as did the simulations in an earlier model intercomparison project [125]. One reason could be that low-resolution models cannot well represent the fresh coastal current [58,164]. The simulated freshwater transport in 2000–2018 was about 17% stronger than that in 1980–2000 in OMIP2.

Observations indicate that in the 20th century, the Barents Sea branch of Atlantic Water inflow lost most of its heat to the atmosphere during its transit through the Barents Sea [53,165], and most of the Atlantic Water flowing into the Arctic basin via the St. Anna Trough was already cooled to below 0°C [165]. However, during the first 2 decades of the 21st century, the efficiency of ocean heat loss in the southern Barents Sea has decreased, causing the outflow water from the Barents Sea to be warmer [69]. A reduction in ocean surface heat loss in the upstream region of the Atlantic Water inflow can cause ocean warming, winter sea ice retreat, and increases in the surface mixed layer depth and ocean surface heat loss in the downstream region along the Atlantic Water pathway [70]. This process changes the role of the Barents Sea branch, resulting in a poleward expansion of Arctic Atlantification in the Arctic basin [70].

3.2.3. Fram Strait

Since 1997, a mooring array at approximately 78°50′ to 79°N in the Fram Strait has been maintained to obtain year-round measurements of ocean currents and hydrography in both the WSC and East Greenland Current [22,23,50,52,87,117,118]. A strong warming trend in the WSC was found in the mooring observation period [52,93]. The warming trend at 75 m depth in the core of the WSC (east of 8°E) was 0.46 ± 0.11°C per decade between 1997 and 2018, and the trend at a depth of 250 m was similar (Fig. 2C). The model simulation reproduced the observed warming trend and interannual variability well, except for the warm anomaly in 2006 (Fig. 2C). The warming and cooling episodes largely coincided with those at the Svinoy Section before 2000. Then, the Atlantic Water experienced 2 strong warming episodes (which peaked in 2006 and 2016) in the Fram Strait, but they were absent at the Svinoy Section (Fig. 2B and C). The Atlantic Water temperature in the Fram Strait reached its highest value over the past 5 decades in 2016 (Fig. 2C). The simulated warming trend at a depth of 75 m in the core of the WSC was also significant (0.32 ± 0.04°C per decade) over the past 5 decades.

The northward volume transport of warm Atlantic Water (warmer than 2°C) in the WSC was estimated to be 3.0 ± 0.2 Sv for 1997–2010 using the mooring observations at 78°50′N [52]. Despite the observed warming trend during this period, the volume transport of Atlantic Water did not display a significant

trend [52]. Model simulations showed that the volume transport of warm Atlantic Water in the WSC was approximately 3 Sv in the 2000s, while it increased by about 1 Sv in the 2010s [93]. The annual mean northward heat transport of the Atlantic Water was estimated to vary between 26 and 50 TW in 2001–2006 based on a stream-tube approach [50]. As both the Atlantic Water temperature (Fig. 2C) and poleward volume transport increased in the 2010s [93,166], northward heat transport increased.

Both observations and model simulations show that part of the warm Atlantic Water recirculates near and north of the mooring array at 78°50′N [89,167,168]. Model simulations reveal that more than 1.5 Sv warm Atlantic Water propagates westward in the Fram Strait, half of which occurs north of 78°50′N [167]. Therefore, a fraction of northward ocean heat transport measured in the WSC returns south again with the East Greenland Current. To estimate the net meridional ocean heat transport through the Fram Strait, the full-width mooring array at 78°50′N (between 6°51′W and 8°40′E) was used. The net heat transport into the Arctic Ocean across this mooring array was estimated to vary between 16 ± 12 and 41 ± 5 TW in 1997–2000 [87], indicating large interannual variability. The Fram Strait net heat transports in the 2 sets of OMIP simulations have similar interannual variability but different magnitudes and trends (Fig. 3G). In OMIP2 simulations, the heat transport in the 1990s was larger than that in the 1970s and 1980s, consistent with the observed warming of the Arctic Atlantic Water layer in the 1990s [169]. The heat transport in OMIP2 continued to increase after 2010 (Fig. 3G), consistent with the results of previous modeling studies [93]. It had a significant trend of 2.65 ± 0.29 TW per decade over the past 5 decades and was 27% higher in 2000–2018 than in 1980–2000 when computed relative to 0°C.

The Fram Strait branch of Atlantic Water inflow directly supplies the warm Atlantic Water layer of the Arctic Ocean. The increase in ocean heat transport in the 2000s and 2010s can partly explain the eastward retreat of the winter sea ice edge northeast Svalbard [102] and contribute to winter sea ice decline in the western Nansen Basin [98]. However, storm-induced ocean mixing is needed in addition to explain recent sea ice melt rates north of Svalbard [100]. The observed warming trend of the Arctic Atlantic Water layer [94,104,169] was accompanied by the weakening of the halocline stratification in the eastern Eurasian Basin and Makarov Basin, which is an indication of Arctic Atlantification [78,104,170,171]. The recent increase in Atlantic Water volume transport through the Fram Strait also implies that an increased amount of nutrients could have been advected into the Arctic basin, with possible impacts on the Arctic marine ecosystem [172]. Increases in the presence and temperature of Atlantic Water since the early 2000s have been observed on the northeast Greenland continental shelf [173], indicating that the signal of Atlantic Water changes observed at the Fram Strait has propagated southward via the Return Atlantic Current.

3.2.4. Davis Strait

The cold, fresh Arctic waters exported through the CAA flow southward in the Baffin Island Current along the western Baffin Bay. On the eastern side of the Davis Strait, low-salinity water of Arctic origin and warm, salty water of North Atlantic origin flow northward into the Baffin Bay. These inflowing waters, after being modified during their cyclonic circulation in the Baffin Bay, join the Baffin Island Current and flow southward in the western Davis Strait. The climatological net volume transport through the Davis Strait is southward and carries freshwater toward the subpolar North Atlantic (see section 3.3). The net heat transport through the Davis Strait is northward, mainly due to the West Greenland Irminger Water (also called Subpolar Mode Water or simply Atlantic origin water) in the eastern Davis Strait [174].

The temperature of the Subpolar Mode Water in the eastern Davis Strait displayed an upward trend of 0.32 ± 0.05°C per decade from 1970 to 2020 in the FESOM simulation (Fig. 2D). A cooling trend occurred in the 2010s, which is consistent with the cooling of the subpolar North Atlantic in this period (see section 4.2.1). The observed net heat transport across Davis Strait was 18 ± 17 TW in 1987–1990 [21] and 20 ± 9 TW in 2004–2005 [174]. In the OMIP2 simulations, the heat transport was 10% lower in 2000–2018 than in 1980–2000, but did not have a statistically significant trend over the past 5 decades (Fig. 3H). The recent reduction in the heat transport can be explained by the inflow cooling in the 2010s (Fig. 2D), and this trend is consistent with the results of a high-resolution regional model that showed a decadal decline in the heat transport between 2005 and 2013 [175].

The net ocean volume transport in Davis Strait and Nares Strait reversed direction (becoming poleward) in a few months at the end of 2010 [175]. This event was unusual and resulted in a reduction in the annual mean ocean volume export in 2010 as shown in OMIP2 (Fig. 3D). Associated with this event, the northward heat transport in the West Greenland Current over the past 5 decades was the highest in 2010, but the net heat transport through the whole Davis Strait was not very high in 2010 due to the compensation of increased southward heat transport in the western Davis Strait in this year (model result not shown).

3.3. Arctic freshwater export

3.3.1. Fram Strait

Year-round salinity and velocity measurements in the East Greenland Current were obtained from the Fram Strait Arctic Outflow mooring array at 78°50′N during the past 2 decades [23,118]. The mooring array covers the outer shelf and continental slope (between 8°W and 2°W) but not the inner shelf where the ocean salinity is the lowest and where there is little knowledge of the year-round flow (Fig. 1B). The mooring observations revealed that the near-surface part of the Polar Water became fresher in the 2010s than in 2004–2009 (by 0.10 in the upper 55 m), while the halocline water experienced an increase in salinity (by 0.09 in 55 to 155 m depth) [118]. The observed salinity in the upper 55 m exhibited a (statistically insignificant) trend of −0.11 ± 0.10 per decade between 2004 and 2019 (Fig. 2G). The model simulation results show consistent interannual variability, with a significant freshening trend of −0.13 ± 0.02 per decade in the upper 55 m in 1970–2020 (Fig. 2G, solid lines). The observed increase in halocline salinity after 2015 was not reproduced (Fig. 2G, dashed lines). The magnitude of the observed halocline salinification in the 2010s (by 0.09) is within the range of simulated decadal variability in the past few decades.

It is challenging to estimate net ocean volume transport through the Fram Strait using available mooring observations because of the partial coverage of the mooring array and the relatively low spatial resolution. The observational estimate for

1997–2007 is an outflow of −2 ± 2.7 Sv with a large uncertainty [50]. The Fram Strait ocean volume transport in 2000–2018 was stronger by −0.3 Sv than that in 1980–2000 in the OMIP2 simulations (Fig. 3C).

An increase in Fram Strait freshwater export was observed in 2010–2013 compared to that in the 2000s, mainly due to a stronger East Greenland Current and secondly freshening anomalies [23]. After 2015, the freshwater export was observed to decrease to the prior-2010 level, mainly due to the slowdown of the East Greenland Current [118]. A considerable fraction of the freshwater export occurs in the inner shelf, which is not covered by mooring observations [22]. A recent study based on all available observational data including dynamic ocean topography reported a large seasonality in the freshwater transport on the shelf and that the shelf region accounts for more than 40% of the total freshwater transport in the shelf-slope system of the western Fram Strait [176].

The total freshwater transport across the whole Fram Strait in the OMIP simulations is depicted in Fig. 3K. The transports in OMIP1 and OMIP2 display similar interannual variability, especially for the 1990s and 2000s (Fig. 3K). The simulations show a moderate increase in freshwater export in 2005–2007 and a strong increase in 2010–2013, consistent with the changes observed by the moorings (Fig. 3K; [23]). As the transports calculated from the model results are for the whole Fram Strait, the consistency of the variability between the models and observations implies that the freshwater export in the East Greenland Current determines the overall variability of the freshwater transport in the Fram Strait. A reduction in freshwater export after 2013 was simulated but not as pronounced as observed. Overall, the simulated variability of the freshwater export is largely consistent with the mooring observations, while the simulated mean freshwater export is biased weak compared with the synthesized climatological value (−2,700 ± 530 km^3/year [16,32]) and the mooring observations (Fig. 3K). In the OMIP2 simulations, the Fram Strait freshwater export was 20% stronger in 2000–2018 than in 1980–2000. It had a strengthening trend of −110 ± 30 km^3/year per decade over the past 5 decades (calculated relative to 34.8; Fig. 3K).

3.3.2. Davis Strait

The freshwater export in the upper Baffin Island Current is mainly composed of Arctic waters, with other contributions including river runoff in Baffin Bay and CAA and glacial meltwater. A short salinity time series in the upper Baffin Island Current (the part west of 59°W) obtained with moored instruments in the Davis Strait shows a decline from 2004 to 2010 [24], which is consistently simulated by the model (Fig. 2H). The model simulations show that there was no significant salinity trend in the upper Baffin Island Current over the past 5 decades. However, an abnormal salinity reduction of about 0.5 occurred in 2016 and 2017 as shown by the simulation (Fig. 2H), coinciding with an enhanced ocean volume export through the CAA driven by the dynamic sea-level drop south of Greenland in that period [134]. The contemporary salinity drop in both the East Greenland Current and Baffin Island Current in 2017 (Fig. 2G and H) reflects the impact of the Arctic cyclonic wind in favor of Arctic freshwater export [134].

The net ocean volume transport and freshwater transport through the whole Davis Strait are −1.6 ± 0.5 Sv and −2,900 ± 190 km^3/year, respectively, based on the 2004–2010 observations [24]. Compared with the observed freshwater export at the end of the 1980s, which was first described by Cuny et al. [21], the freshwater export in 2004–2010 is markedly weaker [24]. The 2 sets of OMIP simulations display very similar variability in the Davis Strait volume and freshwater exports, and consistently represent the observed weakening between the 2 observation periods mentioned above (Fig. 3D and L). Based on analysis of 7 decades of hydrography surveys, it was suggested that high freshwater transport occurred on the Labrador Shelf (downstream Davis Strait) during the 1970s–1980s and low transport occurred in the 1960s and from the mid-1990s to 2016 [177]. Although the decadal variability at this downstream location is impacted by outflow from Hudson Bay, it remains consistent with the simulated variability in Davis Strait obtained in the OMIP simulations. A recent model study revealed that the Arctic Ocean volume and freshwater export through the Davis Strait dramatically strengthened in 2015–2017 [134], as also shown by the OMIP2 simulations (Fig. 3D and L). The freshwater export in this period increased to a level similar to that at the end of the 1980s in the simulations (Fig. 3L).

In the OMIP2 simulations, the mean freshwater transport through the Davis Strait is close to the synthesized climatological value (−3,200 ± 320 km^3/year [16]). The simulated freshwater export in 2000–2018 was 13% weaker than that in 1980–2000 (calculated relative to the reference salinity of 34.8), and the net ocean volume export in 2000–2018 was weaker by 0.3 Sv than in 1980–2000. However, as mentioned in section 3.1, the models did not reproduce the observed increase in Pacific Water inflow. If we add the missing Pacific freshwater to the Davis Strait outflow, the Davis Strait freshwater export is then very similar between the periods of 2000–2020 and 1980–2000 (see section 3.4 for details). Considering the past 5 decades, there were no significant trends in the simulated Davis Strait volume and freshwater transports.

3.3.3. Sea ice export

Sea ice in the Fram Strait has been thinning over the last few decades. Its annual mean thickness declined by 15% per decade (in total about 35%) from 1990 to 2014 [25,178]. Sea ice thickness at the end of the melt season decreased by more than 50% (at a reduction rate of 0.2 m/year) from 2003 to 2012 at 79°N [179] and by 20% from 2001 to 2020 further north (80.5 to 86°N) [180]. Despite a slight increase in sea ice drift, the strong sea ice thinning caused a considerable decline in sea ice volume export through the Fram Strait over the past decades [25,181]. Strong interannual and decadal variability can mask the declining trend if only a short time period is considered. Spreen et al. [182] reported that the sea ice volume export between 2003 and 2008 was lower than that previously observed in the 1990s [183,184], but the reduction was not statistically significant. Based on sea ice thickness from Upward Looking Sonars (ULS) and satellite observations of sea ice drift and area for the period of 1992–2014, a significant decrease of 648 ± 14 km^3/year per decade in the Fram Strait sea ice volume export, equivalent to a decrease of 27 ± 2% per decade, was found [25].

A record low annual mean sea ice volume export through the Fram Strait occurred in 2018 (or 2017/2018 for winter-centered annual mean), as revealed by a model simulation corroborated by satellite observations and reanalysis of sea ice thickness and drift (Fig. 4A) [181]. The positive sea-level pressure anomaly

over the Eurasian Arctic in this year tended to reduce sea ice thickness and drift in the Fram Strait, but model sensitivity experiments revealed that it was the persistent sea ice thinning that preconditioned this event of anomalously low sea ice volume export (Fig. 4B) [181]. This low ice export was further confirmed using a combination of in situ ice draft measurements from the ULS combined with satellite observations [185]. The reduction in sea ice volume export in 2018 amounted to 40% relative to that in the period of 2000–2017 [185].

The previously synthesized sea ice freshwater transport through the Fram Strait is −2,300 ± 340 km^3/year [16], which was based on the observed sea ice volume transport of −2,850 km^3/year in 1990–1996 [183]. This freshwater transport represents the mean condition for 1980–2000 [32]. Observational estimates of annual sea ice volume transport are missing for several years between 2000 and 2020, but a linear regression can reasonably represent the changes in the observed sea ice volume transport [25], from which we estimate the mean sea ice volume transport for 2000–2020 to be −2,000 ± 640 km^3/year. This is equivalent to a freshwater transport (in the form of sea ice) of −1,600 ± 510 km^3/year.

Sea ice is also exported southward through the Davis Strait. Sea ice freshwater transport was estimated to be −420 km^3/year at the end of the 1980s [21], about −400 to −600 km^3/year for 2002–2007 [186], and −320 ± 32 km^3/year for 2004–2010 [24]. A recent estimate was −250 ± 60 km^3/year for 2011–2016 based on an ensemble of different observations and model simulations [187]. The decline in sea ice export through the Davis Strait during the observation period is consistent with the results of a suite of ocean–sea ice models assessed previously [188]. It was shown that the sea ice freshwater export through the Davis Strait had decadal variability with a magnitude of about 200 km^3/year over the past few decades and a decreasing trend starting from the 1990s [188].

The sea ice volume transport into the Arctic Ocean through the Bering Strait remained limited (about 100 km^3/year northward [4,188]), although this rate is currently poorly constrained [189].

3.4. Summary of past changes

Based on the above review, we synthesize the ocean transports in the 4 Arctic Ocean gateways for 2000–2020 (Table 1). Observational estimates for Bering Strait transports are available and adopted directly. For ocean volume transports through other gateways, we first computed the difference between 2000–2018 and 1980–2000 simulated in OMIP2 models (shown in the left column of the 2000–2020 period in Table 1). As the Bering Strait volume transport was observed to be 1.0 ± 0.1 Sv in 2000–2020, 0.2 Sv higher than in 1980–2000, while the OMIP2 simulated volume transport is lower by 0.1 Sv in 2000–2018 than in 1980–2000, a total export of 0.3 Sv should be added to the Fram and Davis straits to correct the model data. An estimate based on summer observations between 1998 and 2011 shows that on average one-third of the Pacific Water is exported through the Fram Strait (but highly variable in time) [190]. We divided the 0.3 Sv export according to this fraction between the 2 export gateways , and obtained the final estimates (shown in the right column of the 2000–2020 period in Table 1). [Note that the partitioning of the Pacific Water exports between the 2 gateways was based on 6 hydrographic surveys between June and September [190,191], so there is uncertainty in using this information to determine the partition of the Pacific Water transports that are not obtained in the simulations. We adopt this observational estimate and consider 1/2 − 1/3 = 1/6 of the 0.3 Sv total volume transport and 700 km^3/year total freshwater export as the error range. As the uncertainty of the unadjusted values is already large, the uncertainty of our correction method does not change the overall uncertainty much. Overall, the correction to model data is a poor-man's approximation and is needed just because of insufficient model accuracy and the lack of direct observational

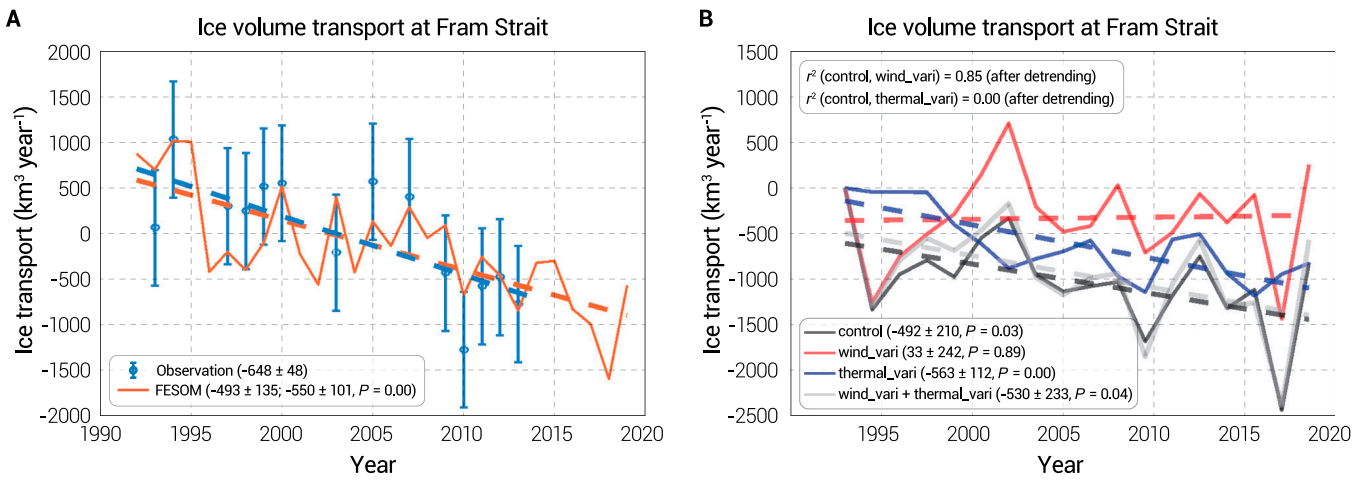

Fig. 4. (A) Anomaly of annual mean sea ice volume transport in the Fram Strait: Observations in blue and FESOM historical simulation in red. The dashed lines depict the linear fit, with the trends shown in the legend. The trends in the model are calculated for the period of available observations and for the whole illustrated period as well. (B) Winter-centered annual mean sea ice volume transport in the Fram Strait in FESOM simulations: (black) control (historical) simulation; (red) sensitivity simulation in which winds have interannual variability, but Arctic thermal forcing is climatology; (blue) sensitivity simulation in which thermal forcing has interannual variability, but Arctic winds are climatology; (gray) sum of the red and blue lines. The anomalies relative to the first year are shown. The dashed lines depict the linear fit, and the trends are shown in the legend. The fractions of the variance in the control simulation that can be explained by the 2 sensitivity simulations are shown at the top of the plot (r^2). In this figure, Arctic sea ice export is defined to be positive, so a downward trend indicates a reduction in sea ice export. The figure is modified from Wang et al. [181]. The observation data in (A) were described by Spreen et al. [25].

Table 1. Ocean and ice transports through Arctic Ocean gateways based on model-observation synthesis. Positive indicates an Arctic inflow, and negative indicates an Arctic outflow. The cells with Δ show changes relative to the 1980–2000 period. The reference salinity is 34.8 psu for freshwater transports, and the reference temperature is 0°C for heat transports. For the period of 2000–2020, the right column shows adjusted values after taking into account the increased Bering Strait inflow, which was not obtained in model simulations (see the text for an explanation). The question marks indicate that estimates of the respective uncertainties are not available.

	1980–2000	2000–2020		2090–2100
		Unadjusted	Adjusted	SSP585
Volume transport (Sv)				
Bering Strait	0.8 ± 0.1[a]	$\Delta = -0.1$	1.0 ± 0.1[b]	$\Delta = -0.4 \pm 0.2$
Fram Strait	-2 ± 2.7[c]	$\Delta = -0.3$	$\Delta = -0.4$	$\Delta = -0.7 \pm 1.2$
Davis Strait	-2.6 ± 1[d]	$\Delta = +0.3$	$\Delta = +0.1$	$\Delta = +0.6 \pm 1.0$
	-1.6 ± 0.5[e]			
Barents Sea Opening	$2.3 \pm ?$[f]	$\Delta = +0.1$		$\Delta = +0.5 \pm 1.2$
Freshwater transport (km^3/yr), relative to 34.8				
Bering Strait	$2{,}400 \pm 300$[g]	$2{,}200 \pm 390$	$3{,}000 \pm 280$[b]	$\Delta = +100 \pm 500$
Fram Strait	$-2{,}700 \pm 530$[g, h]	$-3{,}200 \pm 620$	$-3{,}400 \pm 630$	$\Delta = -3{,}400 \pm 2{,}400$
Davis Strait	$-3{,}200 \pm 320$[g]	$-2{,}800 \pm 570$	$-3{,}300 \pm 580$	$\Delta = -1{,}500 \pm 2{,}300$
Barents Sea Opening	$-90 \pm ?$[g]	$-110 \pm ?$		$\Delta = +1{,}700 \pm 1{,}500$
Fram Strait (ice)	$-2{,}300 \pm 340$[g]	$-1{,}600 \pm 510$[i]		$\Delta = +1{,}500 \pm 900$[j]
Davis Strait (ice)	$-420 \pm ?$[d]	-280 ± 50[k]		$\Delta = +380 \pm 180$
River runoff	$3{,}900 \pm 390$[h]	$4{,}200 \pm 420$[h]		$\Delta = +1{,}400 \pm 650$
P-E	$2{,}000 \pm 200$[g]	$2{,}200 \pm 220$[h]		$\Delta = +2{,}000 \pm 2{,}700$
Heat transport (TW), relative to 0°C				
Bering Strait	4 ± 4[l]	6 ± 4[l]		$\Delta = +19 \pm 7$
	(12 ± 4)[m]	(14 ± 4)[m]		
Fram Strait	29 ± 10[n]	37 ± 11		$\Delta = -8 \pm 22$[o]
Davis Strait	18 ± 17[d]	16 ± 17		$\Delta = -13 \pm 14$[o]
Barents Sea Opening	62 ± 10	70 ± 5[f]		$\Delta = +78 \pm 70$

[a] After Roach et al. [3].

[b] After Woodgate and Peralta-Ferriz [1].

[c] After Schauer et al. [50].

[d] After Cuny et al. [21], for 1987–1990.

[e] After Curry et al. [24], for 2004–2010.

[f] After Smedsrud et al. [53].

[g] After Serreze et al. [16].

[h] After Haine et al. [32].

[i] After Spreen et al. [25].

[j] This reduction renders a nearly vanishing sea ice transport in the models. See Fig. 8F.

[k] The mean value of the estimates by Curry et al. [24] and Min et al. [187].

[l] Recomputed using reference temperature of 0°C from the originally calculated Bering Strait values provided in [1].

[m] The original Bering Strait values using reference temperature of −1.9°C are shown in parentheses.

[n] After Schauer et al. [87], and the median value of the suggested range is used here.

[o] Net transport in the full gateways. Poleward heat transport will increase in the future [74].

estimates.] We concluded that the Fram Strait volume export was increased by 0.4 Sv and the Davis Strait volume export was reduced by 0.1 Sv in 2000–2020 compared to that in 1980–2000.

To estimate ocean freshwater and heat transports in 2000–2020 ($T^{2000-2020}$), we used their percentage changes in 2000–2018 relative to 1980–2000 (denoted as α) obtained in the OMIP2 simulations: $T^{2000-2020} = (1+\alpha)T^{1980-2000}$, where $T^{1980-2000}$ denotes the previously synthesized transports for 1980–2000. This estimation is motivated by the fact that the simulations can capture the variability of the transports, while the magnitudes of the variability (and their mean states) are often biased, as discussed above and suggested in previous model intercomparison studies [124,125]. For freshwater exports through the Fram and Davis straits, we further applied an adjustment similar to that for the ocean volume transport to compensate the models' misrepresentation of the trend of Bering Strait freshwater transport. A value of 800 km^3/year should be added to the simulated Bering Strait freshwater transport to obtain the observational estimate. Considering that the increase in the Arctic liquid freshwater content over the last 2 decades was underestimated by about 2,000 km^3 in the OMIP2 simulations [124] and assuming that an additional 100 km^3/year Bering Strait freshwater transport can correct this underestimation, 700 km^3/year export should be added to the Fram (one-third) and Davis (two-thirds) straits. The resulting estimates are shown in the right column of the 2000–2020 period in Table 1.

The main results of section 3 are summarized below.

• Estimated from our model-observation synthesis, the liquid freshwater transport in the Bering Strait inflow increased by 600 km^3/year in 2000–2020 compared to that in the period of 1980–2000 (Table 1). The liquid freshwater export was 700 km^3/year greater in 2000–2020 than in 1980–2000 in the Fram Strait, while it was very similar between these 2 periods in the Davis Strait. The liquid freshwater exports were not significantly different between the 2 gateways. The sea ice freshwater export in the Fram Strait became less than half of its liquid counterpart in 2000–2020. The sea ice freshwater export through the Davis Strait became even smaller during the past 2 decades than it was before, accounting for about 15% of the total Arctic sea ice export.

• Ocean temperatures in the Atlantic Water inflow in the Fram Strait and Barents Sea Opening and in the Pacific Water inflow in the Bering Strait have been increasing during the past 5 decades (summarized in Table 2). The Atlantic Water inflow into the Norwegian Sea had a cooling trend starting from the late 2000s, but the temperature in the WSC and in the southern Barents Sea continued to increase in the 2010s. The temperature and heat transport in the WSC and in the Pacific inflow reached record highs in the 2010s (Table 2). Comparing the 2000–2020 period with the 1980–2000 period, a pronounced increase in ocean heat transport of 8 TW occurred in both the Barents Sea Opening and Fram Strait (Table 1). The ocean heat transport into Baffin Bay through the Davis Strait was slightly reduced in the 2010s compared to that in the 3 preceding decades.

• Considering both the observations and model results, several record highs and lows were hit in the Arctic Ocean gateways in the 2010s (Table 2): record highs for temperature in the Atlantic Water in the Fram Strait and Barents Sea Opening and in the Pacific Water in the Bering Strait; record lows for salinity in the Pacific inflow in the Bering Strait and in the Arctic outflows in the Fram and Davis straits; record highs for heat transports through the Bering, Fram, and Davis straits, for freshwater import in the Bering Strait, and for freshwater exports through the Fram and Davis straits; record lows for sea ice volume export in the Fram Strait. The contemporary occurrence of these records in the 2010s is an indication of a new status in the linkages between the Arctic Ocean and lower latitudes, suggesting a changing climate.

4. Driving mechanisms

4.1. Pacific Water inflow

It has long been suggested that the variability of the Bering Strait throughflow on annual and interannual time scales is associated with the sea surface height gradient between the Pacific and Arctic oceans [4,192,193]. Those authors used linear regression to quantify the role of far-field drivers versus local winds near the Bering Strait and revealed that the far-field forcing, inferred to be the sea surface height gradient, played a determining role for the recent increase in ocean volume transport through the Bering Strait [144,194].

A conceptual model was used by Danielson et al. [195] to explain the variability of the Bering Strait inflow. They suggested that the sea surface height gradient that drives the inflow variability is mainly determined by the sea surface height in the eastern Bering Sea on the Pacific side and in the western Chukchi Sea and the East Siberian Sea on the Arctic side. On the Pacific side, the longitudinal location of the active center of the atmospheric Aleutian Low regulates the Bering Strait inflow. When the Aleutian Low is centered over the Aleutian Basin, the Ekman transport toward the eastern Bering Sea shelf increases the sea surface height there, thus increasing the Bering Strait inflow through the Bering Strait; when the Aleutian Low is centered over the Gulf of Alaska, the southwestward winds over the eastern Bering shelf reduce the sea surface height there through offshore Ekman transport, thus reducing the Bering Strait inflow. On the Arctic side, changes in the westward winds over the Chukchi and East Siberian seas can change the sea surface height in these shelf seas through onshore/offshore Ekman transport anomalies, thus retarding/enhancing the Bering Strait inflow as well. The changes in the sea surface height in these shelf seas can impact the throughflow with delay on the time scales of shelf wave propagation (hours to days).

Using satellite ocean bottom pressure data from the GRACE mission, Peralta-Ferriz and Woodgate [196] confirmed a strong correlation between a high Bering Sea shelf and low East Siberian Sea ocean bottom pressure pattern with the far-field component of the flow through the Bering Strait, consistent with the expected sea surface height pattern associated with the throughflow in an idealized rotating channel [197]. The analysis of the GRACE data also showed that the Bering Strait throughflow variability was most strongly coupled to sea surface height change in the Arctic, rather than in the Bering Sea for the period of 2002–2016. These results were reinforced by an adjoint model study [198] that used a data-optimized ice-ocean model (for the period of 2002–2013) and its adjoint to link the Bering Strait throughflow variability to wind variability near the coasts, i.e, the eastern Bering Sea shelf south of the strait and the East Siberian Sea north of the strait.

The dynamic framework described above was verified with a global ocean–sea ice model by Zhang et al. [133] using the

Table 2. Whether record high (temperature, heat transport, liquid freshwater transport, and volume transport) or record low (salinity and solid freshwater transport) occurred in the 2010s, and whether there have been statistically significant trends. The absolute values of annual mean transports are considered when judging the record high and low. The results are based on synthesizing observations and model results for the past 5 decades. The reference salinity is 34.8 for freshwater transports, and the reference temperature is 0°C for heat transports. See also the discussion of ambiguities of heat and freshwater transports through open gateways in section 2.3.

	Salinity	Freshwater transport	Temperature	Heat transport	Volume flux
Record high or low in 2010s					
Bering Strait	Yes	Yes	Yes	Yes	Yes
Barents Sea Opening	No[a]	No	Yes[a]	No	No
Fram Strait	Yes[b]	Yes	Yes[a]	Yes	No
Davis Strait	Yes[b]	Yes[c]	No[a]	Yes[d]	No
Fram Strait (sea ice)	/	Yes	/	/	/
Significant trend over the past 5 decades					
Bering Strait	No[e]	Yes[f]	Yes	Yes[f]	Yes
Barents Sea Opening	No[a,g]	No	Yes[a]	Yes	No
Fram Strait	Yes[b]	Yes	Yes[a]	Yes	No
Davis Strait	No[b]	No	Yes[a]	No	No
Fram Strait (sea ice)	/	Yes	/	/	/

[a] In the Atlantic Water inflow.

[b] In the Arctic outflow.

[c] After adding the anomaly of freshwater transport from the Pacific that was not captured in the models.

[d] Record high in the northward heat transport in the West Greenland Current in 2010, but possibly not in the net heat transport.

[e] There was a freshening trend over 5 decades, but it was not statistically significant.

[f] When combining the anomalies of models before 2000 and observations afterward.

[g] There was a weak upward salinity trend, opposite the expected freshening trend associated with the hydrological cycle strengthening projected in future warming climate.

modeling technique described in section 2. By retaining the interannual variability of the atmospheric forcing only inside or outside the Arctic in their simulations, they found that winds in the northern Pacific and in the western Arctic contribute to similar amounts of interannual variance in the Bering Strait volume transport when considering the long historical period of a few decades. However, after the mid-1990s, winds in the western Arctic had a relatively larger contribution as they drove a few high inflow events (also see Fig. 5A), consistent with the aforementioned findings based on satellite observations [196] and the adjoint model [198].

The model results suggest that the interannual variability in ocean freshwater and heat transports in the Bering Strait over the period of 1970–2020 can be explained to a larger extent by the atmospheric forcing outside the Arctic (Fig. 5E and I). Before 2010, winds determined most of the variability in the heat and freshwater transports via the impacts on both ocean volume transport in the Bering Strait and the accumulation of low-salinity and high-temperature water upstream the Bering Strait [133], while thermal and freshwater surface forcing had little impact on heat and freshwater transports [133,198]. In the 2010s, strong ocean warming (Fig. 2A) significantly contributed to the increase in ocean heat transport, reducing the total variance in the ocean heat transport that can be explained by the ocean volume transport (as indicated by the low coefficient of determination between the ocean volume and heat transports in OMIP2; Fig. 3E).

4.2. Atlantic Water inflow

4.2.1. Norwegian Sea inflow

The increases in temperature and salinity from the mid-1990s to the mid-2000s and their subsequent decreases in the Atlantic Water inflow into the Norwegian Sea (Fig. 2B and F) coincide with the changes in the ocean properties in the northeast North Atlantic [149,154]. Winds have been suggested to be the main driver of the variability of the Atlantic inflow to the Norwegian Sea on interannual timescales [148,199,200]. Winds largely determine the interannual variability of both the ocean volume and heat transports across the Iceland–Faroe–Scotland Ridge, while atmospheric buoyancy (heat and freshwater) forcing contributes to decadal changes in the ocean heat transport across the ridge by influencing the inflow temperature [132].

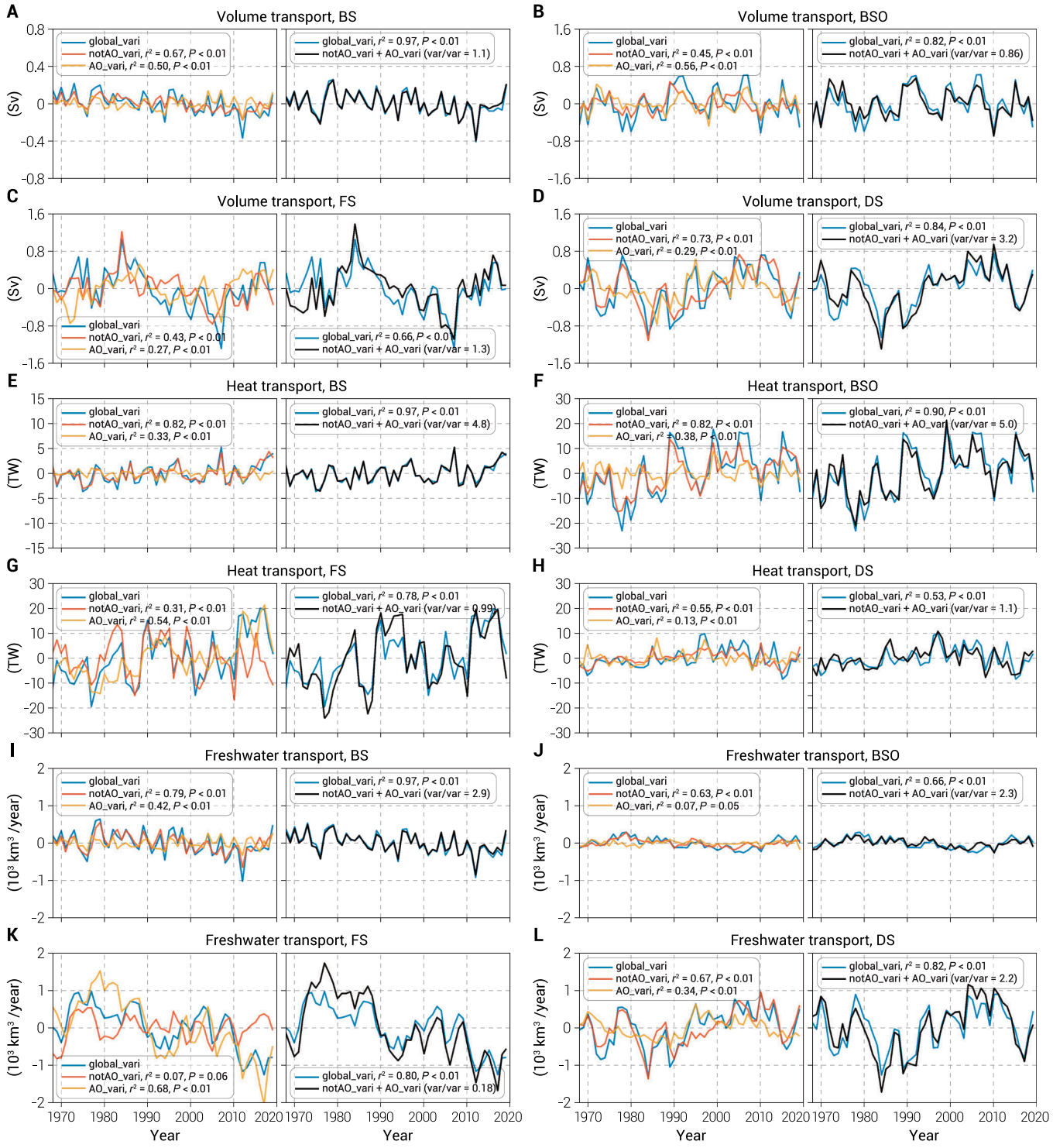

Fig. 5. Anomalies of annual mean ocean volume transport in the FESOM simulations: in the (A) Bering Strait (BS), (B) Barents Sea Opening (BSO), (C) Fram Strait (FS), and (D) Davis Strait (DS). (E to H) The same as (A) to (D), but for heat transport (relative to 0°C). (I to L) The same as (A) to (D), but for freshwater transport (relative to 34.8). In each panel, the left plot shows the results of individual experiments: global_vari (historical simulation), notAO_vari in which atmospheric forcing has interannual variability outside the Arctic, but not inside the Arctic, and AO_vari in which forcing has interannual variability inside the Arctic, but not outside the Arctic. The fractions of explained variance are shown in the legends (r^2). In each panel, the right plot depicts the historical simulation and the sum of the 2 sensitivity experiments. The fractions of explained variance (r^2 of the 2 lines) and the ratio of the individual variances between notAO_vari and AO_vari are shown in the legends.

The changes in the proportions of the subpolar and subtropical waters in the northeast North Atlantic influence the temperature and salinity in this region and thus in the inflow to the Norwegian Sea. Wind variability associated with the second mode of the sea-level pressure over the North Atlantic, the East Atlantic Pattern (EAP; or similarly, the second mode of the wind stress curl) can modulate the strength of the subpolar and subtropical gyres in phase [153]. In a negative EAP phase, both the gyres weaken, with a contraction of the subpolar gyre and an expansion of the subtropical gyre, allowing a larger amount

of warm and saline subtropical water to flow poleward, and vice versa [153,201,202]. It was argued that the changes in the location and alignment of the zero wind stress curl line, mostly associated with the EAP, can influence the interannual variability of the poleward Atlantic Water ocean volume transport [154]. The above understanding of meridional connectivity is in line with the concept of the ocean circulation anomaly between the 2 gyres, the intergyre gyre [203].

The weakening of the subpolar gyre from the mid-1990s to the mid-2000s contributed to the warming and salinification of the Atlantic inflow to the Norwegian Sea, and the strengthening of the subpolar gyre in the 2010s contributed to the cooling and freshening of the Atlantic inflow [202]. The strengthening of the subpolar gyre in the 2010s was associated with a strongly positive EAP [154,204]. On decadal timescales, not only winds but also buoyancy forcing can influence the strength of the subpolar gyre. For example, the surface ocean buoyancy anomaly in the Labrador Sea, which is subject to the impact of surface buoyancy fluxes such as those associated with the North Atlantic Oscillation (NAO), can influence the strength of the subpolar gyre on a timescale of years [205]. Model simulations showed that without buoyancy forcing variability, winds alone would not have strengthened the subpolar gyre in the 2010s as much as observed [134].

The cooling and freshening of the northeast North Atlantic started in the early 2010s before the strengthening of the subpolar gyre [206]. Therefore, it was also suggested that changes in the amount and pathway of fresh, cold surface water exported from the Labrador Sea considerably contributed to the freshening and cooling of the northeast North Atlantic in the 2010s [206,207]. Surface heat loss transforms lighter surface water into denser intermediate and deep waters in the Labrador Sea. The reduced surface heat loss in the Labrador Sea in the late 2000s and early 2010s caused an increased volume of lighter water to remain in the Labrador Sea, which finally supplied the northeast North Atlantic [206]. The later strengthening of the subpolar gyre after 2013 could have further increased the proportion of the subpolar water in the northeast North Atlantic, causing the salinity there to reach a record low in 2016 [207]. The cooling of the eastern subpolar gyre in the 2010s was also suggested to be associated with the weakening of the AMOC [208]. The cooling was mitigated by reduced ocean surface heat loss along the Atlantic Water pathway [209]. There is no full consensus on the main mechanisms that drove the 2010s freshening and cooling of the subpolar gyre, and more research is needed.

4.2.2. Barents Sea Opening

The salinity variability of Atlantic Water inflow propagates from the northeast North Atlantic to the Barents Sea Opening on a timescale of about 2 years, while the timescale for temperature is 1 year or less, indicating that air-sea heat flux along the Atlantic Water pathway has a crucial influence on the Atlantic Water temperature in the downstream region [161]. The observed decoupling of temperature and salinity in the Norwegian Sea in the 2010s was due to reduced surface heat loss [155]. The reduction in surface heat loss in the Norwegian Sea and southwestern Barents Sea was suggested to be one crucial factor that can enhance the progression of Arctic Atlantification via the Barents Sea branch of the Atlantic Water inflow to the Arctic Ocean [69,70,85,210].

The variations in the Atlantic Water current along the Norwegian coast toward the Barents Sea are driven by NAO-like wind forcing, and they correspond to fast barotropic transfer mechanisms without an obvious phase lag [200]. However, the coherence of the currents is reduced at the Barents Sea Opening [51]. First, the amount of Atlantic Water that flows into the Barents Sea can be influenced by the eastward/westward extent of the Atlantic Water current in the Norwegian Sea [211–213]. Cyclonic wind anomalies over the northern Nordic Seas can increase the Atlantic Water inflow to the Barents Sea by pushing the boundary current closer to the entrance [214], with a stronger effect when the center of the wind anomaly is closer to the Barents Sea [132]. Second, winds in the Barents Sea region can also strongly influence the volume transport through the Barents Sea Opening by creating sea surface height gradients [132,215].

The atmospheric forcing inside and outside the Arctic can explain the interannual variability in the volume transport to a similar extent, with the variance explained by the forcing inside the Arctic being slightly larger (Fig. 5B). It was found that the variability of the volume transport is mainly determined by winds [132]. The variability and trend of the ocean heat transport are mainly associated with atmospheric forcing outside the Arctic because ocean temperature is mainly subject to outside forcing, but Arctic winds can still explain a non-negligible part (38%) of the heat transport variability via impacts on the ocean volume transport (Fig. 5F). The interannual variability in the freshwater transport in the Barents Sea Opening, being small in magnitude, is mainly determined by forcing outside the Arctic (Fig. 5J).

4.2.3. Fram Strait

Some of the episodes of high/low heat transport coincide between the Fram Strait and Barents Sea Opening (Fig. 3F and G) because both the branches originate from the Atlantic Water boundary current in the Nordic Seas. The correlation between the heat transports through the 2 gateways is statistically significant ($r = 0.65$, $P < 0.01$ in OMIP2 models). However, there are many differences between the 2 heat transport time series (Fig. 3F and G) because each of them is also subject to distinct forcing mechanisms (see section 4.2.2 for a discussion of the Barents Sea Opening inflow).

A dynamic framework involving wind-driven flow along the potential vorticity f/H contours (where f is the Coriolis parameter and H is the water depth) was proposed to explain the large-scale circulation in the Nordic Seas and Arctic Ocean [216–218]. There exist closed f/H contours that cross the Fram Strait and span the Nordic Seas and Arctic basin. In this region, f does not change much, so the f/H contours effectively coincide with isobaths. Vorticity conservation implies that the depth-integrated flow follows the bottom bathymetry. The dominant vorticity input in the Nordic Seas and Arctic Ocean is the positive wind stress curl exerted over the Nordic Seas, which sustains the cyclonic barotropic flow along the closed f/H contours. The flow covaries with the difference between the surface vorticity input and the bottom dissipation over the area surrounded by the closed f/H contour [217]. This dynamic framework is consistent with the finding that lower sea-level pressure over the Nordic Seas and a stronger Greenland Sea gyre can increase Atlantic Water inflow and temperature in the Fram Strait [214,219]. However, this framework does not account for across-f/H processes, in particular those influencing the recirculation in the Fram Strait.

An estuary framework was proposed to explain the mean status of the Arctic halocline and Atlantic Water circulation

[218,220–222]. In this framework, the freshwater from the Arctic continental shelves drives the cyclonic circulation of the Atlantic Water. Vertical mixing converts the salinity contrast between salty Atlantic Water and Arctic freshwater into potential energy, which drives the horizontal circulation [221]. Vertical mixing and lateral eddy advection of freshwater and Atlantic Water at different depths maintain the Arctic halocline. The estuary framework was intended to understand the basic mean circulation of the Atlantic Water, not its interannual and decadal variability.

A large part of the variability in the heat transport in the Fram Strait stems from the Arctic Ocean (Fig. 5G), for which explanations should be sought. In the Fram Strait, a fraction of the Atlantic Water propagates to the west and joins the southward East Greenland Current [86–89]. In the following, we use wind perturbation experiments (see Materials and Methods) to show that large-scale winds over the Arctic basin (north of Fram Strait) can influence the effective Atlantic Water inflow into the Arctic basin and the recirculation strength in the Fram Strait. Following the vorticity dynamic framework described above, we argue that wind variability inside the Arctic makes a large contribution to the interannual and decadal variability of the Fram Strait branch of the Atlantic Water inflow.

The Arctic wind perturbation of negative Arctic Oscillation (Fig. 6A) accumulates surface freshwater, leading to a positive sea surface height anomaly and an anticyclonic surface geostrophic current anomaly spanning the Eurasian and Makarov basins (Fig. 6B). The imprint of the anticyclonic circulation on the Atlantic Water layer circulation effectively reduces the northward ocean heat transport in the Fram Strait (Fig. 6J). The Atlantic Water entering the Nordic Seas through the Iceland–Scotland–Ridge does not significantly change (not shown), implying a stronger recirculation of the Atlantic Water in the Fram Strait. The temperature at 300 m depth reflects the reduction in both the amount of warm Atlantic Water and the strength of the cyclonic circulation in the Arctic Ocean under the negative Arctic Oscillation wind forcing (Fig. 7A and B).

It is interesting to note that the increased recirculation of the warm Atlantic Water does not increase the temperature in the East Greenland Current or the Greenland Sea; in contrast, the temperature is even lower in these areas in case with a negative Arctic Oscillation forcing (Fig. 7A and B). The reason is that the freshwater export through the western Fram Strait is strongly reduced in this case, which weakens the upper ocean stratification and thus increases ocean surface heat loss in these areas. This could further influence the heat content of the Atlantic Water circulating along the northeast rim of the Greenland Sea gyre. Therefore, the impact of Arctic winds on the Atlantic Water inflow and Arctic freshwater export (see section 4.3.1) should be considered together for a comprehensive understanding.

In the opposite case with a positive Arctic Oscillation perturbation, the Arctic freshwater is released and a negative sea surface height anomaly forms in the Eurasian and Makarov basins (Fig. 6C). The cyclonic circulation anomaly in the Eurasian Basin increases the Atlantic Water inflow (Fig. 6J). The Atlantic Water also penetrates farther into the Canada Basin than it does in the control simulation (Fig. 7A and C).

The wind perturbations representing the changes in the Beaufort High (Fig. 6D) induce strong sea surface height anomalies in the Canada Basin (Fig. 6E and F). The changes in the eastward extent of the along-slope propagation of the warm Atlantic Water are obvious in the Amerasian Basin (Fig. 7D and E). It turns out that the wind stress curl input over the Canada Basin can influence the overall along-f/H-contour circulation, with impacts on the heat inflow through the Fram Strait (Fig. 6J) and thus the temperature along the Atlantic Water circulation pathway in the Arctic basin (Fig. 7D and E). In addition to the impact on the Atlantic Water inflow and its circulation in the Arctic basin, the Beaufort High forcing leads to Beaufort Gyre cooling (through a downwelling anomaly in the case of an anticyclonic wind anomaly) or warming (through an upwelling anomaly in the case of a cyclonic wind anomaly) (Fig. 7D and E).

The Dipole Anomaly wind perturbations (Fig. 6G) lead to a dipole pattern in the sea surface height changes: eastern Eurasian Basin versus north of Greenland (Fig. 6H and I). Although the magnitude of the sea surface height changes is clearly smaller than that in the case of Beaufort High forcing, the strength of the impacts on the Atlantic Water inflow in the Fram Strait is similar in the 2 forcing cases (Fig. 6J, cyan and blue). Specifically, under the negative Dipole Anomaly forcing, the anticyclonic ocean circulation anomaly in the eastern Eurasian Basin (Fig. 6H) weakens the along-topography cyclonic Atlantic Water layer circulation (Fig. 7F) and reduces the Atlantic Water inflow in the Fram Strait (Fig. 6J) and thus the Atlantic Water layer temperature (Fig. 7F). The opposite occurs with positive Dipole Anomaly forcing (Fig. 7G). There are 2 noteworthy aspects. First, the most obvious impacts of the Dipole Anomaly forcing on the cyclonic Atlantic Water layer circulation occur in the Eurasian Basin, including the return circulation along the Lomonosov Ridge (Fig. 7F and G), as expected from the sea surface height anomalies in the eastern Eurasian Basin (Fig. 6H and I). Second, in comparison with the ocean circulation anomalies north of Greenland, the ocean circulation anomalies in the eastern Eurasian Basin play a predominant role in changing the Atlantic Water inflow in the Fram Strait due to their direct impacts on the cyclonic Atlantic Water layer circulation.

The strong impacts of the upper ocean circulation on the Atlantic Water layer circulation in the Arctic Ocean, as shown in Fig. 7, are consistent with previous understanding of the dynamic interplay between the surface and Atlantic Water layers [223–226]. Here, concerning the main scope of this paper, we suggest that the upper ocean circulation variability has stronger impacts on the Atlantic Water layer variability than previously thought because it influences the amount of Atlantic Water entering the Arctic Ocean.

The leading mode of the upper Arctic Ocean circulation is associated with the Arctic Oscillation [170,227]. Therefore, the Arctic Oscillation is expected to have the strongest impact on the Atlantic Water layer circulation and Atlantic Water inflow in the Fram Strait. From the late-1980s to the mid-1990s, the Arctic Oscillation was predominantly in a positive phase, causing the eastward shift of the Transpolar Drift Stream and the strengthening of the Arctic Ocean cyclonic circulation [228–232]. Accordingly, the Arctic Ocean drew in Atlantic Water (Fig. 5G, yellow line). The positive Arctic Oscillation (or NAO) also strengthened the cyclonic Atlantic Water boundary current in the Nordic Seas and thus the heat inflow through the Fram Strait in this period (Fig. 5G, red line). Therefore, the winds both inside and outside the Arctic associated with the positive Arctic Oscillation/NAO drove the high Atlantic Water inflow in the 1990s, which explains the reported correlation between the NAO and Atlantic Water inflow [233]. In the 2010s, the atmospheric forcing inside the Arctic exerted even stronger

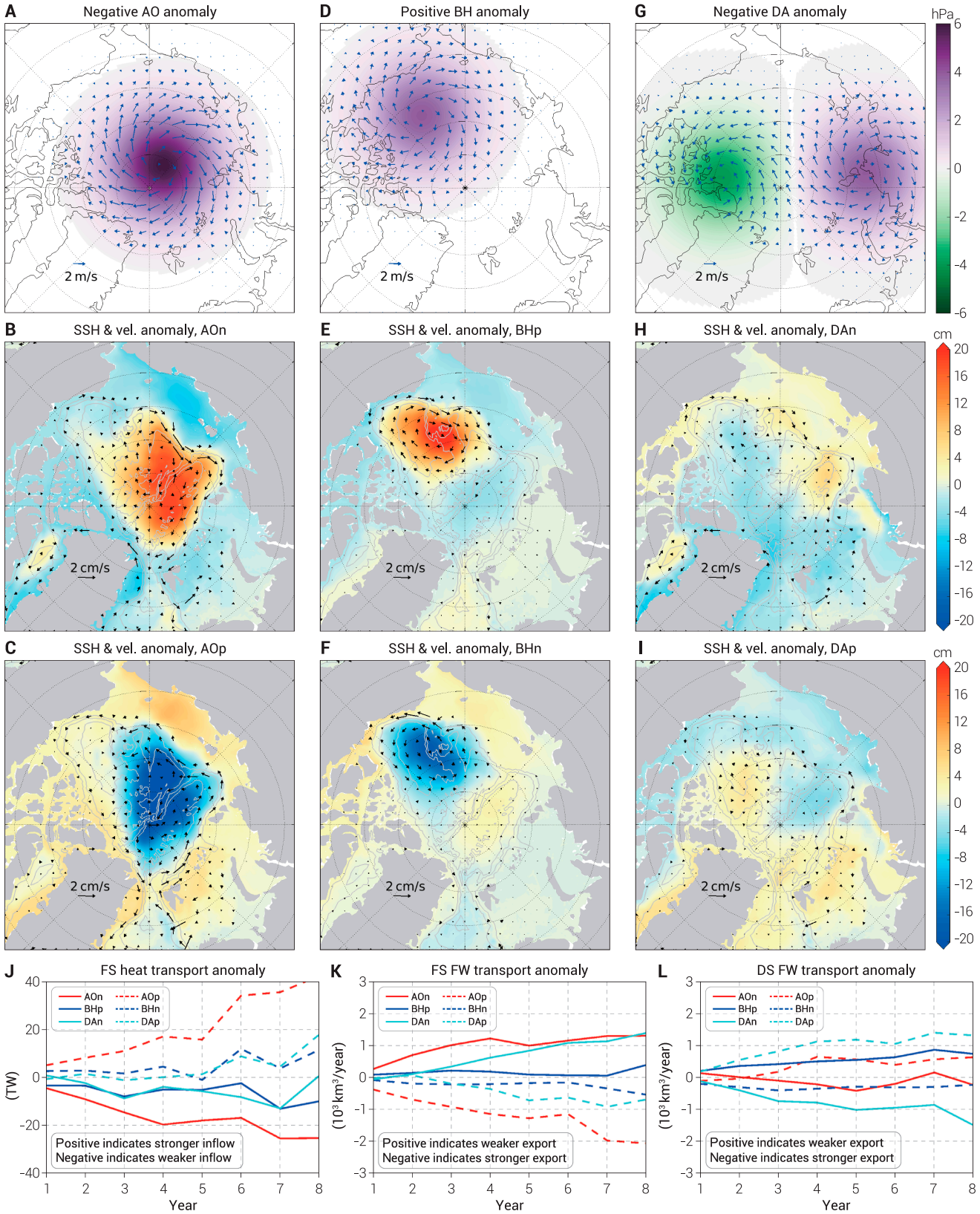

Fig. 6. Winds representing the (A) negative phase of the Arctic Oscillation, (D) positive Beaufort High anomaly, and (G) negative phase of the Arctic Dipole Anomaly that are used in the wind perturbation experiments. The associated sea-level pressure anomalies are also depicted. Sea surface height and velocity differences between the wind perturbation experiments and the control run: perturbed with the (B) negative Arctic Oscillation forcing (AOn), (C) positive Arctic Oscillation forcing (AOp), (E) positive Beaufort High anomaly (BHp), (F) negative Beaufort High anomaly (BHn), (H) negative Dipole Anomaly forcing (DAn), and (I) positive Dipole Anomaly forcing (DAp). (J) Anomalies of heat transport in the Fram Strait relative to the control run. (K) Anomalies of freshwater transport in the Fram Strait relative to the control run. (L) The same as (K), but for the Davis Strait. Ocean heat and freshwater transports are calculated relative to 0°C and 34.8, respectively.

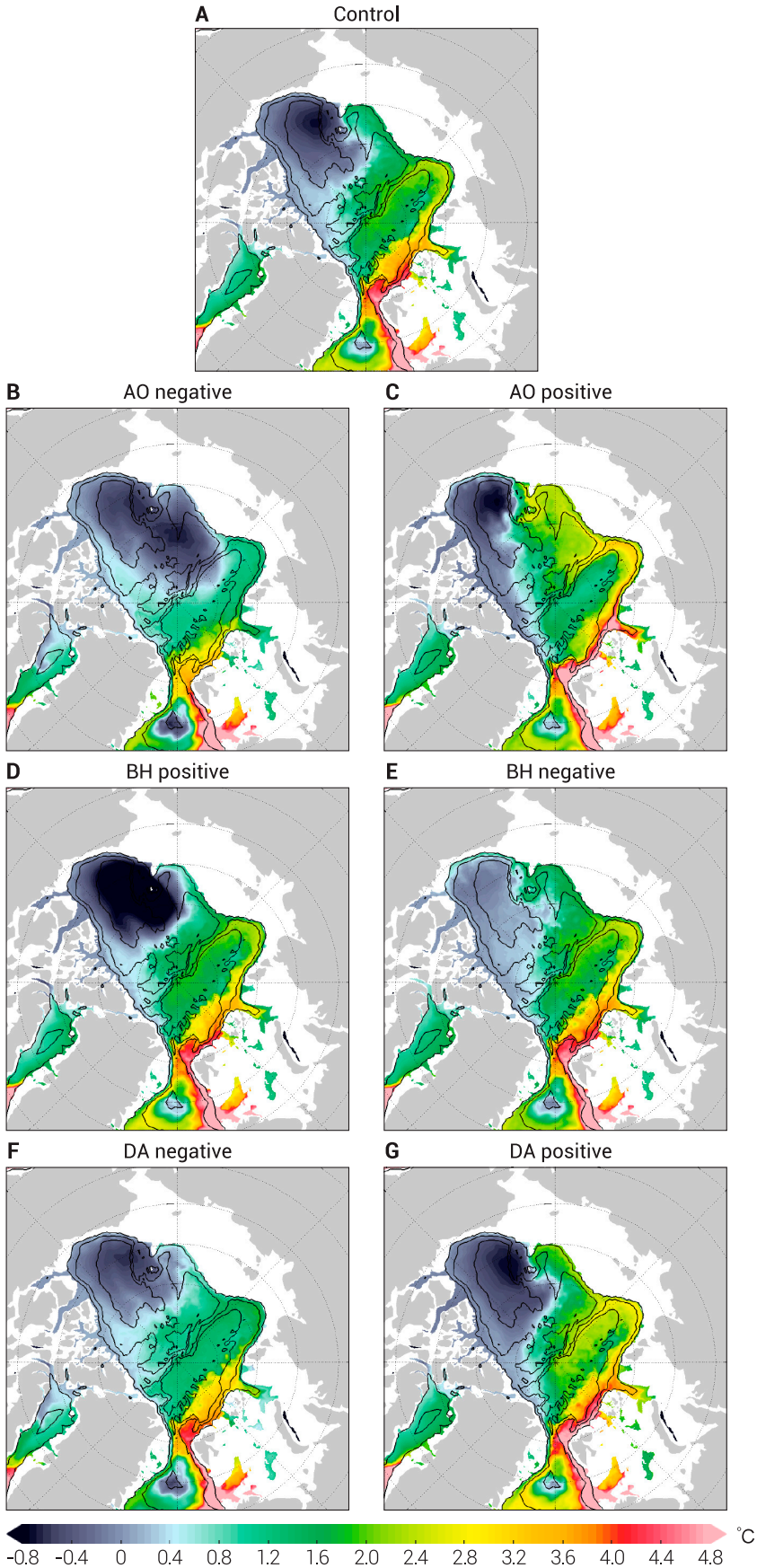

Fig. 7. Temperature at 300 m depth in the last model (8th) year in (A) the control simulation and in experiments perturbed with winds of the (B) negative Arctic Oscillation, (C) positive Arctic Oscillation, (D) positive Beaufort High anomaly, (E) negative Beaufort High anomaly, (F) negative Dipole Anomaly, and (G) positive Dipole Anomaly.

impacts on the Atlantic Water inflow. In addition to the effect of the on-average positive Arctic Oscillation, Arctic sea ice decline was found to have considerably increased the Atlantic Water inflow in the 2010s [93]. The declining sea ice reduced sea ice export through the Fram Strait, which resulted in a salinification and cyclonic circulation anomaly in the Greenland Sea, thus driving the Atlantic Water into the Arctic Ocean [93].

Many local processes can influence Fram Strait inflow as well. In the Arctic Ocean, the strongest mesoscale eddy activity is located in the Fram Strait [234,235]. The ocean circulation in the Fram Strait and the partitioning of the WSC into recirculation and poleward branches can be influenced by eddies [167,236,237], which have large seasonal variability related to surface buoyancy forcing [117,167]. Horizontal eddy transport crossing f/H contours can modify the circulation pathway of the Atlantic Water and thus the partitioning between the recirculation and poleward inflow in the Fram Strait. Regional wind stress in the southern Fram Strait can also influence the circulation pathway of the Atlantic Water relative to the f/H contours and thus the partitioning between the recirculation and poleward inflow [238]. The poleward transport of the Atlantic Water is further separated into 3 branches following different bottom bathymetry features in the northern Fram Strait [239–242]. Eddy fluxes, vertical mixing, wind stress curl, and surface heat loss in the Fram Strait and along the different Atlantic Water branches downstream could influence the amounts of Atlantic Water and ocean heat that finally enter the Eurasian Basin along the continental slope [243–245].

4.2.4. Davis Strait

As implied by its origin, the temperature of the Subpolar Mode Water in the Davis Strait is associated with the ocean temperature in the subpolar North Atlantic. Many factors contribute to the temperature variability in the subpolar North Atlantic, as discussed in section 4.2.1. In addition to the amount of warm subtropical water entering the subpolar gyre and the ocean surface heat flux along the Atlantic Water Current, the Atlantic Multidecadal Variability and anthropogenic North Atlantic ocean warming also affect the subpolar gyre temperature change [246,247].

The exchange of the warm water in the West Greenland Current with water in the interior Labrador Sea can influence ocean heat transport into Baffin Bay. Eddy fluxes can exchange water masses offshore from the West Greenland Current [248]. Ekman transport plays a more important role than eddies in determining the offshore exchange of the West Greenland Current [249,250]. The influence of winds on the ocean currents in the West Greenland Current increases toward the Davis Strait [251]. Normal wind conditions in winter in the northern Labrador Sea support offshore Ekman transport [250]. However, in 2 months at the end of 2010, the anomalous winds associated with a record high of the Greenland Blocking Index and a change in the storm track led to an onshore Ekman transport anomaly and caused most of the waters in the West Greenland Current to remain near the coast, thus strongly increasing the northward ocean volume, heat, and freshwater transports in the eastern Davis Strait in this period [175]. The anomalous atmospheric conditions in 2010 might be part of a larger hemispheric signal [175], but it is not clear whether such anomalous ocean circulations will become more regular in the future.

Both FESOM (Fig. 5H) and previous high-resolution regional model simulations [175] show a (relatively small) decadal decline in net heat transport through the Davis Strait after the mid-2000s. The cause is the cooling of the Subpolar Mode Water in the Davis Strait, which is associated with the ocean cooling in the subpolar North Atlantic in the 2010s (Fig. 2D).

4.3. Arctic freshwater export

4.3.1. Impact from Arctic Ocean

(a) Dynamic processes

The release of liquid freshwater from the Arctic Ocean is dramatically influenced by the large-scale atmospheric circulation in the Arctic, in particular by the variability associated with the Arctic Oscillation [135,139,252–257]. Freshwater export through the Fram Strait strongly decreases in a negative Arctic Oscillation phase, and it increases in a positive phase (Fig. 6K). This tendency in the changes in freshwater export also occurred in the Davis Strait, but only during the first model year (Fig. 6L). Afterward, the negative Arctic Oscillation tends to increase the Davis Strait freshwater export and the positive Arctic Oscillation causes a reduction. The different responses in the 2 export gateways can be explained by the changes in upper ocean circulation pathways in the Arctic Ocean [135,230,258]. With a positive Arctic Oscillation, the cyclonic ocean circulation in the Eurasian and Makarov basins strengthens (Fig. 6C). This circulation pattern favors the release of surface freshwater through the Fram Strait. In contrast, an anticyclonic ocean circulation anomaly in the Eurasian and Makarov basins associated with a negative Arctic Oscillation phase (Fig. 6B) carries surface freshwater toward the CAA.

From the mid-1980s to the mid-1990s, the Arctic Ocean released freshwater, which was suggested to be the cause of the Great Salinity Anomaly in the 1990s [39]. In this period, the Arctic Oscillation was mainly in a positive phase, so an increase in freshwater export occurred in the Fram Strait (Fig. 5K), while a reduction in freshwater export associated with atmospheric forcing inside the Arctic occurred in the Davis Strait (Fig. 5L, yellow line). These results obtained from the global model simulations are consistent with the results of the idealized wind perturbation experiments described above. The total freshwater export through the Davis Strait increased from the late-1980s to the beginning of the 1990s (Fig. 5L, blue line), which was due to atmospheric forcing outside the Arctic (see the next section). In 2011, the freshwater export in the western Fram Strait significantly increased [23] (also see Fig. 5K). The annual mean Arctic Oscillation was strongly positive in 2011, which could have contributed to the increase in the Fram Strait export. Indeed, this increase had an origin inside the Arctic (Fig. 5K, yellow line). The freshwater in the Arctic Ocean was in a high storage state before that event [259–264]. The abundant freshwater could also have contributed to the increased freshwater export in 2011.

The changes in the strength of the atmospheric Beaufort High dynamically drive the accumulation and release of Beaufort Gyre freshwater [262,265,266]. The wind anomalies over the Beaufort Gyre modulate the freshwater export through both gateways (Fig. 6K and L). An anticyclonic wind anomaly reduces freshwater export, more strongly in the Davis Strait than in the Fram Strait, and a cyclonic wind anomaly increases freshwater export, also more strongly in the Davis Strait than in the Fram Strait (Fig. 6K and L). The Beaufort High relaxed at the beginning of the 2010s, and the freshwater

in the Beaufort Gyre was slightly released [170,264], which contributed to the increase in the Davis Strait freshwater export associated with the Arctic forcing in this period (Fig. 5L, yellow line).

We found that the Arctic Dipole Anomaly forcing has strong impacts on freshwater exports through the Davis and Fram straits (Fig. 6K and L), although its overall impacts on the Arctic sea surface height are weaker than those of the other atmospheric modes considered (Fig. 6H and I). The reason is that the Dipole Anomaly forcing modifies the sea surface height and thus upper ocean circulation north of Greenland, which directly influences the distribution of the freshwater release between the Davis and Fram straits. Under a negative Dipole Anomaly forcing, the sea surface height decreases north of Greenland, which results in increased freshwater export through the Davis Strait (Fig. 6L) and decreased freshwater export through the Fram Strait (Fig. 6K). The opposite occurs under a positive Dipole Anomaly forcing. Consistent with the fact that the total freshwater content in the Arctic Ocean does not change much under the Dipole Anomaly forcing (manifested by the relatively small change in sea surface height compared with other forcing cases), the changes in the freshwater exports largely offset between the Fram and Davis straits (Fig. 6K and L). That is, the Dipole Anomaly forcing mainly influences the distribution of freshwater exports between the 2 gateways, while the Arctic Oscillation and Beaufort High forcings have strong impacts on the total amount of freshwater exported in addition to the transports in individual gateways. Our findings suggest that more attention should be given to the impacts of the Dipole Anomaly forcing on ocean transports, which have not been comprehensively studied before. In contrast, the Dipole Anomaly has often been applied to explain the variability in Arctic sea ice transport in the Fram Strait (see section 4.3.3).

(b) Freshwater sources

In addition to the Arctic dynamic processes discussed above, changes in salinity in the upper Arctic Ocean can influence freshwater exports through the 2 gateways. Based on model output, it was found that the Fram Strait freshwater transport is significantly correlated with the ocean–ice water flux north of Greenland [255]. Both Arctic runoff and net precipitation minus evaporation (P-E) have been increasing in response to increased poleward moisture transport in the atmosphere [32,267–270] (see Table 1), but sea ice decline has contributed the most to the increase in Arctic Ocean surface freshwater budget over the past 2 decades [170]. Under a strengthening of the hydrological cycle in a warming climate, the freshening of the Arctic Ocean due to increases in P-E and river runoff will increase freshwater exports through both gateways in the late 21st century, while the water flux between ocean and sea ice will finally be close to zero when Arctic sea ice volume nearly vanishes (see section 5). In observations, the freshwater input to the Arctic Ocean through the Bering Strait also increased in the early 21st century (see section 3.1).

Currently, a large amount of anomalous freshwater (an anomaly of approximately 10,000 km^3 relative to the level in the mid-1990s) is stored in the Arctic Ocean, mainly in the western Arctic [263,264], which resulted from a dominating anticyclonic wind regime and sea ice decline in the Arctic over the past 2 decades [170]. The anomalous freshwater is a potential source for freshwater export when Arctic winds change to a cyclonic regime, which promotes freshwater release. The strengthening of ocean surface stress associated with Arctic sea ice decline dramatically influenced the spatial distribution of the accumulated freshwater in the Arctic Ocean over the past 2 decades, causing the overall accumulation to occur mainly in the western Arctic (see figure 12a,b of [170]). If the Arctic Ocean starts to release freshwater, the partitioning of freshwater export between the Davis and Fram straits might be impacted by the location of the anomalous freshwater content.

The total freshwater discharge (runoff and icebergs) from Greenland reached 1,300 km^3/year in the 2010s, approximately 400 km^3/year higher than that in the 1990s [271]. The signal of Greenland freshwater discharge might already be detectable in the Labrador Sea [272,273], although recent studies cannot confirm this [274]. Freshwater from northern Greenland into the Arctic basin is a very small fraction of the total Greenland discharge [275]. The freshwater discharge into Baffin Bay increased more than those into other individual areas around Greenland in recent decades, with an anomaly of 90 km^3/year after 2000 relative to the 1960–1990 climatology [271]. This increase could contribute to the change in Davis Strait freshwater transport, although it is small in comparison to the interannual and decadal variability of the Davis Strait freshwater transport (Fig. 3L). Greenland has continued to lose ice mass in past decades despite strong interannual variability in the mass change rate associated with the variability in air and ocean temperature [276–278]. In the future warming climate, freshwater from land may make an increasing contribution to the Arctic Ocean freshwater budget.

4.3.2. Impact from downstream sea level

Ocean volume transport largely determines the freshwater transport variability for the CAA throughflow [279,280]. This is also the case for the Davis Strait export (Fig. 3L), so regional freshwater sources in Baffin Bay and inflows of different origins through the eastern Davis Strait to Baffin Bay do not considerably influence the freshwater transport variability stemming from Arctic Ocean export. The variability of the ocean volume transport through the CAA correlates well with the along-strait sea surface height gradient (the sea-level difference between the 2 ends of the main CAA straits), as suggested in model-based studies [280–285]. The anomaly of sea-level changes south of Greenland can propagate quickly through fast waves to the northern Baffin Basin and influence the export through the CAA [280,282].

It has been found that the Davis Strait volume transport is correlated with the NAO index [257,280,282]. The Davis Strait ocean volume export associated with the atmospheric forcing outside the Arctic was high at the beginning of the 1990s when the NAO was high; afterward, it dropped until the mid-2000s following the NAO reduction and then increased in the 2010s when the NAO was mainly positive again (Fig. 5D and L, red line). The NAO influences the Davis Strait export through its impact on the dynamic sea level in the subpolar gyre, especially the Labrador Sea. The enhanced freshwater export through the Davis Strait in the mid-to-late 2010s can be well explained by the dynamic sea-level drop south of Greenland in this period [134]. Surface buoyancy forcing was found to considerably contribute to this dynamic sea-level drop [134]. The atmosphere forcing over the Arctic basin also drives a large part of the total variability of the Davis Strait export through the joint effects of different atmospheric modes (see section 4.3.1), but the forcing outside the Arctic plays a comparatively larger role

(Fig. 5D and L). Notably, the forcing outside the Arctic accounts for 73% of the ocean volume transport variability and 67% of the freshwater transport variability in the Davis Strait (Fig. 5D and L).

An increase in the Davis Strait ocean volume export induced by a dynamic sea-level drop south of Greenland implies a decrease in the Fram Strait ocean volume transport. This is clearly shown by the negative correlation between the volume transports in the Fram and Davis straits associated with forcing outside the Arctic (Fig. 5C and D, red lines). The anti-correlation is comparatively weaker for freshwater exports (Fig. 5K and L, red lines). The reason is that the freshwater transport is not highly correlated with ocean volume transport in the Fram Strait, even for the case only with forcing variability outside the Arctic (Fig. 5C and K), possibly due to the high north- and southward transports of high-salinity waters in the Fram Strait. The anti-correlation between the 2 gateways is at least clearly visible for some extreme events. For example, the increase in the Davis Strait freshwater export in the mid-to-late 2010s coincides with the contemporary decrease in the Fram Strait freshwater export in the case when only the forcing outside the Arctic varies interannually (Fig. 5K and L, red lines). In 2017, the strong cyclonic wind anomaly in the Arctic drove freshwater release, as shown by simulations and observations [118,134]. Without the redirection of the freshwater release toward the Davis Strait due to the dynamic sea-level drop south of Greenland, much more freshwater would have been released through the Fram Strait than actually observed in the 2010s (comparing the 3 lines in the left panel of Fig. 5K); therefore, Fram Strait freshwater export is also subject to remote forcing over the northern North Atlantic [134]. However, when considering the past 5 decades, the interannual variability in the Fram Strait freshwater export is mainly determined by Arctic forcing, in contrast to that in the Davis Strait (Fig. 5K and L).

Local surface stress associated with local winds and sea ice conditions in the CAA can influence the strength of the CAA volume transport [286]. There is currently no evidence to suggest that local surface stress plays an important role in the interannual variability of the CAA volume transport in comparison with the impacts of the Arctic and northern North Atlantic forcing.

4.3.3. Sea ice export

The sea ice volume export through the Fram Strait is positively correlated with both the first (Arctic Oscillation) and second (Arctic Dipole Anomaly) leading modes of sea-level pressure in the Arctic, but the relative importance of the 2 modes varies with season [181]. The Dipole Anomaly can considerably influence the variability of the sea ice in the Transpolar Drift and the amount of sea ice that reaches the Fram Strait, thus affecting the sea ice thickness there [137,287,288]. This effect takes place year round, so the annual mean sea ice volume export can be better explained by the Dipole Anomaly than by the Arctic Oscillation [181]. The Arctic Oscillation exerts very strong impacts on sea ice drift and moderate impacts on sea ice thickness in the Fram Strait in winter [289], so the winter variability in the sea ice volume export can be better explained by the Arctic Oscillation than by the Dipole Anomaly [181]. However, the impact of the Arctic Oscillation on winter sea ice drift and volume export in the Fram Strait is nonstationary, with a much higher impact after the 1970s due to the eastward shift of the NAO active center [290,291].

The sea ice volume transport through the Fram Strait is influenced by both winds and thermal forcing in the Arctic. Winds drive the interannual variability; air and ocean warming has led to a strong declining trend in sea ice thickness and thus in volume export over the past 2 decades (Fig. 4B) [25,181]. It is interesting to note that the decline in the Fram Strait sea ice volume export matches the decline in the overall sea ice volume in the Arctic Ocean. Thus, the percentage of sea ice volume exported every year (≈14%) has remained constant in recent decades [25]. This suggests again that over long time scales, the sea ice thinning is a dominant driver of the decrease in Fram Strait sea ice export. In 2017/2018, the strong positive sea-level pressure anomaly over the Eurasian Arctic, which extended to the western Barents Sea, reduced the sea ice thickness and drift in the Fram Strait, resulting in a low sea ice volume export [181,185]; however, it was the lasting Arctic sea ice thinning trend that caused the export to be extremely low (Fig. 4B) [181].

4.4. Summary of mechanisms

The interannual and decadal variations in the heat and freshwater transports in the 4 Arctic Ocean gateways are subject to drivers both inside and outside the Arctic. In addition to reviewing the literature, we quantified these relative contributions using dedicated numerical simulations. To better understand processes in the Arctic that influence the variability of Atlantic Water inflow through the Fram Strait, which to our knowledge were not well known before, we employed a set of wind perturbation simulations. Section 4 is summarized below.

• Pacific Water inflow: Previous model studies have found that the Pacific Water inflow is mainly determined by the wind-driven changes in the sea surface height gradient between the eastern Bering Sea shelf outside the Arctic and the Chukchi/East Siberian seas in the Arctic. In our simulations, the winds inside and outside the Arctic displayed similarly important effects on the interannual variability of the ocean volume transport in the Bering Strait when the past 5 decades are considered, while the Arctic winds played a more important role in driving the variability over the last 2 decades as revealed by previous satellite data and model studies. Nevertheless, the interannual variations in the heat and freshwater transports respond more to forcings from outside the Arctic because Pacific inflow temperature and salinity changes, associated with wind-driven circulation changes and thermal/freshwater surface forcing outside the Arctic, also influence the variability in the heat and freshwater transports.

• Atlantic Water inflow: Upstream forcing: The variability in the strength and spatial location of the Atlantic Water boundary current in the Nordic Seas can influence the Atlantic Water inflow in the Barents Sea Opening and Fram Strait. A positive NAO phase strengthens the cyclonic Atlantic Water boundary current in the Nordic Seas, thus increasing the Atlantic Water inflows through the 2 gateways. The Atlantic Water temperature in the Barents Sea Opening and Fram Strait is correlated with the temperature in the southern Norwegian Sea, but the air-sea heat flux along the Atlantic Water pathway in the Norwegian Sea strongly affects the ocean temperature. In particular, a reduction in surface heat loss helped maintain the warming trend in the Norwegian Sea and in the inflow into the Arctic Ocean in the 2010s.

• Atlantic Water inflow: Arctic forcing: Winds in the Arctic can also modulate the Atlantic Water inflow in the Barents Sea Opening (by changing the sea surface height gradient in the Barents Sea) and in the Fram Strait (by changing the halosteric sea surface height and thus the flow along the f/H contours in the Arctic basin). A vorticity gain in the Arctic basin, for example, associated with a positive Arctic Oscillation, negative Beaufort High anomaly, or positive Arctic Dipole Anomaly, can enhance the Atlantic Water inflow and thus weaken its recirculation in the Fram Strait. The recent Arctic sea ice decline also contributed to the strong increase in the Fram Strait heat transport in the 2010s because the reduction in the sea ice volume export through the Fram Strait resulted in a cyclonic anomaly in the Greenland Sea gyre circulation.

• Atlantic Water inflow in the Davis Strait: The variability in the heat transport to Baffin Bay through the eastern Davis Strait depends on both the Atlantic Water temperature in the Irminger Sea and modifications to the West Greenland Current by eddies and winds along the pathway. A reduction in offshore Ekman transport from the West Greenland Current can increase the amounts of ocean volume and ocean heat that remain close to the coast and propagate into Baffin Bay.

• Arctic export: Arctic forcing: In the Arctic, various modes of atmospheric circulation can influence Arctic freshwater exports differently. A positive Arctic Oscillation phase leads to the increased export of Arctic freshwater through the Fram Strait and reduced export through the Davis Strait after a short lag. A negative Beaufort High anomaly forces freshwater to be released from the Canada Basin, mainly through the Davis Strait. A positive Arctic Dipole Anomaly forcing increases freshwater export in the Fram Strait and reduces export in the Davis Strait to a similar extent. Freshwater export is also influenced by Arctic salinity changes; on interannual time scales, this is more the case for the Fram Strait export. The Arctic winds associated with the positive Arctic Oscillation in the 2010s are the main dynamic drivers of the increase in freshwater export in the Fram Strait in this period.

• Arctic export: Downstream forcing: The variability in the Davis Strait freshwater export is related to the sea surface height gradient between the northern CAA and northern Baffin Bay. The buoyancy-driven dynamic sea-level change south of Greenland can propagate to northern Baffin Bay as fast coastal waves and drive a considerable portion of the interannual variability in the Davis Strait volume and freshwater exports. When more Arctic waters are drawn out through the Davis Strait by a dynamic sea-level drop south of Greenland, less Arctic waters are exported through the Fram Strait. The strong dynamic sea-level drop in the Labrador Sea in the mid-to-late 2010s was the main dynamic driver for the rapid increase in freshwater export in the Davis Strait in this period.

• Sea ice export: Sea ice volume export variability in the Fram Strait is influenced by both the Arctic Dipole Anomaly and Arctic Oscillation. The Dipole Anomaly is important in different seasons, while the Arctic Oscillation has the largest impact in winter. The declining trend in the export is mainly caused by Arctic sea ice thinning. The recent extremely low sea ice volume export in 2017/2018 was associated with a strong northward wind anomaly in the Eurasian Arctic. However, without the preconditioning of the Arctic sea ice thinning, the wind anomaly alone would not have caused the export to be that low.

5. Future projections

5.1. Arctic Ocean heat budget

In the CMIP6 SSP585 scenario (the highest CO_2 emission scenario in CMIP6), the mean Arctic Ocean temperature is projected to increase by 1.55°C at the end of the 21st century relative to the 1980–2000 average, corresponding to a heat content increase of 8.5×10^{22} J (Fig. 8A). The CMIP6 models suggest that the Atlantic Water layer will experience the strongest warming in the Arctic Ocean, reaching approximately 3°C, which is roughly twice the global mean warming in the same depth range [74,129]. The phenomenon of faster Arctic Ocean warming than the global ocean mean, called Arctic Ocean Amplification, can be attributed to increasing oceanic heat convergence via the inflow of Atlantic and Pacific waters [74]. This phenomenon very possibly emerged at the end of the 20th century according to analyses of coupled model simulations [74].

In CMIP6 simulations, the ocean heat transport through the Barents Sea Opening will contribute the most to the Arctic Ocean heat content change, with an increase of 78 ± 70 TW in 2090–2100 relative to the mean in 1980–2000 (Table 1 and Fig. 8C). The ocean volume transport in the Barents Sea Opening is projected to increase (Table 1), but the major increase in the heat transport can be attributed to the warming of the inflow water [74]. The ocean volume transport in the Bering Strait is projected to decrease in the future [note, however, that numerical models tend to be unable to simulate the currently observed increase in the volume transport through the Bering Strait (see section 3.1), which casts some doubts regarding their ability to correctly predict future volume transport change] (Table 1, [126,128]), but the strong warming of the Pacific Water will cause heat transport to increase. The Bering Strait heat transport in 2090–2100 is projected to be 19 ± 7 TW higher than that in 1980–2000, representing the second largest source of Arctic Ocean warming. According to CMIP6 models, both the Fram Strait and Davis Strait throughflows will become heat sinks of the Arctic Ocean (Fig. 8C and Table 1) because of the warming of the outflow waters in the 2 straits and the increase in Fram Strait net (outflow) volume transport in the future [74].

In response to the overall increase in ocean heat convergence to the Arctic Ocean, the ocean surface heat loss will increase until approximately 2070, followed by a slight drop (Fig. 8C and E) as a result of reduced surface cooling efficiency along the Atlantic and Pacific water inflow pathways [70,74]. The increase in ocean surface heat loss will only partially counterbalance the increase in Arctic Ocean heat gain, so the Arctic Ocean net heat budget will increase persistently over the 21st century (thick black line in Fig. 8E), leading to the accelerated warming of the Arctic Ocean (Fig. 8A).

5.2. Arctic Ocean freshwater budget

The Arctic Ocean salinity is projected to decrease by approximately 0.16 on average at the end of the 21st century in the CMIP6 SSP585 scenario, corresponding to a freshwater content increase of approximately 57,000 km^3 (Fig. 8B, [126]), which is similar to the value projected in the previous CMIP models [32]. The magnitude of the increase in liquid freshwater content depends not only on the changes in freshwater sources but also on the freshwater storage capability of the Arctic Ocean, which is subject to the increase in ocean surface stress associated with sea ice decline [292]. The strongest Arctic Ocean freshening [O(1 psu) on average] will occur in the upper ~100 m [129].

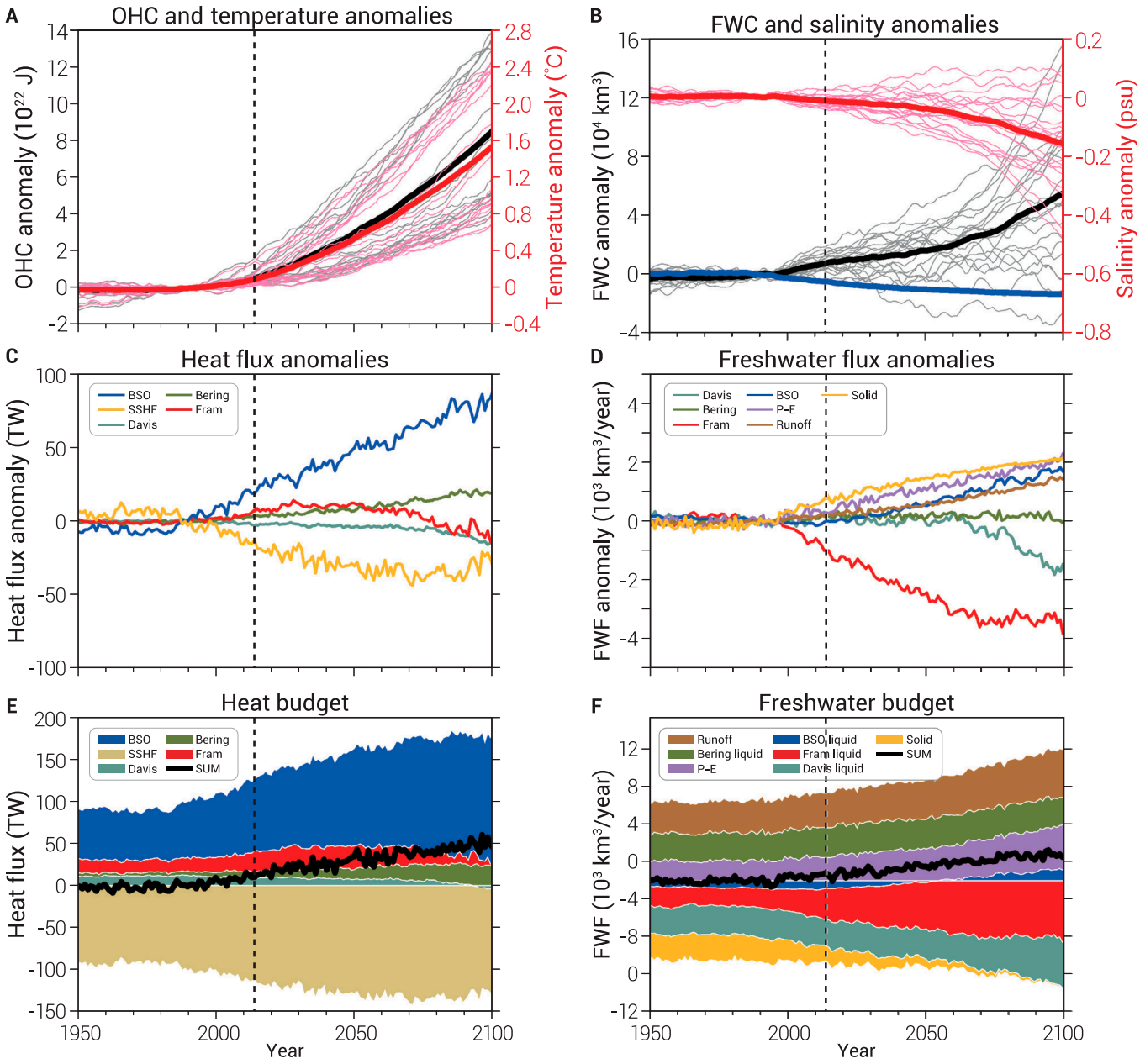

Fig. 8. CMIP6 historical and SSP585 results (periods separated by the vertical dashed lines). Anomalies of the Arctic Ocean (A) heat content (black) and temperature (red), (B) liquid (black) and solid (blue) freshwater contents and salinity (red), (C) heat budget terms, and (D) freshwater budget terms. The anomalies are relative to 1980–2000 means. (E) Arctic Ocean heat budget. (F) Arctic Ocean freshwater budget. Ocean heat and freshwater transports are calculated relative to 0°C and 34.8, respectively. In (A) and (B), the thin lines represent the results of individual models to illustrate the large model spreads. The model data used in this figure are described by Shu et al. [74] and Wang et al. [126]. OHC, ocean heat content; FWC, freshwater content; BSO, Barents Sea Opening; SSHF, sea surface heat flux; P-E, precipitation minus evaporation.

In the SSP585 scenario, the annual mean solid (sea ice) freshwater content will decrease by 13,000 km^3 at the end of the 21st century compared to that in the 1980–2000 period (Fig. 8B), with only 400 km^3 remaining.

Compared to the CMIP5 projection, CMIP6 projected somehow larger and faster changes in the hydrological cycle related to stronger climate sensitivity [293]. Consistent with what can be expected from a strengthened hydrological cycle in a warming climate [18], the river runoff and net precipitation minus evaporation will increase (by 1,400 km^3/year and 2,000 km^3/year, respectively, in the SSP585 scenario; Fig. 8D), and consequently, liquid freshwater exports through the Fram and Davis straits will increase (by 3,400 ± 2,400 km^3/year and 1,500 ± 2,300 km^3/year, respectively) in 2090–2100 relative to 1980–2000 (Table 1 and Fig. 8D). The increase in freshwater export in the Davis Strait will be delayed because the Davis Strait ocean volume export will first decrease until the 2060s and then increase again [126,128]. Accordingly, the Fram Strait ocean volume export will decrease after the 2060s, causing the Fram Strait freshwater export to level off (Fig. 8D). The models predict that the freshwater transport through the Bering Strait is unlikely to undergo marked changes in the future. This is due to the compensating effects of

2 trends: the freshening of the Pacific inflow and the reduction in its volume transport [126]. The latter is a result of the simulated increase in dynamic sea level in the East Siberian and Chukchi seas in the future [note, however, that numerical models tend to be unable to simulate the currently observed increase in the volume transport through the Bering Strait (see section 3.1), which casts some doubts regarding their ability to correctly predict future volume transport change] [126]. Due to the freshening of the Atlantic Water, the Barents Sea Opening 0inflow will become a freshwater source of the Arctic Ocean after the mid-century, with an increase of 1,700 ± 1,500 km^3/year freshwater transport in 2090–2100 relative to 1980–2000 (Table 1 and Fig. 8D). This changing role in the Barents Sea inflow is a robust feature in different sets of CMIP6 models [126,128] and is quantitatively similar to the projected changes in the high emission scenario RCP8.5 of CMIP5 [294]. As expected from persistent Arctic sea ice decline, the Fram Strait sea ice freshwater export is projected to decrease by 1,500 ± 900 km^3/year in 2090–2100 relative to 1980–2000 (Table 1). This reduction actually renders nearly vanishing sea ice transport at the end of the 21st century in the models (Fig. 8F).

In the SSP245 scenario of CMIP6, which represents a medium pathway of future greenhouse gas emissions assuming that climate protection measures are being taken, the projected changes in Arctic freshwater budget and content are qualitatively similar to those in the SSP585 scenario shown in Fig. 8B and D, with increases in the liquid freshwater content and the magnitude of liquid freshwater transports and reductions in the solid freshwater content and the magnitude of solid freshwater transports [126]. Even quantitatively, the projected changes in the liquid freshwater content and transports are very similar between these 2 scenarios before 2060, after which the projected changes in SSP245 become obviously slower than those in SSP585 [126]. The projected changes in the solid (sea ice) freshwater content and transports are more sensitive to greenhouse gas emission levels, with noticeable quantitative differences between the 2 scenarios already in the 2030s [126]. The pace of the changes in the liquid freshwater budget in the most optimistic scenario SSP126 (compatible with the 2°C target) is also very similar to that in the SSP585 scenario before 2050 [128]. It is worth noting that model spreads are large among CMIP simulations and even larger than climate change signals in some cases, as reported in all the CMIP studies cited above.

5.3. Summary of future projections

• According to the CMIP6 results described above, the Arctic Ocean warming rate will remain approximately twice the global mean rate in the depth range of the Arctic Atlantic Water layer (150 to 900 m), which will be sustained by increasing ocean heat transports into the Arctic Ocean (Fig. 9). The increase in ocean heat transports will be mainly due to the warming of the inflow waters, although changes in ocean volume transports can have impacts on ocean heat transports in individual gateways. The net heat transport through the Barents Sea Opening will be the largest heat source of the Arctic Ocean among the net heat transports through different Arctic gateways.

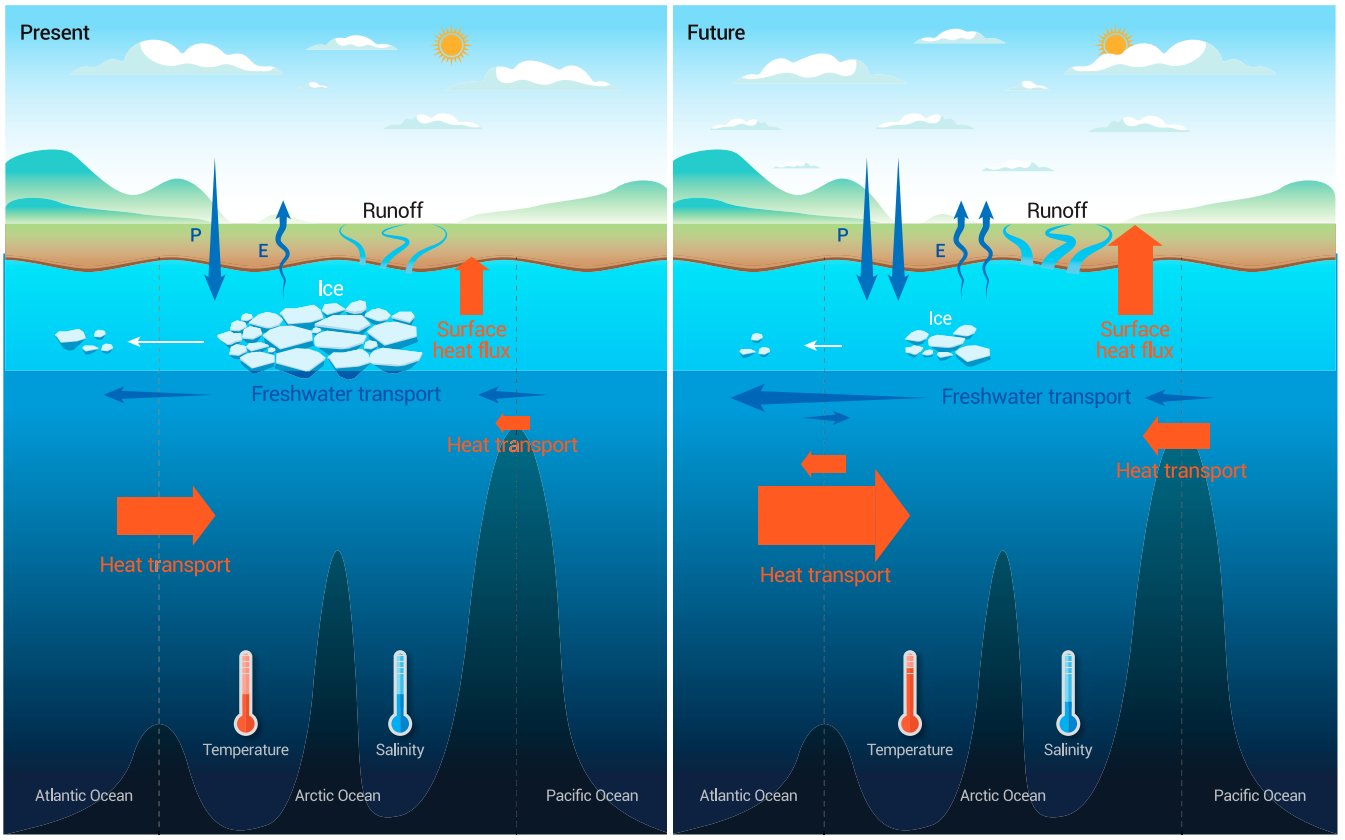

Fig. 9. Schematic showing changes in Arctic Ocean heat (red arrows) and freshwater (blue arrows) budgets in a warming climate. The poleward ocean heat convergence and the hydrological cycle are strengthened with climate warming. P, precipitation; E, evaporation.

• The hydrological cycle will intensify in the future. Consistent with previous coupled model projections [294–298], CMIP6 models suggest increases in the liquid freshwater content, surface fluxes, and gateway exports and reductions in the solid freshwater content and gateway exports over the 21st century (Fig. 9) [126,128]. Over the 21st century, the Arctic Ocean will experience a freshwater content increase of more than 50% in the CMIP6 SSP585 scenario. At the end of the 21st century, river runoff and P-E will be the largest Arctic freshwater sources, followed by Pacific Water inflow through the Bering Strait (Fig. 8F). The largest Arctic freshwater loss will be via the Fram Strait outflow, followed by the Davis Strait outflow.

The projected nonmonotonic changes in the distribution of ocean volume transports between the Davis and Fram straits considerably influence the future evolution of freshwater transports in these 2 gateways (Fig. 8D, [126,128]). Atmospheric forcing and ocean circulations in both the Arctic and subpolar gyre regions can influence the partitioning of ocean volume exports between the 2 gateways (see section 4.3). Our understanding of the long-term changes in the ocean volume transports in these gateways is constrained by the uncertainties of climate models. In particular, the CMIP6 models disagree on the behavior of liquid freshwater export in the Davis Strait in the early-to-mid 21st century due to differences in the magnitude and timing of the simulated decrease in the Davis Strait volume transport [128].

The net heat transport into the Arctic basin through the Fram Strait will not increase much in the coming decades, and it will finally become negative at the end of the 21st century (Fig. 8C). The northward heat transport in the Western Spitsbergen Current actually will increase more than the heat transport in the Barents Sea Opening, but the increase in the southward heat transport in the East Greenland Current will outweigh the increase in the northward transport (figure 4 in [74]). To understand the impact of Fram Strait inflow on the Arctic basin temperature, stratification, and sea ice, it is necessary to know the fraction of Atlantic Water that recirculates in the Fram Strait and the fraction that transits the Arctic subbasins before returning to the Fram Strait. The partitioning is not fully understood for the current climate, and much less is known for the future warming climate. For example, mesoscale ocean eddies are believed to have a strong influence on recirculation in the Fram Strait [167,237], but CMIP6 models typically have horizontal resolutions of a few tens of kilometers, far coarser than the resolution required to resolve eddies in this region [O(1 km)]. The northward heat transport in the Davis Strait is also projected to increase in the future [74], although the net heat transport in the Davis Strait will not change much (Fig. 8C). To assess the potential impacts of ocean warming on marine-terminating glaciers on the western and eastern sides of Greenland, how the northward heat transport through the Davis Strait and the recirculation Atlantic Water from the Fram Strait will change in the future should be better understood, for which eddy-resolving climate model projections with improved representations of physical processes are ultimately needed.

6. Discussion

In this paper, we reviewed the past and projected future changes in the Arctic–Subarctic ocean linkages and the driving mechanisms. We combined observations, historical-period OMIP simulations, and dedicated numerical simulations using the FESOM model to understand the past changes (section 3) and the driving mechanisms (section 4). The future changes were discussed mainly based on CMIP6 simulations (section 5). The reviews were summarized for each topic at the end of the corresponding section. In particular, we concluded that both the ocean heat convergence to the Arctic Ocean and the hydrological cycle were stronger in 2000–2020 than in 1980–2000 and they will continue to be intensified in future warming climate. We also addressed that variabilities and changes in Arctic gateway fluxes could have origins both inside and outside the Arctic.

Changes in the Arctic–Subarctic ocean transports in different Arctic gateways should be interpreted comprehensively. As we noted in this paper, the Fram Strait freshwater outflow can influence the heat budget in the Greenland Sea, with potential impacts on Atlantic Water circulating northeast of the gyre; an increase in freshwater export through the Davis Strait due to a dynamic sea-level drop south of Greenland reduces the freshwater export in the Fram Strait; winds in the Arctic can change the freshwater exports through the Fram and Davis straits simultaneously; the Bering Strait freshwater inflow influences the amount of freshwater exported to the subpolar North Atlantic. To achieve a comprehensive understanding of all the linked changes in the Arctic Ocean and beyond, both observation and modeling capabilities need to be further improved.

We note that one needs to bear in mind the ambiguities concerning heat and freshwater transports across open gateways, as discussed in section 2.3. That is, statements about changes in heat and freshwater transports are valid for the reference temperature and salinity we used, but may not be valid for other reference values.

6.1. Observations

Observations are essential for understanding ocean and sea ice changes and for judging model fidelity. Modern measurements of Arctic–Subarctic ocean and sea ice transports have started since the 1990s, but the lateral and/or vertical resolutions of the year-round ocean observations are relatively low and in some cases only parts of the ocean currents are covered by moorings [54,112]. The moorings in the western Fram Strait do not cover the inner continental shelf (Fig. 1B), and possibly more than 40% of the Fram Strait freshwater export is not observed with year-round instruments [176]. For the Davis Strait, the observational estimates of freshwater export are currently available for only a few years [24]. Challenges have also been reported in comparing simulated and observed Atlantic Water heat transports in the Barents Sea Opening. Although they agree on the upward trend over the past decades, on interannual timescales the simulated and observed heat transports in the Barents Sea Opening are surprisingly anti-correlated [188]. It was speculated that the spatial resolution of mooring instruments in the Barents Sea Opening is too low to capture all the flow variations (Fig. 1B) [63]. One additional challenge is that the observation-based ocean volume transports through the Arctic Ocean gateways have substantial uncertainties (Table 1). The uncertainty of the Fram Strait volume transport could be even larger than the mean transport values of other gateways. An imbalance in the ocean volume transports through the gateways causes uncertainty in the estimates of the Arctic Ocean heat and freshwater budgets [299].

The observation capability for monitoring the Arctic–Subarctic ocean and sea ice transports has recently been improved to some extent. This paper addresses the rich dynamics of the

warm water inflow in the Fram Strait, which is subject to remote forcing over the Nordic Seas and Arctic Ocean, and to local eddy dynamics and winds. The partitioning of the Atlantic Water into recirculation and poleward branches is one of the key factors influencing the final inflow into the Arctic deep basin, and a single traditional longitudinal mooring array might not suffice for capturing all the important processes. The recent deployment of moorings and the new observations from gliders and cruises in the northeastern Fram Strait and north of Svalbard are expected to improve the observations of Atlantic Water circulation, inflow, and transformation [103,168,240]. In the western part of the Fram Strait mooring array at 78°50′N, one additional mooring and more sampling points at most of the existing moorings have been added since 2015, which improved the measurements of temperature, salinity, and currents, especially near the surface and in the 100 to 150 m depth range [118]. This significantly enhanced the monitoring of ocean transports via the East Greenland Current, although year-round measurements of transports across the inner continental shelf are still lacking [176].

Different techniques have been applied to address the issue of lacking or insufficient observations. Inverse modeling that combines current and temperature observations in different Arctic gateways was successfully used to infer ocean heat transports [158]. However, the obtained estimates might not be fully consistent with individual observations focusing on Atlantic heat inflow into the Nordic Seas [154], possibly due to the sparseness of the observational data input for inverse modeling. The recent development of an Arctic Ocean state estimate product for the period of 2002–2017 using a dynamically and kinematically consistent approach to combine modeling and observations can effectively reduce some of the model misfits [300]. However, challenges remain. For example, the estimated freshwater transports in the Fram and Bering straits are much lower than the estimates based on observations. Therefore, using models constrained by the currently available observations cannot fully resolve issues related to insufficient observations. It is necessary to improve and increase observations for key ocean and sea ice parameters.

6.2. Modeling

Models have been increasingly used for understanding ocean dynamics and changes, including for the Arctic Ocean [301]. It is known that models have different issues in the representation of the Arctic Ocean and sea ice as shown in previous model intercomparison studies [125,126,128,129,188,226,279,302–307]. The model spreads in the simulated ocean states and transports are large in both the OMIP and CMIP6 simulations, and they should be considered when interpreting the simulated climate change signals.

Using multi-model-mean values reduces the risk of obtaining extremely biased results with a single model, but common model biases remain. For example, none of the publicly available OMIP2 models reproduced the observed upward trends in ocean volume and heat transports through the Bering Strait. A comparison of simulated and observed sea-level changes indicated that the model deficiency is likely associated with a pronounced sea surface height drop in the northern Bering Sea and (to a lesser extent) with an overestimated sea surface height increase in the western Chukchi Sea in the 2010s in the models, but the exact reasons for the erroneous sea surface height changes remain unknown [124]. The inability of ocean–ice models to simulate past changes raises concerns about whether the simulated future decreasing trends in Pacific Water inflow in CMIP6 coupled climate models are reliable.

CMIP6 models tend to project different magnitudes and timings of the decrease in the Davis Strait volume transport in future warming climate [128]. First, the typically used model resolutions cannot adequately resolve the narrow straits in the CAA, which could influence the distribution of Arctic exports between the Davis and Fram straits. This was suggested to be one of the main reasons for the large biases in Davis Strait volume and freshwater transports in some models [124,125]. The resolution required to accurately resolve the throughflow in the CAA is high, given the narrowness of the straits [280]. This poses a challenge for the current coupled climate models. Second, the Davis Strait volume transport is sensitive to different atmospheric circulation modes in the Arctic and to the sea surface height south of Greenland (section 4.3). Uncertainties in projected changes in Arctic winds and in North Atlantic circulations could then contribute to the uncertainty of the simulated Davis Strait transports. Therefore, to reduce the uncertainty of Davis Strait transports in coupled climate models, it is necessary to improve different components of climate models.

It was suggested that the low resolution of the ocean models is one of the main reasons for the underestimation of Atlantic heat transport into the Arctic Ocean in current coupled climate models [308]. Using eddy-resolving resolution could more realistically represent the Atlantic Water circulation in the Fram Strait [167]. Additionally, the transport of Atlantic Water in the Norwegian Atlantic Current and freshwater in the Norwegian Coastal Current could be more reasonably simulated at high resolutions [58,164]. Improved ocean hindcasts and future projections are expected if high model resolutions are used in the next phases of CMIP and OMIP. However, investigations into model parameterizations, numerics, and the coupling between model components are also needed, as not all model issues are related to model resolution [131,198,226,309]. A recent analysis of CMIP6 simulations revealed that future increases in ocean heat transports into the Arctic Ocean and thus the changes in the Arctic sea ice cover, ocean surface heat flux, mixed layer depth, and air temperature in wintertime are strongly influenced by the ocean model component of coupled climate models, with one particular family of climate models predicting much larger future Arctic climate change than other climate models [310]. This implies that improving ocean models in terms of representing poleward ocean heat transports could substantially reduce the overall uncertainty of the Arctic climate change projections obtained with coupled climate models.

Despite the limitations associated with the current observations and models, our review provides an updated understanding of the status, changes, and driving mechanisms of the Arctic–Subarctic ocean linkages. Warming trends in the Arctic inflow waters in the 20th and early 21st centuries can be well determined based on the synthesis of observations and models (Table 2), even if masked by multi-decadal variability. The unprecedented warming observed in the Arctic Atlantic Water layer is consistent with the increase in the ocean heat transports through the Arctic gateways [104,170]. CMIP6 simulations further suggest that Arctic Ocean Amplification emerged at the end of the 20th century and will continue through the 21st century as a result of poleward ocean heat convergence [74], although, currently, observational corroboration is difficult due to the sparseness of ocean observations at depth in the past and the low signal-to-noise ratio. The emergence of climate change signals in freshwater transports

through Arctic gateways has been mainly studied based on climate model results [298]. Our synthesis of observations and hindcast model simulations suggests the occurrence of record lows in salinity and record highs in freshwater transports in the Pacific inflow and Arctic outflows in the 2010s (Table 2). Record highs and lows beyond the range of natural variability imply forced ocean changes in a changing climate. Future improvements in both model fidelity and observation capability will facilitate the enhanced identification and understanding of climate change signals in Arctic–Subarctic ocean linkages.

Acknowledgments

This study was motivated by the plenary discussions in the Arctic–Subarctic Ocean Fluxes (ASOF) workshops over the last few years. The authors thank the 3 anonymous reviewers for their helpful comments. **Funding:** Q.W. was supported by the German Helmholtz Climate Initiative REKLIM (Regional Climate Change and Humans) and the German Federal Ministry for Education and Research (BMBF) within the EPICA project (grant no. 03F0889A). Q.S. was supported by the Taishan Scholars Program (no. tsqn202211264) and the Shandong Provincial Natural Science Foundation (ZR2022JQ17). S.W. was supported by the National Natural Science Foundation of China (grant no. 42005044). G.S. was supported by the German Research Foundation (DFG, Deutsche Forschungsgemeinschaft) through the Transregional Collaborative Research Center TRR 172 "(AC)3 – Arctic Amplification" (grant no. 268020496) and the European Union's Horizon 2020 research and innovation programme via project CRiceS (grant no. 101003826). The Bering Strait work is supported by NSF-OPP Arctic Observing Network grants 1758565 and 2153942. P.G.M. was supported by the Natural Sciences and Engineering Research Council of Canada via research grant rgpin227438-09. The Fram Strait Arctic Outflow Observatory is supported by the Norwegian Polar Institute and by the Norwegian Research Council through the FRIPRO program (FreshArc, grant 286971). C.M.L. and the Davis Strait observing system are supported by the U.S. National Science Foundation Arctic Observing Network under grant 1902595. **Author contributions:** Q.W. performed and analyzed the FESOM simulations and wrote the first draft of the paper. Q.S. and S.W. analyzed the OMIP and CMIP6 simulations and created corresponding plots. All authors contributed to the discussions of the scientific content and to the improvement of the manuscript. **Competing interests:** The authors declare that they have no competing interests.

References

1. Woodgate RA, Peralta-Ferriz C. Warming and freshening of the Pacific inflow to the Arctic from 1990-2019 implying dramatic shoaling in Pacific Winter water ventilation of the Arctic water column. *Geophys Res Lett*. 2021;48(9):Article e2021GL092528.
2. Aagaard K, Carmack EC. The role of sea ice and other fresh water in the Arctic circulation. *J Geophys Res*. 1989;94(C10):14485–14498.
3. Roach AT, Aagaard K, Pease C, Salo SA, Weingartner T, Pavlov V, Kulakov M. Direct measurements of transport and water properties through the Bering Strait. *J Geophys Res Oceans*. 1995;100(C9):18443–18457.
4. Woodgate RA, Aagaard K. Revising the Bering Strait freshwater flux into the Arctic Ocean. *Geophys Res Lett*. 2005;32(2):Article L02602.
5. Woodgate RA, Weingartner T, Lindsay R. The 2007 Bering Strait oceanic heat flux and anomalous Arctic sea-ice retreat. *Geophys Res Lett*. 2010;37(1):Article L01602.
6. Woodgate RA, Aagaard K, Swift JH, Falkner KK, Smethie WM Jr. Pacific ventilation of the Arctic Ocean's lower halocline by upwelling and diapycnal mixing over the continental margin. *Geophys Res Lett*. 2005;32(18):Article L18609.
7. Shaffer G, Bendtsen J. Role of the Bering Strait in controlling North Atlantic ocean circulation and climate. *Nature*. 1994;367:354–357.
8. Goosse H, Fichefet T, Campin JM. The effects of the water flow through the Canadian Archipelago in a global ice-ocean model. *Geophys Res Lett*. 1997;24(12):1507–1510.
9. De Boer AM, Nof D. The Bering Strait's grip on the northern hemisphere climate. *Deep Sea Res I Oceanogr Res Pap*. 2004;51(10):1347–1366.
10. de Boer AM, Nof D. The exhaust valve of the North Atlantic. *J Clim*. 2004;17(3):417–422.
11. Hu A, Meehl GA, Han W. Role of the Bering Strait in the thermohaline circulation and abrupt climate change. *Geophys Res Lett*. 2007;34(5):Article L05704.
12. Hu A, Meehl GA, Otto-Bliesner BL, Waelbroeck C, Han W, Loutre M-F, Lambeck K, Mitrovica JX, Rosenbloom N. Influence of Bering Strait flow and North Atlantic circulation on glacial sea-level changes. *Nat Geosci*. 2010;3:118–121.
13. Walsh JJ, McRoy CP, Coachman LK, Goering JJ, Nihoul JJ, Whitledge TE, Blackburn TH, Parker PL, Wirick CD, Shuert PG, et al. Carbon and nitrogen cycling within the Bering/Chukchi Seas: Source regions for organic matter effecting AOU demands of the Arctic Ocean. *Prog Oceanogr*. 1989;22(4):277–359.
14. Popova EE, Yool A, Aksenov Y, Coward AC. Role of advection in Arctic Ocean lower trophic dynamics: A modeling perspective. *J Geophys Res Oceans*. 2013;118(3):1571–1586.
15. Torres-Valdés S, Tsubouchi T, Bacon S, Naveira-Garabato AC, Sanders R, McLaughlin FA, Petrie B, Kattner G, Azetsu-Scott K, Whitledge TE. Export of nutrients from the Arctic Ocean. *J Geophys Res Oceans*. 2013;118(4):1625–1644.
16. Serreze MC, Barrett AP, Slater AG, Woodgate RA, Aagaard K, Lammers RB, Steele M, Moritz R, Meredith M, Lee CM. The large-scale freshwater cycle of the Arctic. *J Geophys Res Oceans*. 2006;111(C11):C11010.
17. Dickson R, Rudels B, Dye S, Karcher M, Meincke J, Yashayaev I. Current estimates of freshwater flux through Arctic and subarctic seas. *Prog Oceanogr*. 2007;73(3-4):210–230.
18. Carmack E, Yamamoto-Kawai M, Haine T, Bacon S, Bluhm BA, Lique C, Melling H, Polyakov IV, Straneo F, Timmermans M-L, et al. Freshwater and its role in the Arctic Marine System: Sources, disposition, storage, export, and physical and biogeochemical consequences in the Arctic and global oceans. *J Geophys Res Biogeosci*. 2016;121(3):675–717.
19. Kwok R, Rothrock DA. Variability of Fram Strait ice flux and North Atlantic Oscillation. *J Geophys Res Oceans*. 1999;104(C3):5177–5189.
20. Vinje T. Fram strait ice fluxes and atmospheric circulation: 1950-2000. *J Clim*. 2001;14(16):3508–3517.

21. Cuny J, Rhines PB, Kwok R. Davis Strait volume, freshwater and heat fluxes. *Deep Sea Res I Oceanogr Res Pap*. 2005;52:519–542.
22. de Steur L, Hansen E, Gerdes R, Karcher M, Fahrbach E, Holfort J. Freshwater fluxes in the east greenland current: A decade of observations. *Geophys Res Lett*. 2009;36(23):Article L23611.
23. de Steur L, Peralta-Ferriz C, Pavlova O. Freshwater export in the East Greenland Current freshens the North Atlantic. *Geophys Res Lett*. 2018;45(24):13,359–13,366.
24. Curry B, Lee CM, Petrie B, Moritz RE, Kwok R. Multiyear volume, liquid freshwater, and sea ice transports through Davis Strait, 2004–10. *J Phys Oceanogr*. 2014;44(4): 1244–1266.
25. Spreen G, de Steur L, Divine D, Gerland S, Hansen E, Kwok R. Arctic sea ice volume export through Fram Strait from 1992 to 2014. *J Geophys Res Oceans*. 2020;125(6):Article e2019JC016039.
26. Prinsenberg SJ, Hamilton J. Monitoring the volume, freshwater and heat fluxes passing through Lancaster Sound in the Canadian Arctic Archipelago. *Atmos Ocean*. 2005;43(1):1–22.
27. Prinsenberg S, Hamilton J, Peterson I, Pettipas R. Observing and interpreting the seasonal variability of the oceanographic fluxes passing through Lancaster Sound of the Canadian Arctic Archipelago. In: Nihoul J, editor. *Influence of climate change on the changing Arctic and sub-Arctic conditions.* Dordrecht: Springer; 2009. p. 125–143.
28. Melling H. Exchanges of freshwater through the shallow straits of the North American Arctic. In: Lewis EL, editor. *The freshwater budget of the Arctic Ocean.* New York (NY): Springer; 2000. p. 479–502.
29. Melling H, Agnew TA, Falkner KK, Greenberg DA, Lee CM, Münchow A, Petrie B, Prinsenberg SJ, Samelson RM, Woodgate RA. Fresh-water fluxes via Pacific and Arctic outflows across the Canadian polar shelf. In: Dickson PR, Meincke J, editors. *Arctic-Subarctic ocean fluxes: Defining the role of the northern seas in climate.* Dordrecht: Springer; 2008. p. 193–247.
30. Peterson I, Hamilton J, Prinsenberg S, Pettipas R. Wind-forcing of volume transport through Lancaster Sound. *J Geophys Res Oceans*. 2012;117(C11):Article C11018.
31. Münchow A. Volume and freshwater flux observations from Nares Strait to the west of Greenland at daily time scales from 2003 to 2009. *J Phys Oceanogr*. 2016;46(1):141–157.
32. Haine T, Curry B, Gerdes R, Hansen E, Karcher M, Lee C, Rudels B, Spreen G, de Steur L, Stewart K, et al. Arctic freshwater export: Status, mechanisms, and prospects. *Glob Planet Chang*. 2015;125:13–35.
33. Aagaard K, Swift JH, Carmack E. Thermohaline circulation in the Arctic mediterranean seas. *J Geophys Res Oceans*. 1985;90(C3):4833–4846.
34. Hakkinen S. A simulation of thermohaline effects of a great salinity anomaly. *J Clim*. 1999;12(6):1781–1795.
35. Arzel O, Fichefet T, Goosse H, Dufresne J-L. Causes and impacts of changes in the Arctic freshwater budget during the 20th and 21st centuries in an AOGCM. *Clim Dyn*. 2008;30:37–58.
36. Le Bras I, Straneo F, Muilwijk M, Smedsrud LH, Li F, Lozier MS, Holliday NP. How much Arctic fresh water participates in the subpolar overturning circulation? *J Phys Oceanogr*. 2021;51(3):955–973.
37. Zhang J, Weijer W, Steele M, Cheng W, Verma T, Veneziani M. Labrador Sea freshening linked to Beaufort Gyre freshwater release. *Nat Commun*. 2021;12:Article 1229.
38. Dickson R, Meincke J, Malmberg S, Lee AJ. The "great salinity anomaly" in the Northern North Atlantic 1968–1982. *Prog Oceanogr*. 1988;20(2):103–151.
39. Belkin IM. Propagation of the "Great Salinity Anomaly"of the 1990s around the northern North Atlantic. *Geophys Res Lett*. 2004;31(8):Article L08306.
40. Stouffer RJ, Yin J, Gregory JM, Dixon KW, Spelman MJ, Hurlin W, Weaver AJ, Eby M, Flato GM, Hasumi H, et al. Investigating the causes of the response of the thermohaline circulation to past and future climate changes. *J Clim*. 2006;19(8):1365–1387.
41. Jahn A, Holland MM. Implications of arctic sea ice changes for North Atlantic deep convection and the meridional overturning circulation in CCSM4-CMIP5 simulations. *Geophys Res Lett*. 2013;40(6):1206–1211.
42. Weijer W, Cheng W, Drijfhout SS, Fedorov AV, Hu A, Jackson LC, Liu W, McDonagh EL, Mecking JV, Zhang J. Stability of the atlantic meridional overturning circulation: A review and synthesis. *J Geophys Res Oceans*. 2019;124(8):5336–5375.
43. Komuro Y, Hasumi H. Intensification of the Atlantic deep circulation by the Canadian Archipelago throughflow. *J Phys Oceanogr*. 2005;35(5):775–789.
44. Wang H, Legg S, Hallberg R. The effect of Arctic freshwater pathways on North Atlantic convection and the Atlantic Meridional Overturning Circulation. *J Clim*. 2018;31(13):5165–5188.
45. Azetsu-Scott K, Clarke A, Falkner K, Hamilton J, Jones EP, Lee C, Petrie B, Prinsenberg S, Starr M, Yeats P. Calcium carbonate saturation states in the waters of the Canadian Arctic Archipelago and the Labrador Sea. *J Geophys Res Oceans*. 2010;115(C11):Article C11021.
46. Hátún H, Azetsu-Scott K, Somavilla R, Rey F, Johnson C, Mathis M, Mikolajewicz U, Coupel P, Tremblay JE, Hartman S, et al. The subpolar gyre regulates silicate concentrations in the North Atlantic. *Sci Rep*. 2017;7:14576.
47. Rudels B, Friedrich H. The transformation of the Atlantic Water in the Arctic Ocean and their significance for the freshwaer budget. In: Lewis EL, editor. *The freshwater budget of the Arctic Ocean*. Dordrecht: Springer; 2000. p. 503–532.
48. Rudels B. Arctic Ocean circulation, processes and water masses: A description of observations and ideas with focus on the period prior to the International Polar Year 2007–2009. *Prog Oceanogr*. 2015;132:22–67.
49. Ingvaldsen R, Loeng H, Asplin L. Variability in the Atlantic inflow to the Barents Sea based on a one-year time series from moored current meters. *Cont Shelf Res*. 2002;22(3):505–519.
50. Schauer U, Beszczynska-Möller A, Walczowski W, Fahrbach E, Piechura J, Hansen E. Variation of measured heat flow through the Fram Strait between 1997 and 2006. In: Dickson RR, Meincke J, Rhines P, editors. *Arctic-Subarctic ocean fluxes: Defining the role of the northern seas in climate.* Dordrecht: Springer; 2008. p. 65–85.
51. Skagseth O, Furevik T, Ingvaldsen R, Mork H, Orvik K, Ozhigi V. Volume and heat transports to the Arctic Ocean via the Norwegian and Barents Seas. In: Dickson RR,

Meincke J, Rhines P, editors. *Arctic-Subarctic ocean fluxes: Defining the role of the northern seas in climate*. Dordrecht: Springer; 2008. p. 45–64.
52. Beszczynska-Moeller A, Fahrbach E, Schauer U, Hansen E. Variability in Atlantic water temperature and transport at the entrance to the Arctic Ocean, 1997–2010. *ICES J Mar Sci*. 2012;69:852–863.
53. Smedsrud LH, Esau I, Ingvaldsen RB, Eldevik T, Haugan PM, Li C, Lien VS, Olsen A, Omar AM, Otterå OH, et al. The role of the Barents Sea in the Arctic climate system. *Rev Geophys*. 2013;51(3):415–449.
54. Østerhus S, Woodgate R, Valdimarsson H, Turrell B, de Steur L, Quadfasel D, Olsen SM, Moritz M, Lee CM, Larsen KMH, et al. Arctic Mediterranean exchanges: A consistent volume budget and trends in transports from two decades of observations. *Ocean Sci*. 2019;15:379–399.
55. Orvik KA, Niiler P. Major pathways of Atlantic water in the northern North Atlantic and Nordic Seas toward Arctic. *Geophys Res Lett*. 2002;29(19):1896.
56. Koszalka I, LaCasce JH, Andersson M, Orvik KA, Mauritzen C. Surface circulation in the Nordic Seas from clustered drifters. *Deep Sea Res I Oceanogr Res Pap*. 2011;58(4):468–485.
57. Johannessen JA, Raj RP, Nilsen JEØ, Pripp T, Knudsen P, Counillon F, Stammer D, Bertino L, Andersen OB, Serra N, et al. Toward improved estimation of the dynamic topography and ocean circulation in the high latitude and Arctic Ocean: The importance of GOCE. *Surv Geophys*. 2014;35:661–679.
58. Wekerle C, Wang Q, Danilov S, Schourup-Kristensen V, von Appen W-J, Jung T. Atlantic Water in the Nordic Seas: Locally eddy-permitting ocean simulation in a global setup. *J Geophys Res Oceans*. 2017;122(2):914–940.
59. Broomé S, Chafik L, Nilsson J. A satellite-based lagrangian perspective on Atlantic Water fractionation between Arctic gateways. *J Geophys Res Oceans*. 2021;126(11):Article e2021JC017248.
60. Basedow SL, Sundfjord A, von Appen W-J, Halvorsen E, Kwasniewski S, Reigstad M. Seasonal variation in transport of zooplankton into the Arctic basin through the Atlantic gateway, Fram Strait. *Front Mar Sci*. 2018;5:194.
61. Wassmann P, Slagstad D, Ellingsen I. Advection of mesozooplankton into the northern Svalbard shelf region. *Front Mar Sci*. 2019;6:458.
62. Vernet M, Ellingsen IH, Seuthe L, Slagstad D, Cape MR, Matrai PA. Influence of phytoplankton advection on the productivity along the Atlantic Water inflow to the Arctic Ocean. *Front Mar Sci*. 2019;6:Article 583.
63. Årthun M, Eldevik T, Smedsrud LH, Skagseth O, Ingvaldsen RB. Quantifying the influence of Atlantic heat on Barents Sea ice variability and retreat. *J Clim*. 2012;25(13):4736–4743.
64. Koenigk T, Brodeau L, Graversen R, Karlsson J, Svensson G, Tjernström M, Willén U, Wyser K. Arctic climate change in 21st century CMIP5 simulations with EC-Earth. *Clim Dyn*. 2013;40:2719–2743.
65. Årthun M, Eldevik T, Smedsrud LH. The role of Atlantic heat transport in future Arctic winter sea ice loss. *J Clim*. 2019;32(11):3327–3341.
66. Docquier D, Koenigk T. A review of interactions between ocean heat transport and Arctic sea ice. *Environ Res Lett*. 2021;16(12):Article 123002.
67. Oziel L, Sirven J, Gascard J-C. The Barents Sea frontal zones and water masses variability (1980–2011). *Ocean Sci*. 2016;12(1):169–184.
68. Barton BI, Lenn Y-D, Lique C. Observed Atlantification of the Barents Sea causes the polar front to limit the expansion of winter sea ice. *J Phys Oceanogr*. 2018;48(8):1849–1866.
69. Skagseth Ø, Eldevik T, Årthun M, Asbjørnsen H, Lien VS, Smedsrud LH. Reduced efficiency of the Barents Sea cooling machine. *Nat Clim Chang*. 2020;10:661–666.
70. Shu Q, Wang Q, Song Z, Qiao F. The poleward enhanced Arctic Ocean cooling machine in a warming climate. *Nat Commun*. 2021;12:Article 2966.
71. Screen JA, Simmonds I. The central role of diminishing sea ice in recent Arctic temperature amplification. *Nature*. 2010;464:1334–1337.
72. Nummelin A, Li C, Hezel P. Connecting ocean heat transport changes from the midlatitudes to the Arctic Ocean. *Geophys Res Lett*. 2017;44(4):1899–1908.
73. Onarheim IH, Årthun M. Toward an ice-free Barents Sea. *Geophys Res Lett*. 2017;44(16):8387–8395.
74. Shu Q, Wang Q, Årthun M, Wang S, Song Z, Zhang M, Qiao F. Arctic Ocean Amplification in a warming climate in CMIP6 models. *Sci Adv*. 2022;8(30):Article eabn9755.
75. Isaksen K, Nordli O, Ivanov B, Køltzow MAO, Aaboe S, Gjelten HM, Mezghani A, Eastwood S, Førland E, Benestad RE, et al. Exceptional warming over the Barents area. *Sci Rep*. 2022;12:Article 9371.
76. Overland JE, Dethloff K, Francis JA, Hall RJ, Hanna E, Kim S-J, Screen JA, Shepherd TG, Vihma T. Nonlinear response of mid-latitude weather to the changing Arctic. *Nat Clim Chang*. 2016;6:992–999.
77. Cohen J, Zhang X, Francis J, Jung T, Kwok R, Overland J, Ballinger TJ, Bhatt US, Chen HW, Coumou D, et al. Divergent consensuses on Arctic amplification influence on midlatitude severe winter weather. *Nat Clim Chang*. 2020;10:20–29.
78. Polyakov I, Pnyushkov AV, Alkire MB, Ashik IM, Baumann TM, Carmack EC, Goszczko I, Guthrie J, Ivanov VV, Kanzow T, et al. Greater role for Atlantic inflows on sea-ice loss in the Eurasian Basin of the Arctic Ocean. *Science*. 2017;356(6335):285–291.
79. Lind S, Ingvaldsen RB, Furevik T. Arctic warming hotspot in the northern Barents Sea linked to declining sea-ice import. *Nat Clim Chang*. 2018;8:634–639.
80. Oziel L, Baudena A, Ardyna M, Massicotte P, Randelhoff A, Sallée JB, Ingvaldsen RB, Devred E, Babin M. Faster Atlantic currents drive poleward expansion of temperate phytoplankton in the Arctic Ocean. *Nat Commun*. 2020;11:Article 1705.
81. Ingvaldsen RB, Assmann KM, Primicerio R, Fossheim M, Polyakov IV, Dolgov AV. Physical manifestations and ecological implications of Arctic Atlantification. *Nat Rev Earth Environ*. 2021;2:874–889.
82. Yeager SG, Karspeck AR, Danabasoglu G. Predicted slowdown in the rate of Atlantic sea ice loss. *Geophys Res Lett*. 2015;42(24):10,704–10,713.
83. Årthun M, Eldevik T, Viste E, Drange H, Furevik T, Johnson HL, Keenlyside NS. Skillful prediction of northern climate provided by the ocean. *Nat Commun*. 2017;8:Article 15875.
84. Koul V, Sguotti C, Årthun M, Brune S, Düsterhus A, Bogstad B, Ottersen G, Baehr J, Schrum C. Skilful prediction

of cod stocks in the North and Barents Sea a decade in advance. *Commun Earth Environ*. 2021;2:Article 140.
85. Asbjørnsen H, Årthun M, Skagseth Ø, Eldevik T. Mechanisms of ocean heat anomalies in the Norwegian Sea. *J Geophys Res Oceans*. 2019;124(4):2908–2923.
86. Quadfasel D, Gascard J-C, Koltermann K-P. Large-scale oceanography in Fram Strait during the 1984 Marginal Ice Zone Experiment. *J Geophys Res Oceans*. 1987;92(C7):6719–6728.
87. Schauer U, Fahrbach E, Østerhus S, Rohardt G. Arctic warming through the fram strait: Oceanic heat transport from 3 years of measurements. *J Geophys Res*. 2004;109(C6):Article C06026.
88. Marnela M, Rudels B, Houssais M-N, Beszczynska-Möller A, Eriksson PB. Recirculation in the Fram Strait and transports of water in and north of the Fram Strait derived from CTD data. *Ocean Sci*. 2013;9:499–519.
89. de Steur L, Hansen E, Mauritzen C, Beszczynska-Möller A, Fahrbach E. Impact of recirculation on the East Greenland Current in Fram Strait: Results from moored current meter measurements between 1997 and 2009. *Deep Sea Res I Oceanogr Res Pap*. 2014;92:26–40.
90. Håvik L, Pickart RS, Våage K, Torres D, Thurnherr AM, Beszczynska-Möller A, Walczowski W, von Appen WJ. Evolution of the East Greenland Current from Fram Strait to Denmark Strait: Synoptic measurements from summer 2012. *J Geophys Res Oceans*. 2017;122(3):1974–1994.
91. Woodgate RA, Aagaard K, Muench RD, Gunn J, Björk G, Rudels B, Roach AT, Schauer U. The Arctic Ocean boundary current along the Eurasian slope and the adjacent Lomonosov Ridge: Water mass properties, transports and transformations from moored instruments. *Deep Sea Res I Oceanogr Res Pap*. 2001;48(8):1757–1792.
92. Karcher MJ, Gerdes R, Kauker F, Koberle C. Arctic warming: Evolution and spreading of the 1990s warm event in the Nordic seas and the Arctic Ocean. *J Geophys Res Oceans*. 2003;108(C2):3034.
93. Wang Q, Wekerle C, Wang X, Danilov S, Koldunov N, Sein D, Sidorenko D, von Appen W-J, Jung T. Intensification of the Atlantic Water supply to the Arctic Ocean through Fram Strait induced by Arctic sea ice decline. *Geophys Res Lett*. 2020;47(3):Article e2019GL086682.
94. Dmitrenko I, Kirillov S, Tremblay L. The long-term and interannual variability of summer fresh water storage over the eastern Siberian Shelf: Implication for climatic change. *J Geophys Res-Oceans*. 2008;113(C3):Article C03003.
95. Polyakov IV, Pnyushkov AV, Timokhov LA. Warming of the intermediate Atlantic Water of the Arctic Ocean in the 2000s. *J Clim*. 2012;25(23):8362–8370.
96. Polyakov I, Timokhov L, Alexeev V, Bacon S, Dmitrenko I, Fortier L, Frolov I, Gascard J, Hansen E, Ivanov V, et al. Arctic ocean warming contributes to reduced polar ice cap. *J Phys Oceanogr*. 2010;40(12):2743–2756.
97. Onarheim IH, Smedsrud LH, Ingvaldsen RB, Nilsen F. Loss of sea ice during winter north of Svalbard. *Tellus A Dyn Meteorol Oceanogr*. 2014;66:Article 23933.
98. Ivanov V, Smirnov A, Alexeev V, Koldunov NV, Repina I, Semenov V. Contribution of convection-induced heat flux to winter ice decay in the western Nansen Basin. *J Geophys Res Oceans*. 2018;123(9):6581–6597.
99. Athanase M, Provost C, Pérez-Hernández MD, Sennéchael N, Bertosio C, Artana C, Garric G, Lellouche J-M. Atlantic Water modification north of Svalbard in the Mercator Physical System from 2007 to 2020. *J Geophys Res Oceans*. 2020;125(10):Article e2020JC016463.
100. Duarte P, Sundfjord A, Meyer A, Hudson SR, Spreen G, Smedsrud LH. Warm Atlantic Water explains observed sea ice melt rates north of Svalbard. *J Geophys Res Oceans*. 2020;125(8):Article e2019JC015662.
101. Lundesgaard Ø, Sundfjord A, Renner AHH. Drivers of interannual sea ice concentration variability in the Atlantic Water inflow region north of Svalbard. *J Geophys Res Oceans*. 2021;126(4):Article e2020JC016522.
102. Herbaut C, Houssais M-N, Blaizot A-C, Molines J-M. A role for the ocean in the winter sea ice distribution north of Svalbard. *J Geophys Res Oceans*. 2022;127(6):Article e2021JC017852.
103. Koenig Z, Kalhagen K, Kolås E, Fer I, Nilsen F, Cottier F. Atlantic Water properties, transport and heat loss from mooring observations north of Svalbard. *J Geophys Res Oceans*. 2022;127(8):Article e2022JC018568.
104. Polyakov IV, Alkire MB, Bluhm BA, Brown KA, Carmack EC, Chierici M, Danielson SL, Ellingsen I, Ershova EA, Gårdfeldt K, et al. Borealization of the Arctic Ocean in response to anomalous advection from sub-Arctic seas. *Front Mar Sci*. 2020;7:491.
105. Tang CCL, Ross CK, Yao T, Petrie B, DeTracey BM, Dunlap E. The circulation, water masses and sea-ice of Baffin Bay. *Prog Oceanogr*. 2004;63(4):183–228.
106. Myers PG, Kulan N, Ribergaard MH. Irminger water variability in the West Greenland Current. *Geophys Res Lett*. 2007;34(17):Article L17601.
107. Holland DM, Thomas RH, de Young B, Ribergaard MH, Lyberth B. Acceleration of Jakobshavn Isbræ triggered by warm subsurface ocean waters. *Nat Geosci*. 2008;1:659–664.
108. Straneo F, Sutherland DA, Holland D, Gladish C, Hamilton GS, Johnson HL, Rignot E, Xu Y, Koppes M. Characteristics of ocean waters reaching Greenland's glaciers. *Ann Glaciol*. 2012;53(60):202–210.
109. Myers PG, Ribergaard MH. Warming of the polar water layer in disko bay and potential impact on jakobshavn isbrae. *J Phys Oceanogr*. 2013;43(12):2629–2640.
110. Gladish CV, Holland DM, Lee CM. Oceanic boundary conditions for Jakobshavn Glacier. part II: Provenance and sources of variability of Disko Bay and Ilulissat Icefjord waters, 1990–2011. *J Phys Oceanogr*. 2015;45(1):33–63.
111. Rysgaard S, Boone W, Carlson D, Sejr MK, Bendtsen J, Juul-Pedersen T, Lund H, Meire L, Mortensen J. An updated view on water masses on the pan-west Greenland continental shelf and their link to proglacial fjords. *J Geophys Res Oceans*. 2020;125(2):Article e2019JC015564.
112. Beszczynska-Moeller A, Woodgate RA, Lee C, Melling H, Karcher M. A synthesis of exchanges through the main oceanic gateways to the Arctic Ocean. *Oceanography*. 2011;24:82–99.
113. Smedsrud LH, Muilwijk M, Brakstad A, Madonna E, Lauvset SK, Spensberger C, Born A, Eldevik T, Drange H, Jeansson E, et al. Nordic Seas heat loss, Atlantic inflow, and Arctic sea ice cover over the last century. *Rev Geophys*. 2022;60(1):Article e2020RG000725.
114. IHO, "Limits of oceans and seas," IHO Special Publication, International Hydrographic Organization, Technical Report, 1953.
115. Tsubouchi T, Bacon S, Aksenov Y, Naveira Garabato AC, Beszczynska-Möller A, Hansen E, de Steur L, Curry B,

Lee CM. The Arctic Ocean seasonal cycles of heat and freshwater fluxes: Observation-based inverse estimates. *J Phys Oceanogr*. 2018;48(9):2029–2055.
116. Woodgate R. Increases in the Pacific inflow to the Arctic from 1990 to 2015, and insights into seasonal trends and driving mechanisms from year-round Bering Strait mooring data. *Prog Oceanogr*. 2018;160:124–154.
117. von Appen W-J, Schauer U, Hattermann T, Beszczynska-Möller A. Seasonal cycle of mesoscale instability of the West Spitsbergen Current. *J Phys Oceanogr*. 2016;46(4):1231–1254.
118. Karpouzoglou T, de Steur L, Smedsrud LH, Sumata H. Observed changes in the Arctic freshwater outflow in Fram Strait. *J Geophys Res Oceans*. 2022;127(3):Article e2021JC018122.
119. González-Pola C, Larsen KMH, Fratantoni P, Beszczynska-Möller A, "Ices report on ocean climate 2019," ICES Cooperative Research Reports, Technical Report 350, 2020. p. 36. [Online]. https://doi.org/10.17895/ices.pub.7537.
120. Griffies SM, Danabasoglu G, Durack PJ, Adcroft AJ, Balaji V, Böning CW, Chassignet EP, Curchitser E, Deshayes J, Drange H, et al. OMIP contribution to CMIP6: Experimental and diagnostic protocol for the physical component of the Ocean Model Intercomparison Project. *Geosci Model Dev*. 2016;9(9):3231–3296.
121. Tsujino H, Urakawa LS, Griffies SM, Danabasoglu G, Adcroft AJ, Amaral AE, Arsouze T, Bentsen M, Bernardello R, Böning CW, et al. Evaluation of global ocean–sea-ice model simulations based on the experimental protocols of the Ocean Model Intercomparison Project phase 2 (OMIP-2). *Geosci Model Dev*. 2020;13(8):3643–3708.
122. Large WG, Yeager SG. The global climatology of an interannually varying air-sea flux data set. *Clim Dyn*. 2009;33:341–364.
123. Tsujino H, Urakawa S, Nakano H, Small RJ, Kim WM, Yeager SG, Danabasoglu G, Suzuki T, Bamber JL, Bentsen M, et al. JRA-55 based surface dataset for driving ocean–sea-ice models (JRA55-do). *Ocean Modell*. 2018;130:79–139.
124. Shu Q, Wang Q, Guo C, Song Z, Wang S, He Y, Qiao F. Arctic Ocean simulations in the CMIP6 Ocean Model Intercomparison Project (OMIP). *Geosci Model Dev*. 2023;16:2539–2563.
125. Wang Q, Ilicak M, Gerdes R, Drange H, Aksenov Y, Bailey DA, Bentsen M, Biastoch A, Bozec A, Böning C, et al. An assessment of the Arctic Ocean in a suite of interannual CORE-II simulations. Part II: Liquid freshwater. *Ocean Modell*. 2016;99:86–109.
126. Wang S, Wang Q, Wang M, Lohmann G, Qiao F. Arctic Ocean freshwater in CMIP6 coupled models. *Earth's Future*. 2022;10(9):Article e2022EF002878.
127. O'Neill BC, Tebaldi C, van Vuuren DP, Eyring V, Friedlingstein P, Hurtt G, Knutti R, Kriegler E, Lamarque J-F, Lowe J, et al. The Scenario Model Intercomparison Project (ScenarioMIP) for CMIP6. *Geosci Model Dev*. 2016;9:3461–3482.
128. Zanowski H, Jahn A, Holland MM. Arctic Ocean freshwater in CMIP6 ensembles: Declining sea ice, increasing ocean storage and export. *J Geophys Res Oceans*. 2021;126(4):Article e2020JC016930.
129. Khosravi N, Wang Q, Koldunov N, Hinrichs C, Semmler T, Danilov S, Jung T. Arctic Ocean in CMIP6 models: Historical and projected temperature and salinity in the deep basins. *Earth's Future*. 2022; 10: Article e2021EF002282.
130. Wang Q, Danilov S, Sidorenko D, Timmermann R, Wekerle C, Wang X, Jung T, Schröter J. The Finite Element Sea Ice-Ocean Model (FESOM) v.1.4: Formulation of an ocean general circulation model. *Geosci Model Dev*. 2014;7(2):663–693.
131. Wang Q, Wekerle C, Danilov S, Wang X, Jung T. A 4.5 km resolution Arctic Ocean simulation with the global multi-resolution model FESOM 1.4. *Geosci Model Dev*. 2018;11(4):1229–1255.
132. Wang Q, Wang X, Wekerle C, Danilov S, Jung T, Koldunov N, Lind S, Sein D, Shu Q, Sidorenko D. Ocean heat transport into the Barents Sea: Distinct controls on the upward trend and interannual variability. *Geophys Res Lett*. 2019;46(22):13180–13190.
133. Zhang W, Wang Q, Wang X, Danilov S. Mechanisms driving the interannual variability of the Bering Strait throughflow. *J Geophys Res Oceans*. 2020;125(2):Article e2019JC015308.
134. Wang Q, Shu Q, Danilov S, Sidorenko D. An extreme event of enhanced Arctic Ocean export west of Greenland caused by the pronounced dynamic sea level drop in the North Atlantic subpolar gyre in the mid-to-late 2010s. *Environ Res Lett*. 2022;17(4):Article 044046.
135. Wang Q. Stronger variability in the Arctic Ocean induced by sea ice decline in a warming climate: Freshwater storage, dynamic sea level and surface circulation. *J Geophys Res Oceans*. 2021;126(3):Article e2020JC016886.
136. Thompson DWJ, Wallace JM. The Arctic oscillation signature in the wintertime geopotential height and temperature fields. *Geophys Res Lett*. 1998;25(9):1297–1300.
137. Wu B, Wang J, Walsh J. Dipole Anomaly in the winer arctic atmosphere and its association with sea ice motion. *J Clim*. 2006;19(2):210–225.
138. Serreze MC, Barry RG. Processes and impacts of Arctic amplification: A research synthesis. *Glob Planet Chang*. 2011;77(1):85–96.
139. Steele M, Morison J, Ermold W, Rigor I, Ortmeyer M, Shimada K. Circulation of summer Pacific halocline water in the Arctic Ocean. *J Geophys Res Oceans*. 2004;109(C2):Article C02027.
140. Schauer U, Beszczynska-Möller A. Problems with estimation and interpretation of oceanic heat transport—Conceptual remarks for the case of fram strait in the arctic ocean. *Ocean Sci*. 2009;5(4):487–494.
141. Bacon S, Aksenov Y, Fawcett S, Madec G. Arctic mass, freshwater and heat fluxes: Methods and modelled seasonal variability. *Phil Trans R Soc A*. 2015;373:Article 20140169.
142. Schauer U, Losch M. "Freshwater" in the ocean is not a useful parameter in climate research. *J Phys Oceanogr*. 2019;49(9):2309–2321.
143. Danielson SL, Ahkinga O, Ashjian C, Basyuk E, Cooper LW, Eisner L, Farley E, Iken KB, Grebmeier JM, Juranek L, et al. Manifestation and consequences of warming and altered heat fluxes over the Bering and Chukchi Sea continental shelves. *Deep Sea Res II Top Stud Oceanogr*. 2020;177:Article 104781.
144. Woodgate RA, Stafford KM, Prahl FG. A synthesis of year-round interdisciplinary mooring measurements in the Bering Strait (1990–2014) and the RUSALCA years (2004–2011). *Oceanography*. 2015;28(3):46–67.
145. Muilwijk M, Smedsrud LH, Ilicak M, Drange H. Atlantic water heat transport variability in the 20th century Arctic

Ocean from a global ocean model and observations. *J. Geophys. Res. Oceans*. 2018;123(11):8159–8179.
146. Hansen B, Østerhus S. North Atlantic–Nordic Seas exchanges. *Prog Oceanogr*. 2000;45(2):109–208.
147. Hansen B, Østerhus S, Hátún H, Kristiansen R, Larsen KMH. The Iceland–Faroe inflow of Atlantic water to the Nordic Seas. *Prog Oceanogr*. 2003;59:443–474.
148. Mork K, Blindheim J. Variations in the Atlantic inflow to the Nordic Seas, 1955–1996. *Deep Sea Res I Oceanogr Res Pap*. 2000;47(6):1035–1057.
149. Holliday NP, Hughes SL, Bacon S, Beszczynska-Möller A, Hansen B, Lavin A, Loeng H, Mork KA, Østerhus S, Sherwin T, et al. Reversal of the 1960s to 1990s freshening trend in the northeast North Atlantic and Nordic Seas. *Geophys Res Lett*. 2008;35(3):Article L03614.
150. Gerdes R, Karcher MJ, Kauker F, Schauer U. Causes and development of repeated Arctic Ocean warming events. *Geophys Res Lett*. 2003;30(19):1980.
151. Polyakov IV, Alekseev GV, Timokhov LA, Bhatt US, Colony RL, Simmons HL, Walsh D, Walsh JE, Zakharov VF. Variability of the intermediate Atlantic Water of the Arctic Ocean over the last 100 years. *J Clim*. 2004;17(23): 4485–4497.
152. Polyakov IV, Beszczynska A, Carmack EC, Dmitrenko IA, Fahrbach E, Frolov IE, Gerdes R, Hansen E, Holfort J, Ivanov VV, et al. One more step toward a warmer Arctic. *Geophys Res Lett*. 2005;32(17):L17605.
153. Häkkinen S, Rhines PB, Worthen DL. Warm and saline events embedded in the meridional circulation of the northern North Atlantic. *J Geophys Res Oceans*. 2011;116(C3):Article C03006.
154. Orvik KA. Long-term moored current and temperature measurements of the Atlantic inflow into the Nordic Seas in the Norwegian Atlantic Current; 1995–2020. *Geophys Res Lett*. 2022;49(3):Article e2021GL096427.
155. Mork KA, Skagseth O, Soiland H. Recent warming and freshening of the Norwegian Sea observed by Argo data. *J Clim*. 2019;32(12):3695–3705.
156. Rossby T, Flagg C, Chafik L, Harden B, Søiland H. A direct estimate of volume, heat, and freshwater exchange across the Greenland-Iceland-Faroe-Scotland ridge. *J Geophys Res Oceans*. 2018;123(10):7139–7153.
157. Orvik KA, Skagseth Ø, Mork M. Atlantic inflow to the nordic seas: Current structure and volume fluxes from moored current meters, VM-ADCP and SeaSoar-CTD observations, 1995–1999. *Deep Sea Res I Oceanogr Res Pap*. 2001;48(4):937–957.
158. Tsubouchi T, Våge K, Hansen B, Larsen KMH, Østerhus S, Johnson C, Jónsson S, Valdimarsson H. Increased ocean heat transport into the Nordic Seas and Arctic Ocean over the period 1993–2016. *Nat Clim Chang*. 2021;11:21–26.
159. Chafik L, Rossby T. Volume, heat, and freshwater divergences in the subpolar north atlantic suggest the nordic seas as key to the state of the meridional overturning circulation. *Geophys Res Lett*. 2019;46(9):4799–4808.
160. Furevik T. Annual and interannual variability of Atlantic Water temperatures in the Norwegian and Barents Seas: 1980–1996. *Deep Sea Res I Oceanogr Res Pap*. 2001;48(2):383–404.
161. Yashayaev I, Seidov D. The role of the atlantic water in multidecadal ocean variability in the Nordic and Barents Seas. *Prog Oceanogr*. 2015;132:68–127.
162. Huang J, Pickart RS, Chen Z, Huang RX. Role of air-sea heat flux on the transformation of Atlantic Water encircling the Nordic Seas. *Nat Commun*. 2023;14(1):141.
163. Skagseth Ø, Drinkwater KF, Terrile E. Wind- and buoyancy-induced transport of the Norwegian Coastal Current in the Barents Sea. *J Geophys Res Oceans*. 2011;116(C8):Article C08007.
164. Veneziani M, Maslowski W, Lee YJ, D'Angelo G, Osinski R, Petersen MR, Weijer W, Craig AP, Wolfe JD, Comeau D, et al. An evaluation of the E3SMv1 Arctic ocean and sea-ice regionally refined model. *Geosci Model Dev*. 2022;15(7):3133–3160.
165. Schauer U, Loeng H, Rudels B, Ozhigin VK, Dieck W. Atlantic water flow through the barents and kara seas. *Deep Sea Res I Oceanogr Res Pap*. 2002;49(12):2281–2298.
166. Athanase M, Provost C, Artana C, Pérez-Hernández MD, Sennéchael N, Bertosio C, Garric G, Lellouche J-M, Prandi P. Changes in Atlantic Water circulation patterns and volume transports north of Svalbard over the last 12 years (2008–2020). *J Geophys Res Oceans*. 2021;126(1):Article e2020JC016825.
167. Wekerle C, Wang Q, von Appen W-J, Danilov S, Schourup-Kristensen V, Jung T. Eddy-resolving simulation of the Atlantic Water circulation in the Fram Strait with focus on the seasonal cycle. *J Geophys Res Oceans*. 2017;122(11):8385–8405.
168. Hofmann Z, von Appen W-J, Wekerle C. Seasonal and mesoscale variability of the two Atlantic Water recirculation pathways in Fram Strait. *J Geophys Res Oceans*. 2021;126(7):Article e2020JC017057.
169. Polyakov I, Bhatt U, Walsh J, Abrahamsen EP, Pnyushkov A, Wassmann P. Recent oceanic changes in the Arctic in the context of long-term observations. *Ecol Appl*. 2013;23(8):1745–1764.
170. Wang Q, Danilov S. A synthesis of the upper Arctic Ocean circulation during 2000–2019: Understanding the roles of wind forcing and sea ice decline. *Front Mar Sci*. 2022;9:Article 863204.
171. Bertosio C, Provost C, Athanase M, Sennéchael N, Garric G, Lellouche J-M, Kim J-H, Cho K-H, Park T. Changes in Arctic halocline waters along the East Siberian slope and in the Makarov Basin from 2007 to 2020. *J Geophys Res Oceans*. 2022;127(9):Article e2021JC018082.
172. Oziel L, Schourup-Kristensen V, Wekerle C, Hauck J. The pan-Arctic continental slope as an intensifying conveyer belt for nutrients in the central Arctic Ocean (1985–2015). *Glob Biogeochem Cycles*. 2022;36(6):Article e2021GB007268.
173. Gjelstrup CVB, Sejr MK, de Steur L, Christiansen JS, Granskog MA, Koch BP, Møller EF, Winding MHS, Stedmon CA. Vertical redistribution of principle water masses on the Northeast Greenland Shelf. *Nat Commun*. 2022;13:Article 7660.
174. Curry B, Lee CM, Petrie B. Volume, freshwater, and heat fluxes through Davis Strait, 2004–05. *J Phys Oceanogr*. 2011;41(3):429–436.
175. Myers PG, Castro de la Guardia L, Fu C, Gillard LC, Grivault N, Hu X, Lee CM, Moore GWK, Pennelly C, Ribergaard MH, et al. Extreme high Greenland Blocking Index leads to the reversal of Davis and Nares Strait net transport toward the Arctic Ocean. *Geophys Res Lett*. 2021;48(17):Article e2021GL094178.
176. Karpouzoglou T, de Steur L, Dodd PA. Freshwater transport over the northeast Greenland shelf in Fram Strait. *Geophys Res Lett*. 2023;50(2):e2022GL101775.

177. Florindo-López C, Bacon S, Aksenov Y, Chafik L, Colbourne E, Holliday NP. Arctic Ocean and Hudson Bay freshwater exports: New estimates from seven decades of hydrographic surveys on the Labrador Shelf. *J Clim*. 2020;33(20):8849–8868.
178. Hansen E, Gerland S, Granskog MA, Pavlova O, Renner AHH, Haapala J, Løyning TB, Tschudi M. Thinning of Arctic sea ice observed in Fram Strait: 1990–2011. *J Geophys Res Oceans*. 2013;118(10):5202–5221.
179. Renner AHH, Gerland S, Haas C, Spreen G, Beckers JF, Hansen E, Nicolaus M, Goodwin H. Evidence of Arctic sea ice thinning from direct observations. *Geophys Res Lett*. 2014;41(14):5029–5036.
180. Belter HJ, Krumpen T, von Albedyll L, Alekseeva TA, Birnbaum G, Frolov SV, Hendricks S, Herber A, Polyakov I, Raphael I, et al. Interannual variability in Transpolar Drift summer sea ice thickness and potential impact of Atlantification. *Cryosphere*. 2021;15(6):2575–2591.
181. Wang Q, Ricker R, Mu L. Arctic sea ice decline preconditions events of anomalously low sea ice volume export through Fram Strait in the early 21st century. *J Geophys Res Oceans*. 2021;126(2):Article e2020JC016607.
182. Spreen G, Kern S, Stammer D, Hansen E. Fram Strait sea ice volume export estimated between 2003 and 2008 from satellite data. *Geophys Res Lett*. 2009;36(19):L19502.
183. Vinje T, Nordlund N, Kvambekk A. Monitoring ice thickness in Fram Strait. *J Geophys Res Oceans*. 1998;103(C5):10437–10449.
184. Kwok R, Cunningham GF, Pang SS. Fram Strait sea ice outflow. *J Geophys Res Oceans*. 2004;109:C01009.
185. Sumata H, de Steur L, Gerland S, Divine DV, Pavlova O. Unprecedented decline of Arctic sea ice outflow in 2018. *Nat Commun*. 2022;13:1747.
186. Kwok R. Baffin Bay ice drift and export: 2002–2007. *Geophys Res Lett*. 2007;34(19):L19501.
187. Min C, Yang Q, Mu L, Kauker F, Ricker R. Ensemble-based estimation of sea-ice volume variations in the Baffin Bay. *Cryosphere*. 2021;15(1):169–181.
188. Wang Q, Ilicak M, Gerdes R, Drange H, Aksenov Y, Bailey DA, Bentsen M, Biastoch A, Bozec A, Böning C, et al. An assessment of the Arctic Ocean in a suite of interannual CORE-II simulations. Part I: Sea ice and solid freshwater. *Ocean Modell*. 2016;99:110–132.
189. Travers CS, Quantifying sea-ice volume flux using moored instrumentation in the Bering Strait [thesis]. [Seattle (WA)]: University of Washington; 2012. [Online] https://digital.lib.washington.edu/researchworks/handle/1773/20503.
190. Rabe B, Dodd P, Hansen E, Falck E, Schauer U, Mackensen A, Beszczynska-Möller A, Kattner G, Rohling EJ, Cox K. Liquid export of Arctic freshwater components through the Fram Strait 1998–2011. *Ocean Sci*. 2013;9:91–109.
191. Dodd PA, Rabe B, Hansen E, Falck E, Mackensen A, Rohling E, Stedmon C, Kristiansen S. The freshwater composition of the Fram Strait outflow derived from a decade of tracer measurements. *J Geophys Res Oceans*. 2012;117(C11):Article C11005.
192. Coachman LK, Aagaard K. On the water exchange through Bering Strait. *Limnol Oceanogr*. 1966;11(1):44–59.
193. Aagaard K, Weingartner TJ, Danielson SL, Woodgate RA, Johnson GC, Whitledge TE. Some controls on flow and salinity in Bering Strait. *Geophys Res Lett*. 2006;33(19):Article L19602.
194. Woodgate RA, Weingartner TJ, Lindsay R. Observed increases in Bering Strait oceanic fluxes from the Pacific to the Arctic from 2001 to 2011 and their impacts on the Arctic Ocean water column. *Geophys Res Lett*. 2012;39(24):Article L24603.
195. Danielson SL, Weingartner TJ, Hedstrom KS, Aagaard K, Woodgate R, Curchitser E, Stabeno PJ. Coupled wind-forced controls of the Bering–Chukchi shelf circulation and the Bering Strait throughflow: Ekman transport, continental shelf waves, and variations of the Pacific–Arctic sea surface height gradient. *Prog Oceanogr*. 2014;125:40–61.
196. Peralta-Ferriz C, Woodgate RA. The dominant role of the East Siberian Sea in driving the oceanic flow through the bering strait—Conclusions from GRACE ocean mass satellite data and in situ mooring observations between 2002 and 2016. *Geophys Res Lett*. 2017;44(22):11,472–11,481.
197. Toulany B, Garrett C. Geostrophic control of fluctuating barotropic flow through straits. *J Phys Oceanogr*. 1984;14(4):649–655.
198. Nguyen AT, Woodgate RA, Heimbach P. Elucidating large-scale atmospheric controls on bering strait throughflow variability using a data-constrained ocean model and its adjoint. *J Geophys Res Oceans*. 2020;125(9):Article e2020JC016213.
199. Skagseth Ø, Orvik K. Identifying fluctuations in the Norwegian Atlantic Slope Current by means of empirical orthogonal functions. *Cont Shelf Res*. 2002;22(4):547–563.
200. Skagseth Ø. Monthly to annual variability of the Norwegian Atlantic slope current: Connection between the northern North Atlantic and the Norwegian Sea. *Deep Sea Res I Oceanogr Res Pap*. 2004;51(3):349–366.
201. Hatun H, Sando AB, Drange H, Hansen B, Valdimarsson H. Influence of the Atlantic Subpolar Gyre on the thermohaline circulation. *Science*. 2005;309(5742):1841–1844.
202. Kenigson JS, Timmermans M-L. Arctic cyclone activity and the Beaufort High. *J Clim*. 2021;34(10):4119–4127.
203. Marshall J, Johnson H, Goodman J. A study of the interaction of the North Atlantic Oscillation with ocean circulation. *J Clim*. 2001;14(7):1399–1421.
204. Sanders RNC, Jones DC, Josey SA, Sinha B, Forget G. Causes of the 2015 North Atlantic cold anomaly in a global state estimate. *Ocean Sci*. 2022;18(4):953–978.
205. Kostov Y, Messias M-J, Mercier H, Johnson HL, Marshall DP. Fast mechanisms linking the Labrador Sea with subtropical Atlantic overturning. *Clim Dyn*. 2023;60:2687–2712.
206. Fox AD, Handmann P, Schmidt C, Fraser N, Rühs S, Sanchez-Franks A, Martin T, Oltmanns M, Johnson C, Rath W, et al. Exceptional freshening and cooling in the eastern subpolar North Atlantic caused by reduced Labrador Sea surface heat loss. *Ocean Sci*. 2022;18(5):1507–1533.
207. Holliday NP, Bersch M, Berx B, Chafik L, Cunningham S, Florindo-López C, Hátún H, Johns W, Josey SA, Larsen KMH, et al. Ocean circulation causes the largest freshening event for 120 years in eastern subpolar North Atlantic. *Nat Commun*. 2020;11:585.
208. Bryden HL, Johns WE, King BA, McCarthy G, McDonagh EL, Moat BI, Smeed DA. Reduction in ocean heat transport at 26°N since 2008 cools the eastern subpolar gyre of the North Atlantic Ocean. *J Clim*. 2020;33(5):1677–1689.
209. Foukal NP, Lozier MS. Examining the origins of ocean heat content variability in the eastern north atlantic subpolar gyre. *Geophys Res Lett*. 2018;45(20):11,275–11,283.

210. Asbjørnsen H, Årthun M, Skagseth Ø, Eldevik T. Mechanisms underlying recent Arctic Atlantification. *Geophys Res Lett*. 2020;47:e2020GL088036.
211. Furevik T. On the atlantic water flow in the nordic seas: Bifurcation and variability [thesis]. [Bergen, Norway]: University of Bergen; 1998.
212. Zhang J, Rothrock D, Steele M. Warming of the Arctic Ocean by a strengthened Atlantic Inflow: Model results. *Geophys Res Lett*. 1998;25:1745–1748.
213. Blindheim J, Borovkov V, Hansen B, Malmberg S, Turrell W, Osterhus S. Upper layer cooling and freshening in the Norwegian Sea in relation to atmospheric forcing. *Deep Sea Res I Oceanogr Res Pap*. 2000;47:655–680.
214. Muilwijk M, Ilicak M, Cornish SB, Danilov S, Gelderloos R, Gerdes R, Haid V, Haine TWN, Johnson HL, Kostov Y, et al. Arctic Ocean response to Greenland Sea wind anomalies in a suite of model simulations. *J Geophys Res Oceans*. 2019;124(8):6286–6322.
215. Ingvaldsen R, Asplin L, Loeng H. Velocity field of the western entrance to the Barents Sea. *J Geophys Res*. 2004;109(C3):Article C03021.
216. Nøst O, Isachsen P. The large-scale time-mean ocean circulation in the Nordic Seas and Arctic Ocean estimated from simplified dynamics. *J Mar Res*. 2003;61:175–210.
217. Isachsen PE, LaCasce JH, Mauritzen C, Häkkinen S. Wind-driven variability of the large-scale recirculating flow in the Nordic Seas and Arctic Ocean. *J Phys Oceanogr*. 2003;33:2534–2550.
218. Timmermans M-L, Marshall J. Understanding Arctic Ocean circulation: A review of ocean dynamics in a changing climate. *J Geophys Res Oceans*. 2020;125:e2018JC014378.
219. Chatterjee S, Raj RP, Bertino L, Skagseth Ø, Ravichandran M, Johannessen OM. Role of Greenland Sea gyre circulation on Atlantic Water temperature variability in the Fram Strait. *Geophys Res Lett*. 2018;45(16):8399–8406.
220. Rudels B. The formation of polar surface water, the ice export and the exchanges through the Fram Strait. *Prog Oceanogr*. 1989;22:205–248.
221. Spall MA. On the circulation of Atlantic Water in the Arctic Ocean. *J Phys Oceanogr*. 2013;43:2352–2371.
222. Haine TWN. A conceptual model of polar overturning circulations. *J Phys Oceanogr*. 2021;51:727–744.
223. Karcher M, Smith J, Kauker F, Gerdes R, Smethie W. Recent changes in Arctic Ocean circulation revealed by iodine-129 observations and modeling. *J Geophys Res Oceans*. 2012;117(C8):C08007.
224. Lique C, Johnson HL, Davis PED. On the interplay between the circulation in the surface and the intermediate layers of the Arctic Ocean. *J Phys Oceanogr*. 2015;45:1393–1409.
225. Smith JN, Karcher M, Casacuberta N, Williams WJ, Kenna T, Smethie WM Jr. A changing Arctic Ocean: How measured and modeled ^{129}I distributions indicate fundamental shifts in circulation between 1994 and 2015. *J Geophys Res Oceans*. 2021;126(3):e2020JC016740.
226. Hinrichs C, Wang Q, Koldunov N, Mu L, Semmler T, Sidorenko D, Jung T. Atmospheric wind biases: A challenge for simulating the Arctic Ocean in coupled models? *J Geophys Res Oceans*. 2021;126(10):e2021JC017565.
227. Morison J, Kwok R, Dickinson S, Andersen R, Peralta-Ferriz C, Morison D, Rigor I, Dewey S, Guthrie J. The cyclonic mode of arctic ocean circulation. *J Phys Oceanogr*. 2021;51:1053–1075.
228. Carmack EC, Macdonald R, Perkin RG, McLaughlin FA, Pearson RJ. Evidence for warming of Atlantic water in the Southern Canadian Basin of the Arctic Ocean: Results from the Larsen-93 Expedition. *Geophys Res Lett*. 1995;22(9):1061–1064.
229. Morison J, Steele M, Andersen R. Hydrography of the upper Arctic Ocean measured from the nuclear submarine U.S.S. *Pargo*. *Deep Sea Res I*. 1998;45(1):15–38.
230. Steele M, Boyd T. Retreat of the cold halocline layer in the Arctic Ocean. *J Geophys Res Oceans*. 1998;103(C5):10419–10435.
231. Ekwurzel B, Schlosser P, Mortlock RA, Fairbanks RG, Swift JH. River runoff, sea ice meltwater, and Pacific water distribution and mean residence times in the Arctic Ocean. *J Geophys Res Oceans*. 2001;106:9075–9092.
232. McLaughlin F, Carmack E, Macdonald R, Weaver AJ, Smith J. The Canada Basin, 1989–1995: Upstream events and far-field effects of the Barents Sea. *J Geophys Res Oceans*. 2002;107(C7):3082.
233. Dickson RR, Osborn TJ, Hurrell JW, Meincke J, Blindheim J, Adlandsvik B, Vinje T, Alekseev G, Maslowski W. The Arctic Ocean Response to the North Atlantic Oscillation. *J Clim*. 2000;13:2671–2696.
234. Wang Q, Koldunov NV, Danilov S, Sidorenko D, Wekerle C, Scholz P, Bashmachnikov IL, Jung T. Eddy kinetic energy in the Arctic Ocean from a global simulation with a 1-km Arctic. *Geophys Res Lett*. 2020;47(14):e2020GL088550.
235. von Appen W-J, Baumann T, Janout M, Koldunov N, Lenn Y-D, Pickart R, Scott R, Wang Q. Eddies and the distribution of eddy kinetic energy in the Arctic Ocean. *Oceanography*. 2022;35:42–51.
236. Gascard J-C, Kergomard C, Jeannin P-F, Fily M. Diagnostic study of the Fram Strait marginal ice zone during summer from 1983 and 1984 Marginal Ice Zone Experiment Lagrangian observations. *J Geophys Res Oceans*. 1988;93:3613–3641.
237. Hattermann T, Isachsen PE, von Appen W-J, Albretsen J, Sundfjord A. Eddy-driven recirculation of Atlantic Water in Fram Strait. *Geophys Res Lett*. 2016;43:3406–3414.
238. Heukamp F, Kanzow T, Wang Q, Wekerle C, Gerdes R. Impact of cyclonic wind anomalies caused by massive winter sea ice retreat in the Barents Sea on Atlantic Water transport toward the Arctic: A model study. *J Geophys Res Oceans*. 2023;128:e2022JC019045.
239. Gascard J-C, Richez C, Rouault C. New insights on large-scale oceanography in Fram Strait: The West Spitsbergen current. In: Smith S, Grebmeier J, editors. *Arctic oceanography: Marginal ice zones and continental shelves*, Washington (DC): American Geophysical Union; 1995; p. 131–182.
240. Koenig Z, Provost C, Sennéchael N, Garric G, Gascard J-C. The Yermak Pass Branch: A major pathway for the Atlantic Water north of Svalbard? *J Geophys Res Oceans*. 2017;122:9332–9349.
241. Crews L, Sundfjord A, Hattermann T. How the Yermak Pass Branch regulates Atlantic Water inflow to the Arctic Ocean. *J Geophys Res Oceans*. 2019;124:267–280.
242. Artana C, Provost C, Koenig Z, Athanase M, Asgari A. Atlantic Water inflow through the Yermak Pass Branch: Evolution since 2007. *J Geophys Res Oceans*. 2022;127:e2021JC018006.
243. Kolås EH, Koenig Z, Fer I, Nilsen F, Marnela M. Structure and transport of Atlantic Water north of Svalbard from observations in summer and fall 2018. *J Geophys Res Oceans*. 2020;125:e2020JC016174.

244. Nilsen F, Ersdal EA, Skogseth R. Wind-driven variability in the Spitsbergen polar current and the Svalbard branch across the Yermak Plateau. *J Geophys Res Oceans*. 2021;126:e2020JC016734.
245. Koenig Z, Meyer A, Provost C, Sennéchael N, Sundfjord A, Gascard J-C. Atlantic Water circulation and properties northwest of Svalbard during anomalous southerly winds. *J Geophys Res Oceans*. 2022;127:e2021JC018357.
246. Straneo F, Heimbach P. North Atlantic warming and the retreat of Greenland's outlet glaciers. *Nature*. 2013;504:36–43.
247. Zhang R. On the persistence and coherence of subpolar sea surface temperature and salinity anomalies associated with the Atlantic multidecadal variability. *Geophys Res Lett*. 2017;44:7865–7875.
248. de Jong MF, Bower AS, Furey HH. Seasonal and interannual variations of Irminger Ring formation and boundary–interior heat exchange in FLAME. *J Phys Oceanogr*. 2016;46:1717–1734.
249. Luo H, Castelao RM, Rennermalm AK, Tedesco M, Bracco A, Yager PL, Mote TL. Oceanic transport of surface meltwater from the southern Greenland ice sheet. *Nat Geosci*. 2016;9:528–532.
250. Schulze Chretien LM, Frajka-Williams E. Wind-driven transport of fresh shelf water into the upper 30 m of the Labrador Sea. *Ocean Sci*. 2018;14:1247–1264.
251. Gou R, Pennelly C, Myers PG. The changing behavior of the West Greenland Current system in a very high-resolution model. *J Geophys Res Oceans*. 2022;127:e2022JC018404.
252. Maslowski W, Newton B, Schlosser A, an Semtner P, Martinson D. Modeling recent climate variability in the Arctic Ocean. *Geophys Res Lett*. 2000;27:3743–3746.
253. Zhang X, Ikeda M, Walsh JE. Arctic sea ice and freshwater changes driven by the atmospheric leading mode in a coupled sea ice–ocean model. *J Clim*. 2003;16:2159–2177.
254. Condron A, Winsor P, Hill C, Menemenlis D. Simulated response of the arctic freshwater budget to extreme NAO wind forcing. *J Clim*. 2009;22:2422–2437.
255. Lique C, Treguier AM, Scheinert M, Penduff T. A model-based study of ice and freshwater transport variability along both sides of Greenland. *Clim Dyn*. 2009;33:685–705.
256. Aksenov Y, Bacon S, Coward AC, Holliday NP. Polar outflow from the Arctic Ocean: A high resolution model study. *J Mar Syst*. 2010;83:14–37.
257. Jahn A, Tremblay B, Mysak LA, Newton R. Effect of the large-scale atmospheric circulation on the variability of the Arctic Ocean freshwater export. *Clim Dyn*. 2010;34:201–222.
258. Bertosio C, Provost C, Athanase M, Sennéchael N, Garric G, Lellouche J-M, Bricaud C, Kim J-H, Cho K-H, Park T. Changes in freshwater distribution and pathways in the Arctic Ocean since 2007 in the Mercator Ocean Global Operational System. *J Geophys Res Oceans*. 2022;127:e2021JC017701.
259. Giles KA, Laxon SW, Ridout AL, Wingham DJ, Bacon S. Western Arctic Ocean freshwater storage increased by wind-driven spin-up of the Beaufort Gyre. *Nat Geosci*. 2012;5:194–197.
260. Morison J, Kwok R, Peralta-Ferriz C, Alkire M, Rigor I, Andersen R, Steele M. Changing Arctic Ocean freshwater pathways. *Nature*. 2012;481:66–70.
261. Rabe B, Karcher M, Kauker F, Schauer U, Toole JM, Krishfield RA, Pisarev S, Kikuchi T, Su J. Arctic ocean basin liquid freshwater storage trend 1992–2012. *Geophys Res Lett*. 2014;41(3):961–968.
262. Wang Q, Wekerle C, Danilov S, Koldunov N, Sidorenko D, Sein D, Rabe B, Jung T. Arctic sea ice decline significantly contributed to the unprecedented liquid freshwater accumulation in the Beaufort Gyre of the Arctic Ocean. *Geophys Res Lett*. 2018;45:4956–4964.
263. Wang Q, Wekerle C, Danilov S, Sidorenko D, Koldunov N, Sein D, Rabe B, Jung T. Recent sea ice decline did not significantly increase the total liquid freshwater content of the Arctic Ocean. *J Clim*. 2019;32:15–32.
264. Proshutinsky A, Krishfield R, Toole JM, Timmermans ML, Williams W, Zimmermann S, Yamamoto-Kawai M, Armitage TWK, Dukhovskoy D, Golubeva E, et al. Analysis of the Beaufort Gyre freshwater content in 2003–2018. *J Geophys Res Oceans*. 2019;124(12):9658–9689.
265. Proshutinsky A, Krishfield R, Timmermans M-L, Toole J, Carmack E, McLaughlin F, Williams WJ, Zimmermann S, Itoh M, Shimada K. Beaufort Gyre freshwater reservoir: State and variability from observations. *J Geophys Res Oceans*. 2009;114(C1):C00A10.
266. Zhang J, Steele M, Runciman K, Dewey S, Morison J, Lee C, Rainville L, Cole S, Krishfield R, Timmermans M-L, et al. The Beaufort Gyre intensification and stabilization: A model-observation synthesis. *J Geophys Res Oceans*. 2016;121(11):7933–7952.
267. Zhang X, He J, Zhang J, Polyakov I, Gerdes R, Inoue J, Wu P. Enhanced poleward moisture transport and amplified northern high-latitude wetting trend. *Nat Clim Chang*. 2013;3:47–51.
268. Vihma T, Screen J, Tjernström M, Newton B, Zhang X, Popova V, Deser C, Holland M, Prowse T. The atmospheric role in the Arctic water cycle: A review on processes, past and future changes, and their impacts. *J Geophys Res Biogeo*. 2016;121:586–620.
269. Villamil-Otero GA, Zhang J, He J, Zhang X. Role of extratropical cyclones in the recently observed increase in poleward moisture transport into the Arctic Ocean. *Adv Atmos Sci*. 2018;35:85–94.
270. Nygård T, Naakka T, Vihma T. Horizontal moisture transport dominates the regional moistening patterns in the Arctic. *J Clim*. 2020;33:6793–6807.
271. Bamber JL, Tedstone AJ, King MD, Howat IM, Enderlin EM, van den Broeke MR, Noel B. Land ice freshwater budget of the Arctic and North Atlantic Oceans: 1. Data, methods, and results. *J Geophys Res Oceans*. 2018;123:1827–1837.
272. Böning CW, Behrens E, Biastoch A, Getzlaff K, Bamber JL. Emerging impact of Greenland meltwater on deepwater formation in the North Atlantic Ocean. *Nat Geosci*. 2016;9:523–527.
273. Yang Q, Dixon TH, Myers PG, Bonin J, Chambers D, van den Broeke MR, Ribergaard MH, Mortensen J. Recent increases in Arctic freshwater flux affects Labrador Sea convection and Atlantic overturning circulation. *Nat Commun*. 2016;7:10525.
274. Stolzenberger S, Rietbroek R, Wekerle C, Uebbing B, Kusche J. Simulated signatures of Greenland melting in the North Atlantic: A model comparison with Argo floats, satellite observations, and ocean reanalysis. *J Geophys Res Oceans*. 2022;127:e2022JC018528.
275. Bamber J, van den Broeke M, Ettema J, Lenaerts J, Rignot E. Recent large increases in freshwater fluxes from Greenland into the North Atlantic. *Geophys Res Lett*. 2012;39(19):L19501.
276. Shepherd A, Ivins E, Rignot E, Smith B, van den Broeke M, Velicogna I, Whitehouse P, Briggs K, Joughin I, Krinner G, et al. Mass balance of the Greenland Ice Sheet from 1992 to 2018. *Nature*. 2020;579:233–239.

277. Sasgen I, Wouters B, Gardner AS, King MD, Tedesco M, Landerer FW, Dahle C, Save H, Fettweis X. Return to rapid ice loss in Greenland and record loss in 2019 detected by the GRACE-FO satellites. *Commun Earth Environ*. 2020;1:8.
278. Khan SA, Bamber JL, Rignot E, Helm V, Aschwanden A, Holland DM, van den Broeke M, King M, Noël B, Truffer M, et al. Greenland mass trends from airborne and satellite altimetry during 2011–2020. *J Geophys Res Earth*. 2022;127:e2021JF006505.
279. Jahn A, Aksenov Y, de Cuevas BA, de Steur L, Hakkinen S, Hansen E, Herbaut C, Houssais MN, Karcher M, Kauker F, et al. Arctic Ocean freshwater: How robust are model simulations? *J Geophys Res Oceans*. 2012;117:C00D16.
280. Wekerle C, Wang Q, Danilov S, Jung T, Schröter J. The Canadian Arctic Archipelago throughflow in a multiresolution global model: Model assessment and the driving mechanism of interannual variability. *J Geophys Res Oceans*. 2013;118(9):4525–4541.
281. Kliem N, Greenberg DA. Diagnostic simulations of the summer circulation in the Canadian Arctic Archipelago. *Atmosphere-Ocean*. 2003;41:273–289.
282. Houssais M-N, Herbaut C. Atmospheric forcing on the Canadian Arctic Archipelago freshwater outflow and implications for the Labrador Sea variability. *J Geophys Res Oceans*. 2011;116:C00D02.
283. McGeehan T, Maslowski W. Evaluation and control mechanisms of volume and freshwater export through the Canadian Arctic Archipelago in a high-resolution pan-Arctic ice-ocean model. *J Geophys Res*. 2012;117:C00D14.
284. Lu Y, Higginson S, Nudds S, Prinsenberg S, Garric G. Model simulated volume fluxes through the Canadian Arctic Archipelago and Davis Strait: Linking monthly variations to forcing in different seasons. *J Geophys Res Oceans*. 2014;119:1927–1942.
285. Wang Z, Hamilton J, Su J. Variations in freshwater pathways from the Arctic Ocean into the North Atlantic Ocean. *Prog Oceanogr*. 2017;155:54–73.
286. Grivault N, Hu X, Myers PG. Impact of the surface stress on the volume and freshwater transport through the Canadian Arctic Archipelago from a high-resolution numerical simulation. *J Geophys Res Oceans*. 2018;123:9038–9060.
287. Wang J, Zhang J, Watanabe E, Ikeda M, Mizobata K, Walsh JE, Bai X, Wu B. Is the Dipole Anomaly a major driver to record lows in Arctic summer sea ice extent? *Geophys Res Lett*. 2009;36(5):L05706.
288. Lei R, Heil P, Wang J, Zhang Z, Li Q, Li N. Characterization of sea-ice kinematic in the Arctic outflow region using buoy data. *Polar Res*. 2016;35:22658.
289. Ricker R, Girard-Ardhuin F, Krumpen T, Lique C. Satellite-derived sea ice export and its impact on Arctic ice mass balance. *Cryosphere*. 2018;12:3017–3032.
290. Hilmer M, Jung T. Evidence for a recent change in the link between the North Atlantic Oscillation and Arctic sea ice export. *Geophys Res Lett*. 2000;27:989–992.
291. Jung T, Hilmer M. The link between the North Atlantic oscillation and Arctic Sea ice export through Fram Strait. *J Clim*. 2001;14:3932–3943.
292. Wang S, Wang Q, Shu Q, Song Z, Lohmann G, Danilov S, Qiao F. Nonmonotonic change of the Arctic Ocean freshwater storage capability in a warming climate. *Geophys Res Lett*. 2021;48:e2020GL090951.
293. McCrystall MR, Stroeve J, Serreze M, Forbes BC, Screen JA. New climate models reveal faster and larger increases in Arctic precipitation than previously projected. *Nat Commun*. 2021;12:6765.
294. Shu Q, Qiao F, Song Z, Zhao J, Li X. Projected freshening of the Arctic Ocean in the 21st century. *J Geophys Res Oceans*. 2018;123:9232–9244.
295. Holland MM, Finnis J, Serreze MC. Simulated Arctic Ocean freshwater budgets in the twentieth and twenty-first centuries. *J Clim*. 2006;19:6221–6242.
296. Holland MM, Finnis J, Barrett AP, Serreze MC. Projected changes in Arctic Ocean freshwater budgets. *J Geophys Res Biogeosci*. 2007;112:G04S55.
297. Koenigk T, Mikolajewicz U, Haak H, Jungclaus J. Arctic freshwater export in the 20th and 21st centuries. *J Geophys Res Biogeo*. 2007;112:G04S41.
298. Jahn A, Laiho R. Forced changes in the Arctic freshwater budget emerge in the early 21st century. *Geophys Res Lett*. 2020;47:e2020GL088854.
299. Rudels B, Marnela M, Eriksson P. *Constraints on estimating mass, heat and freshwater transports in the Arctic Ocean: An exercise*. Netherlands: Springer; 2008. p. 315–341.
300. Nguyen AT, Pillar H, Ocaña V, Bigdeli A, Smith TA, Heimbach P. The Arctic Subpolar Gyre sTate Estimate: Description and assessment of a data-constrained, dynamically consistent ocean-sea ice estimate for 2002–2017. *J Adv Model Earth Syst*. 2021;13(5):e2020MS002398.
301. Lique C, Holland MM, Dibike YB, Lawrence DM, Screen JA. Modeling the Arctic freshwater system and its integration in the global system: Lessons learned and future challenges. *J Geophys Res Biogeo*. 2016;121:540–566.
302. Ilicak M, Drange H, Wang Q, Gerdes R, Aksenov Y, Bailey D, Bentsen M, Biastoch A, Bozec A, Böning C, et al. An assessment of the Arctic Ocean in a suite of interannual CORE-II simulations. Part III: Hydrography and fluxes. *Ocean Model*. 2016;100:141–161.
303. Aksenov Y, Karcher M, Proshutinsky A, Gerdes R, de Cuevas B, Golubeva E, Kauker F, Nguyen AT, Platov GA, Wadley M, et al. Arctic pathways of Pacific Water: Arctic Ocean model intercomparison experiments. *J Geophys Res Oceans*. 2016;121(1):27–59.
304. Shu Q, Wang Q, Su J, Li X, Qiao F. Assessment of the Atlantic Water layer in the Arctic Ocean in CMIP5 climate models. *Clim Dyn*. 2019;53:5279–5291.
305. Shu Q, Wang Q, Song Z, Qiao F, Zhao J, Chu M, Li X. Assessment of sea ice extent in CMIP6 with comparison to observations and CMIP5. *Geophys Res Lett*. 2020;47:e2020GL087965.
306. Muilwijk M, Nummelin A, Heuzé C, Polyakov IV, Zanowski H, Smedsrud LH. Divergence in climate model projections of future Arctic Atlantification. *J Clim*. 2023;1727–1748.
307. Heuzé C, Zanowski H, Karam S, Muilwijk M. The deep Arctic Ocean and Fram Strait in CMIP6 models. *J Clim*. 2023;2551–2584.
308. Docquier D, Grist JP, Roberts MJ, Roberts CD, Semmler T, Ponsoni L, Massonnet F, Sidorenko D, Sein DV, Iovino D, et al. Impact of model resolution on Arctic sea ice and North Atlantic Ocean heat transport. *Clim Dyn*. 2019;53:4989–5017.
309. Chassignet EP, Yeager SG, Fox-Kemper B, Bozec A, Castruccio F, Danabasoglu G, Horvat C, Kim WM, Koldunov N, Li Y, et al. Impact of horizontal resolution

on global ocean–sea ice model simulations based on the experimental protocols of the Ocean Model Intercomparison Project phase 2 (OMIP-2). *Geosci Model Dev*. 2020;13:4595–4637.

310. Pan R, Shu Q, Wang Q, Wang S, Song Z, He Y, Qiao F. Future Arctic climate change in CMIP6 strikingly intensified by NEMO-family climate models. *Geophys Res Lett*. 2023;50:e2022GL102077.